DEFECT DETECTION IN SUBMERGED PLATE STRUCTURES CONSIDERING INHERENT IRREGULARITIES

Thesis submitted in partial fulfillment of the requirements for the award of degree of

Master of Engineering

In

CAD/CAM AND ROBOTICS

By

Gurjot Singh

Roll No 800881007

Under the supervision of:

Dr. Abhijit Mukherjee	**Mr. Sandeep Sharma**
Director	**Assistant Prof., MED**
Thapar University, Patiala	**Thapar University, Patiala**

MECHANICAL ENGINEERING DEPARTMENT

THAPAR UNIVERSITY PATIALA – 147004

July 2010

CERTIFICATE

I hereby certify that the work being presented in the thesis entitled "**Defect Detection in Submerged Plate Structures Considering Inherent Irregularities** " in partial fulfilment of requirement for the award of the master degree in CAD/CAM & Robotics submitted in the mechanical engineering department, Thapar University, Patiala, is an authentic record of the work carried out by me under the guidance of Dr. Abhijit Mukherjee, Director, Thapar University, Patiala and Mr. Sandeep Sharma , Assistant Prof., Mechanical Engineering Department, Thapar University, Patiala.

The matter embodied in this report has not been submitted in part or full to any other university or institute for the award of any degree.

Dated: 15th July 2010

(Gurjot Singh)

This is to certify that above declaration made by the student concerned is correct to the best of my knowledge & belief.

Dr. Abhijit Mukherjee
Director
Thapar University,
Patiala

Mr. Sandeep Sharma
Assistant Prof., MED
Thapar University,
Patiala

Countersigned by

Dr. S.K. Mohopatra
Professor & Head, MED
Thapar University, Patiala

Dr. R.K. Sharma 3/9/10
Dean (Academic Affairs)
Thapar University, Patiala

ACKNOWLEDGEMENT

I take this opportunity to express my sincere gratitude to Dr. Abhijit Mukherjee, Director, Thapar University, Patiala for giving me the opportunity of doing my thesis work under his guidance. I am also thankful to him for his constant supervision and valuable suggestions.

It is my proud privilege to express regards and sincere gratitude to Mr. Sandeep Sharma, Assistant Prof, Mechanical Engineering Department, Thapar University, Patiala for his patient listening of my ideas and also suggesting new ways for implementing my ideas by his expert guidance throughout my work.

I would like to extend my thanks to Mrs. Shruti Sharma, Assistant Prof, Civil Engineering Department, Thapar University, Patiala, for her guidance and providing necessary information and facilities needed for my thesis work.

I am also thankful to Dr. S.K. Mohapatra, Head Mechanical Engineering Department, Thapar University, Patiala for the motivation and inspiration that triggered me for the present work.

I also take this opportunity to thank to the entire faculty and staff of Mechanical Engineering Department, Civil Engineering Department, and Central Workshop Thapar University, Patiala for their help, inspiration and moral support, which went a long way in successfully completion of this report.

I am especially thankful to Mr. Surinder Pal, the Dynamics Lab helper, who offered his helping hand for the successful completion of the experimental work and kept me in high spirits.

Gurjot Singh

80081007

ABSTRACT

Health monitoring for damage detection utilizing ultrasonic waves is an emerging field. It uses transmission of stress waves into a material to detect imperfections, damages or to locate changes in material properties. It becomes even more challenging when the specimen being monitored is submerged in water. But water can be used to advantage, as it acts a natural couplant.

This report presents the use of above two techniques to detect the damage in steel plates, submerged in water, with seeded defects in the form of notches, considering the inherent irregularities in the plate specimen. Presence of the seeded defects in the plates has been detected by pulse transmission technique and the pulse echo method is used to localize the same. Negative spike pulse is used as an input signal to sending transducer through Pulser/Receiver system and transmitted pulse is received at the other end by receiving transducer. Ultrasonic waves are introduced at different angles to excite the different modes in the subject specimen in both pulse echo and through transmission technique. The signals thus obtained are digitized using digitizer card.

Before scanning a plate seeded with defects, specimen plate is tested in healthy condition, for inherent irregularities in it. These inherent irregularities can lead to misinformation regarding the presence, extent and location of the defect. So a correction factor has been formulated to nullify the effect of the inherent irregularities present.

The combination of pulse echo and pulse transmission readings has been successfully used to generate the tomograms of the specimen plate. Application of the correction factor on the readings obtained has been found to significantly improve the tomograms regarding the extent and location of the defect.

TABLE OF CONTENTS

LIST of Figures

List of Tables

CHAPTER 1

INTRODUCTION

1.1 General

Non-destructive testing has been practiced for many decades, with initial rapid developments in instrumentation spurred by the technological advances that occurred during World War II and the subsequent defence effort. During the earlier days, the primary purpose was the detection of defects. As a part of "safe life" design, it was intended that a structure should not develop macroscopic defects during its life, with the detection of such defects being a cause for removal of the component from service. In response to this need, increasingly sophisticated techniques using ultrasonics, eddy currents, x-rays, dye penetrants, magnetic particles and other forms of interrogating energy emerged.

In the early 1970's, two events occurred which caused a major change in the NDT field. First, improvements in the technology led to the ability to detect small flaws, which caused more parts to be rejected even though the probability of component failure had not changed. However, the discipline of fracture mechanics emerged, which enabled one to predict whether a crack of a given size will fail under a particular load when a material's fracture toughness properties are known. Other laws were developed to predict the growth rate of cracks under cyclic loading (fatigue). With the advent of these tools, it became possible to accept structures containing defects if the sizes of those defects were known. This formed the basis for the new philosophy of “damage tolerant" design. Components having known defects could continue in service as long as it could be established that those defects would not grow to a critical, failure producing size.

A new challenge was thus presented to the non-destructive testing community. Detection was not enough. One needed to also obtain quantitative information about flaw size to serve as an input to fracture mechanics based predictions of remaining life. The need for quantitative information was particularly strong in the defence and nuclear power industries and led to the emergence of quantitative non-destructive evaluation (QNDE) as a new engineering/research discipline[1].

1.2 Techniques for NDT

The aim of all NDT **techniques** is to detect and locate defects, without causing any damage to the component under inspection. Some of the most commonly used NDT techniques like visual and optical testing, penetrant testing, electromagnetic testing are used for testing only surface defects, while techniques such as radiography and ultrasonic testing are used to detect both surface and buried-in defects.

Some of the commonly used NDT techniques are as follows:

•**Visual and Optical Testing:** Visual inspection involves using an inspector's eyes to look for defects. The inspector may also use special tools such as magnifying glasses or mirrors gain access and more closely inspect the subject area.

• **Penetrant Testing:** Test specimens are coated with visible or fluorescent dye solution. Excess dye is then wiped out from the surface, and a developer is applied. The developer acts as blotter, drawing trapped penetrant out of imperfections open to the surface. With visible dyes, vivid colour contrasts between the penetrant and developer make “bleed out" easy to see.

• **Magnetic Particle Testing (MT):** In this method a magnetic field in a ferromagnetic material is induced and then dusting the surface with iron particles (either dry or suspended in liquid) is done. Surface and near-surface imperfections distort the magnetic field and concentrate iron particles near imperfections, previewing a visual indication of the flaw.

• **Electromagnetic Testing (ET) or Eddy Current Testing:** Eddy currents are generated in a conductive material by an induced alternating magnetic field and they flow in circles at just below the surface of the material. Interruptions in the flow of eddy currents, caused by imperfections, dimensional changes, or changes in the materials conductive and permeability properties, can be detected with the proper equipment.

• **Radiography (RT):** Radiography involves the use of penetrating gamma or X radiation to examine parts and products for imperfections. An X-ray generator or radioactive isotope is used as a source of radiation. The resulting shadowgraph shows the dimensional features of the part. Possible imperfections are indicated as density changes on the film in the same manner as medical X-ray shows broken bones.

• **Ultrasonic Testing (UT):** ultrasonic testing use transmission of high-frequency sound waves into a material to detect imperfections or to locate changes in material properties. The most commonly used ultrasonic testing technique is pulse echo, wherein sound is introduced into a test object and reflections (echoes) are returned to a receiver from internal imperfections or from the part's geometrical surfaces.

• **Acoustic Emission Testing (AE):** when a solid material is stressed, imperfections within the material emit short bursts of acoustic energy called "emissions." as in ultrasonic testing; acoustic emissions can be detected by special receivers. Emission sources can be evaluated through the study of their intensity, rate, and location.

• **Leak Testing (LT):** Several techniques are used to detect and locate leaks in pressure containment parts, pressure vessels, and structures. Leaks can be detected by using electronic listening devices, pressure gauge measurements, liquid and gas Penetrant techniques, and/or a simple soap-bubble test.

• **Electromagnetic Acoustic Transducers (EMATs): T**hey generate and detect ultrasonic waves via electromagnetic coupling between the EMAT and the metal samples. They operate via the Lorentz force or magneto elastic mechanisms or both simultaneously.

• **X-Ray Fluorescence (XRF):** X-ray fluorescence is one of the methods for NDT. The equipment contains radioactive sources or a low voltage x-ray generator, which sends out radiation. The exposed material then sends temporarily element specific radiation back, generating energy. As every element has its own atomic structure, this reflection will generate a different energy level for every element. This energy is measured and detected, thus identifying the alloy elements.

•**Infrared Thermography:** It is a fast NDT inspection method which does not influence the process and maps the temperature differences of any object in a range from -50ºC to 1500ºC. Instead of detecting the temperature point by point, thermo graphic camera is able to detect the temperature across a complete surface. This gives an excellent image of local temperature differences. [2]

When it is possible to use several inspection techniques, the choice of a specific technique will depend on the accuracy and cost of the inspection, balancing the money spent on safety measures with the business return of the system being maintained. The accuracy of a given technique must also be sufficient to detect defects considerably smaller than those that could result in failure because these defects can grow in size between inspections. The diverse nature of different NDT processes results in different sources of variance and possible impact on detection output capabilities. It is important to recognize the source and nature of variance in each NDT process and to take such information into consideration when applying margins to the NDT processes. The NDT methods and procedures are selected using a variety of practical implementation criteria, are represented in Table 1.1.

Table 1.1 Comparative analyses of various NDT techniques.

Parameter	**Penetrant Testing**	**Magnetic Particle Testing**	**Ultrasonic Testing**	**Eddy Current Testing**	**Radiographic Testing**
	Advantages:				
Range of inspection	Large surface areas or large volumes of parts can be inspected rapidly.	Large surface areas of complex parts can be inspected rapidly.	Depth of penetration for flaw detection is superior to other methods.	Detects surface and near surface defects.	Can be used to inspect virtually all materials.
Geometry of part to be inspected	Parts with complex geometry are routinely inspected.	Can detect surface and subsurface flaws.	Only single sided access is required.	Test probe does not need to contact the part.	Detects surface and subsurface defects.
Geometry of part to be inspected	Indications are produced directly on surface of the part providing a visual image of the discontinuity.	Indications are produced directly on the surface of the part and form an image of the discontinuity.	Provides distance information.	Method can be used for more than flaw detection.	Ability to inspect complex shapes and multi-layered structures without disassembly.
Cost of inspection	Low	Low	Low	Low	Moderate

Cost of equipment	Low	Moderate	Moderate	High	High
Surface preparation	Surface preparation is critical.	Surface preparation is less critical.	Minimum part preparation is required.	Minimum part preparation is required.	Minimum part preparation is required.
	Disadvantages:				
Type of material to be inspected	Detects only surface breaking defects.	Only ferromagnetic materials can be inspected.	Surface must be accessible to probe and couplant.	Only conductive materials can be inspected.	Extensive operator training and skill required.
Type of surface needed	Requires a relatively smooth and nonporous surface.	Proper alignment of magnetic field and defect is critical.	Surface finish and roughness can interfere with inspection.	Ferromagnetic materials require special treatment for magnetic permeability.	Access to both sides of the structure is usually required.
Exceptions in detection	Sub-surface defects go undetected.	Large currents are needed for very large parts.	Linear defects oriented parallel to sound beam can't be detected.	Flaws that lie parallel to the inspection probe coil winding direction can go undetected	Orientation of the radiation beam to non-volumetric defects is critical.
Post inspection treatment	Post cleaning is necessary to remove chemicals.	Demagnetization and post cleaning is usually necessary.	Thin parts may be difficult to inspect.	Surface finish and roughness may interfere.	Inspection of thick section can be time consuming.
Personnel needed	Requires multiple operations	Skill and trained staff is required.	Skill required is more	Skill and trained staff is required.	Skill and trained staff is required.

Safety concerns	Chemical handling precautions are necessary.	Relatively safe method	extensive Relatively safest method	Relatively safe method	Possible radiation hazard [3].

1.3 NDT Technique Selection

Each NDT technique has its own set of advantages and disadvantages and, therefore, some are better suited than others for a particular application. The NDT technician or engineer must select the method that will detect the defect or make the measurement with the highest sensitivity and reliability. The cost effectiveness of the technique must also be taken into consideration.

Table 1.2 provides some guidance in the selection of NDT techniques for common flaw detection and measurement applications [4].

Table 1.2 selections of NDT Techniques.

Flaw type ↓	**Method →**	**Visual**	**Dye penetrant**	**Magnetic particle***	**Ultrasonic**	**Eddy current****	**x- ray**
Surface breaking linear		1	3	3	2	3	1
Surface breaking volumetric		3	3	3	3	3	3
Near surface, linear and parallel to surface		0	0	2	2	3	1
Near surface, linear and normal to surface		0	0	0	3	0	0
Near surface		0	0	2	3	3	3

volumetric						
Sub-surface linear and normal to surface	0	0	0	2	0	1
Sub-surface linear and parallel to surface	0	0	0	3	0	1
Subsurface volumetric	0	0	0	3	0	3

* Ferromagnetic materials only ** Conductive materials only

(0) Will Not Detect

(1) Not Well Suited

(2) Fairly Suitable

(3) Ideal Application

From the above comparison between various techniques, it is concluded that Ultrasonic Waves being capable of detecting most of surface and sub-surface defects. It is cost effective and no special training required for the personnel. It has no safety hazard and can be used for damage detection in plate structures efficiently.

CHAPTER 2

ULTRASONICS AS AN NDT TOOL

2.1 Introduction

Ultrasonic non-destructive testing introduces high frequency (greater than 20 kHz) sound waves into a test object to obtain information about the object without altering or damaging it. It is used for detection of damage in structures. This is one of the best non destructive testing methods where ultrasonic wave is send into the structure to find the location and magnitude of the defect. Ultrasonic wave propagation varies with change in the medium in which the wave propagates.

Ultrasonic waves are simply organized mechanical vibrations travelling through a medium, which may be in any state of matter. These waves travel through a given medium at a specific speed or velocity, in a predictable direction, and when they encounter a boundary with a different medium they will be reflected or transmitted according to simple rules. This is the principle of physics that underlies ultrasonic flaw detection.

Some of the generally used terms to define the ultrasonic waves are [5]:

• **Frequency (υ):** All sound waves oscillate at a specific frequency, or number of vibrations or cycles per second, which we experience as pitch in the familiar range of audible sound. Human hearing extends to a maximum frequency of about 20,000 cycles per second (20 KHz), while the majority of ultrasonic flaw detection applications utilize frequencies between 500 KHz to 10 MHz. At frequencies in the Megahertz range, sound energy does not travel efficiently through air or other gasses, but it travels freely through most liquids and common engineering materials.

• **Wave Speed:** The speed of a sound wave varies depending on the medium through which it is travelling, affected by the medium's density and elastic properties. Different types of sound waves will travel at different velocities.

• **Wavelength (λ)**: It is the distance between any two corresponding points in the wave cycle as it travels through a medium. Wavelength is related to frequency and velocity by the simple equation

$\lambda = c/\upsilon$ …(2.1)

Where, λ = wavelength, c = sound velocity, υ = frequency

In ultrasonic flaw detection, the generally accepted lower limit of detection for a small flaw is one-half wavelength, and anything smaller than that will be invisible. In ultrasonic thickness gauging, the theoretical minimum measurable thickness is one wavelength.

• **Acoustic impedance (**Z**):** Sound travels through materials under the influence of sound pressure. Because molecules or atoms of a solid are bound elastically to one another, the excess pressure results in a wave propagating through the solid. The Acoustic impedance (Z) of a material is defined as the product of its density (ρ) and acoustic speed in medium

$Z = \rho/c$.(2.2)

Acoustic impedance is important in determining acoustic transmission and reflection at the boundary of two materials having different acoustic impedances.

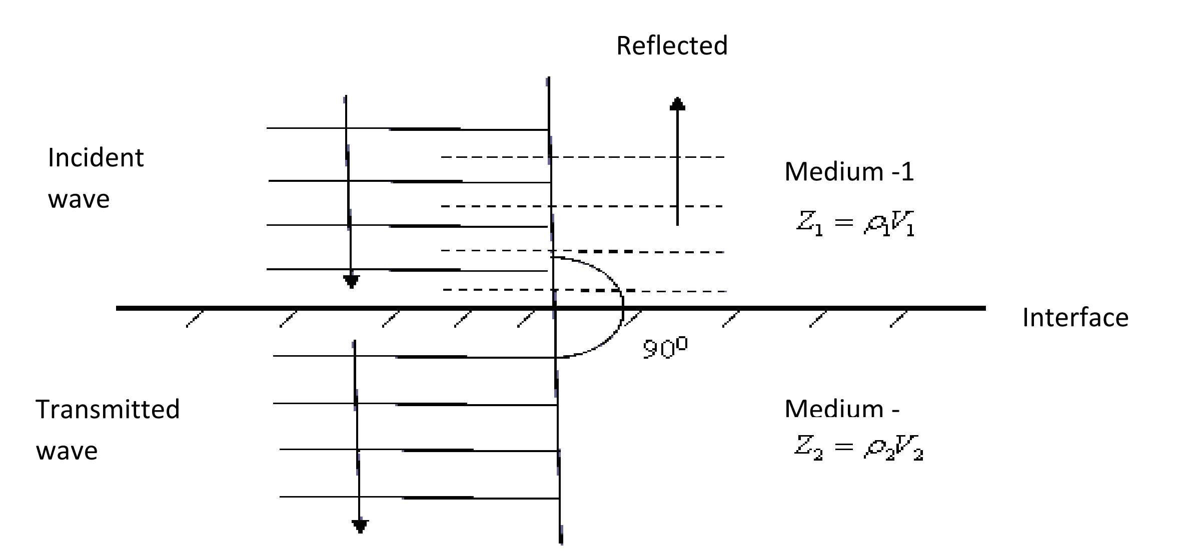

Fig.: 2.1 Reflection and Transmission of sound wave at normal incidence

• **Reflection and Transmission Coefficients:** Ultrasonic waves are reflected at boundaries where there is a difference in acoustic impedances (Z) of the materials on each side of the boundary as shown in the **Fig. 2.1**. This difference in Z is commonly referred to as the impedance mismatch. The greater the impedance mismatch, the greater the percentage of energy that will be reflected at the interface or boundary between one medium and another.

The fraction of the incident wave intensity that is refracted can be derived because particle velocity and local particle pressures must be continuous across the boundary. When the acoustic impedances of the materials on both sides of the boundary are known, the fraction of the incident wave intensity that is reflected can be calculated with the equation below. The value produced is known as the reflection coefficient.

Reflection coefficient, $R = \dfrac{Z_1 - Z_2}{Z_1 + Z_2}$ …(2.3)

Transmission coefficient, $T = \dfrac{2Z_1}{Z_1 + Z_2}$ …(2.4)

2.2 Reflection, Refraction and Mode Conversion

When sound travels in a solid material, one form of wave energy can be transformed into another form. For example, when a longitudinal wave hits an interface at an angle, some of the energy can cause particle movement in the transverse direction to start a shear (transverse) wave. Mode conversion occurs when a wave encounters an interface between materials of different acoustic impedances and the incident angle is not normal to the interface.

When sound waves pass through an interface between materials having different acoustic velocities, refraction takes place at the interface. The larger the difference in acoustic velocities between the two materials, the more the sound is refracted. Notice that the shear wave is not refracted as much as the longitudinal wave. This occurs because shear waves travel slower than longitudinal waves. Therefore, the velocity difference between the incident longitudinal wave and the shear wave is not as great as longitudinal waves but it is between the incident and refracted longitudinal waves. Also note that when a longitudinal wave is reflected inside the material, the reflected shear wave is reflected at a smaller angle than the reflected longitudinal wave (ref. **Fig.: 2.2**). This is also due to the fact that the shear velocity is less than the longitudinal velocity within a given material. Snell’s Law holds true for shear waves as well as longitudinal waves and can be written as

$$\frac{\sin\,\theta_1}{VL_1}=\frac{\sin\,\theta_2}{VL_2}=\frac{\sin\,\theta_3}{VS_3}=\frac{\sin\,\theta_4}{VS_4}$$

2.3 Critical Angle

For small angles of incidence sound waves travelling at an angle from medium 1give rise to the longitudinal as well as shear waves, in the medium 2. Such a situation is very confusing for NDT inspection, as both of these waves present in the medium 2, travel at different velocities and give rise to separate on the flaw detector screen.

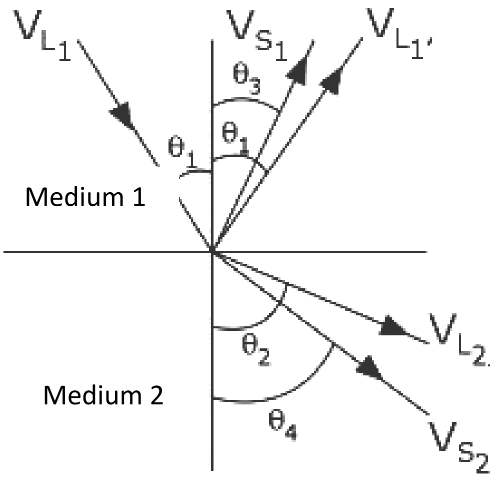

$$\frac{\sin\,\theta_1}{VL_1}=\frac{\sin\,\theta_2}{VL_2}=\frac{\sin\,\theta_3}{VS_3}=\frac{\sin\,\theta_4}{VS_4}$$

Where:

VL_1 – is the longitudinal wave velocity in medium 1.

VL_2 – is the longitudinal wave velocity in medium 2.

VS_1 – is the shear wave velocity in medium 1.

VS_2 – is the shear wave velocity in medium 2.

Fig. 2.2 Snell's Law

As a solution to this problem the longitudinal wave is not allowed to enter the test piece and is eliminated by total internal reflection. Therefore, a clear knowledge about the formation of critical angles becomes important, especially in the case of designing of angle beam transducers.

2.3.1 First Critical Angle

If the angle of incidence A is increased in the particular case when c2 > c1, angle B of the refraction longitudinal wave also increases till, for some specific value of angle A, the angle B becomes equal to 90^o. At this angle A1, (**Fig. 2.3**) there would be no refraction longitudinal wave in the medium 2 and only the shear wave would be propagating. This value of angle A is called First Critical Angle (A_1). Generally, the angle beyond the first critical angle is used for ultrasonic inspection at oblique incidence. Taking the refracted angle B for the longitudinal wave as 90^o, the Snell's equation can be written as

$$\frac{\sin\,A_1}{C_1}=\frac{\sin\,90}{C_2(long\,)} \qquad (5)$$

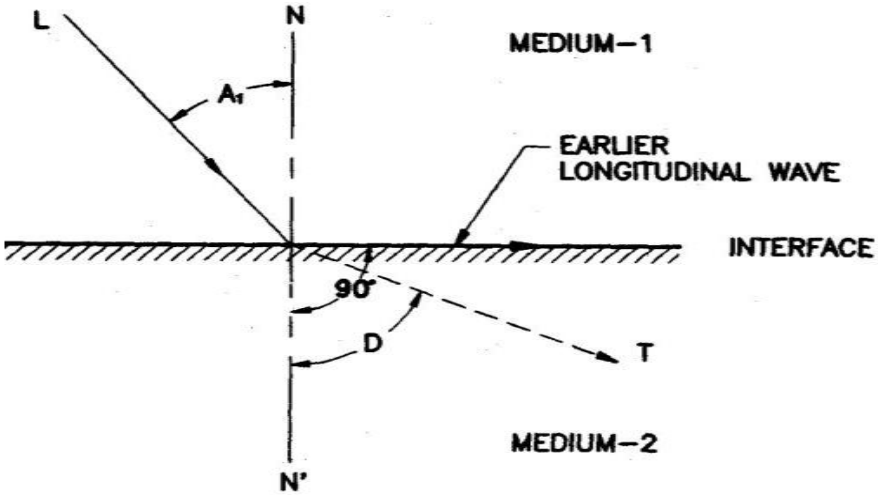

Fig. 2.3 First Critical Angle

Or $A_1 = \sin^{-1}\frac{C_1}{C_2}$ (6)

Where C1 and C2 are longitudinal velocities in two media

2.3.2 Second Critical Angle

If the angle of incidence A is further increased beyond A1, a situation would arrive, when angle D of the refracted shear wave would be equal to 90^{o}. The value of angle A is now known as second critical Angle (A2) (**Fig. 2.4**). At this position the Snell's equation can be written as

$$\frac{\sin A_2}{C_1(long)} = \frac{\sin 90}{C_2(trans)} \quad (7)$$

$$A_2 = \sin^{-1}\frac{C_1(long)}{C_2(long)} \quad (8)$$

The **Fig. 2.4** shows the formation of Second Critical Angle. At this position there would be no sound beam entering the medium 2 and the shear wave would appear as surface wave.

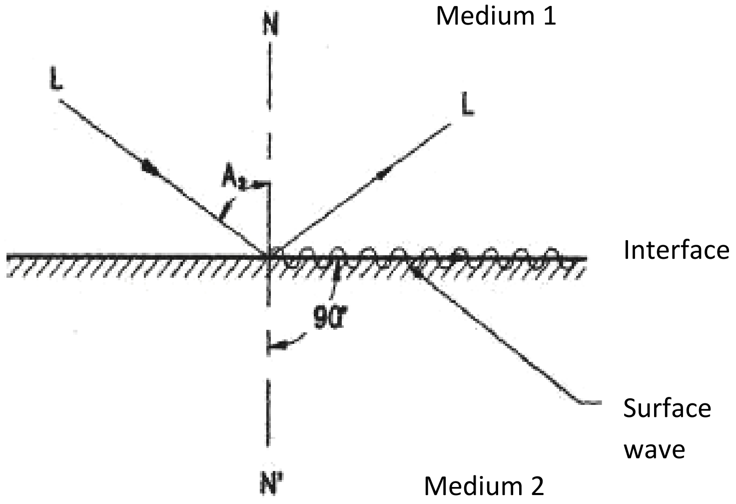

Fig. 2.4 Second Critical Angle

2.4 Modes of Wave Propagation

The ultrasonic waves propagate in different ways in a medium. Wave propagation depends on material properties of the structure. On the basis of the mode of particle displacement, these waves can be classified as follows:

Table 2.1 Types of Waves Propagation

Sr. no	Type of wave	Direction of motion of particles
1	Longitudinal or Compression waves (L-waves)	Parallel to wave direction
2	Transverse or Shear waves (S-waves)	Perpendicular to wave direction
3	Surface or Rayleigh waves	Elliptical orbit – symmetrical mode
4	Plate waves- Lamb	Component perpendicular to surface (extensional wave)
5	Plate waves- Love	Parallel to plane layer, perpendicular to wave direction
6	Stoneley (Leaky Rayleigh Waves)	Wave guided along interface
7	Sezawa	Anti symmetric mode

Out of these longitudinal and transverse wave propagations are most important and are extensively used in ultrasonic NDT applications [6].

2.4.1 Longitudinal or Compressional waves

As shown in **Fig 2.5**, the oscillations occur in the longitudinal direction or the direction of wave propagation. Since compression forces are active in these waves, they are also called pressure or compression waves. They are also sometimes called density waves because their particle density fluctuates as the wave travels. Compression waves can be generated in liquids, as well as solids because the energy travels through the atomic structure by a series of compression and expansion (rarefaction) movements.

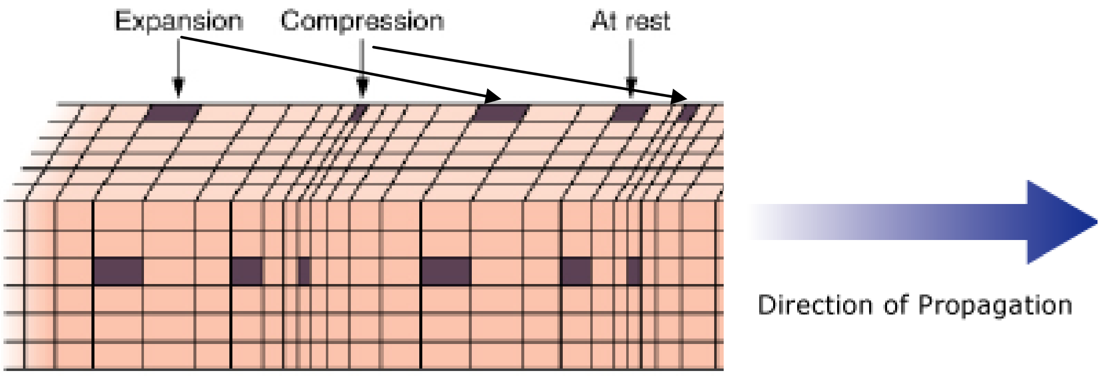

Fig 2.5 Longitudinal or Compressional wave

2.4.2 Transverse or Shear wave

As shown in **Fig 2.6,** the particles oscillate at a right angle to the direction of propagation. Shear waves require an acoustically solid material for effective propagation, and therefore, are not effectively propagated in materials such as liquids or gasses. Shear waves are relatively weak when compared to longitudinal waves. In fact, shear waves are usually generated in materials using some of the energy from longitudinal waves.

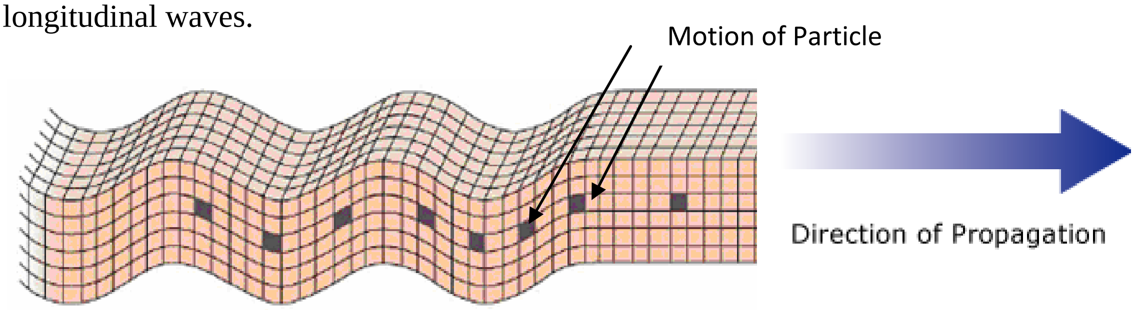

Fig 2.6 Transverse or Shear wave

2.4.3 Surface (or Rayleigh) waves

It travels at the surface of a relatively thick solid material penetrating to a depth of one wavelength. Surface waves combine both a longitudinal and transverse motion to create an elliptic orbit motion as shown in the **Fig 2.7**. The major axis of the ellipse is perpendicular to the surface of the solid. As the depth of an individual atom from the surface increases, the width of its elliptical motion decreases. Surface waves are generated when a longitudinal wave intersects a surface near the second critical angle and they travel at a velocity between 0.87 and 0.95 of a shear wave. Rayleigh waves are useful because they are very sensitive to surface defects (and other surface features) and they follow the surface around curves. Because of this, Rayleigh waves can be used to inspect areas that other waves might have difficulty reaching

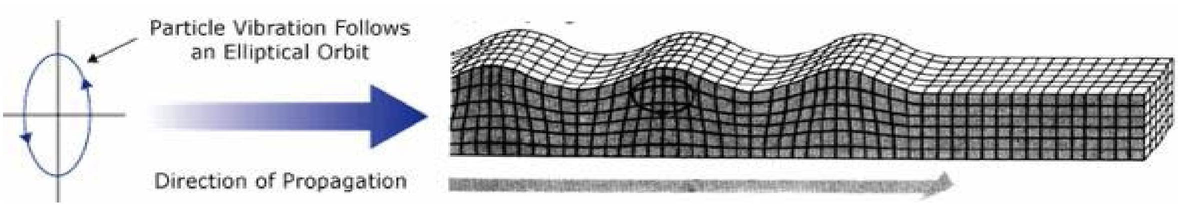

Fig. 2.7 Surface (or Rayleigh) waves

2.4.4 Plate waves or Lamb waves

These are similar to surface waves except they can only be generated in specimen which is a few wavelengths thick. Lamb waves are the most commonly used plate waves in NDT. They are complex vibration waves that propagate parallel to the test surface throughout the thickness of the material. Propagation of Lamb waves depends on the density and the elastic material properties of a component. They are also highly influenced by the test frequency and material thickness. Lamb waves are generated at an incident angle in which the parallel component of the velocity of the wave in the source is equal to the velocity of the wave in the test material. Lamb waves can travel several meters in steel and so are useful to scan plate, wire, and tubes.

With these waves a number of modes of particle vibration are possible, but the two most common are symmetrical and asymmetrical as shown in **Fig. 2.8(a) & (b)**. The complex motion of the particles is similar to the elliptical orbits for surface waves.

Symmetrical Lamb waves move in a symmetrical fashion about the median plane of the plate. This is sometimes called the extensional mode because the wave is “stretching and compressing" the plate in the wave motion direction. Wave motion in the symmetrical mode (S mode) is most efficiently produced when the exciting force is parallel to the plate.

The asymmetrical Lamb wave mode (A mode) is often called the "flexural mode" because a large portion of the motion moves in a normal direction to the plate, and a little motion occurs in the direction parallel to the plate. In this mode, the body of the plate bends as the two surfaces move in the same direction.

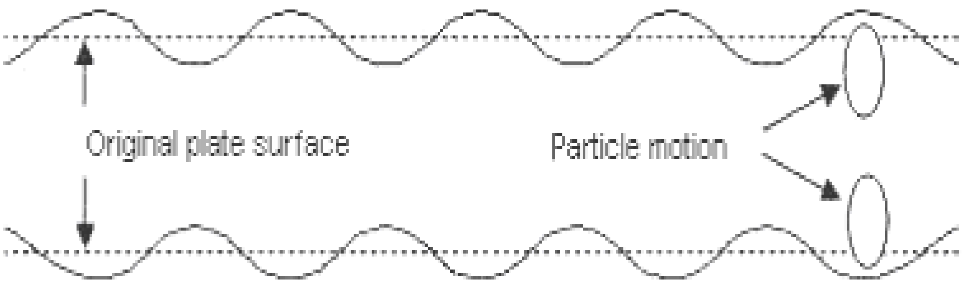

Fig. 2.8 (a) Lamb Wave Symmetric mode(S mode)

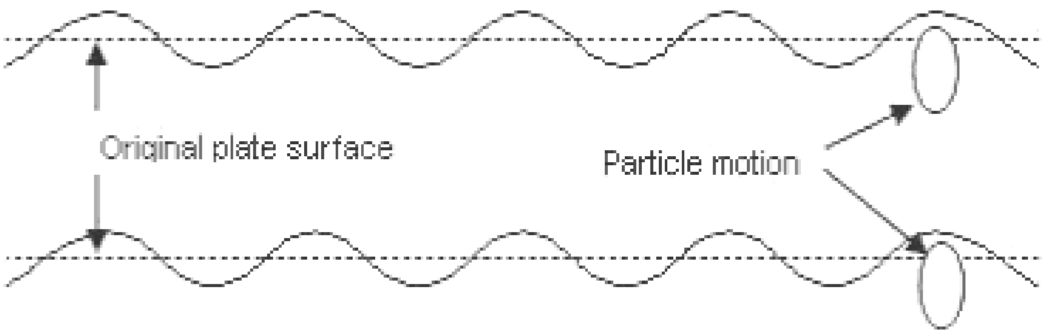

Fig. 2.8 (b) Lamb Wave Anti-symmetric Mode (A mode)

2.5 Piezoelectric Transducers for Ultrasonic Wave Generation

The conversion of electrical pulses to mechanical vibrations and the conversion of returned mechanical vibrations back into electrical energy is the basis for ultrasonic testing. The active element is the heart of the transducer as it converts the electrical energy to acoustic energy, and vice versa. The active element is basically a piece of polarized material with electrodes attached to two of its opposite faces. When an electric field is applied across the material, as shown in **Fig. 2.9**, the polarized molecules will align themselves with the electric field, resulting in induced dipoles within the molecular or crystal structure of the material. This alignment of molecules will cause the material to change dimensions. This phenomenon is known as electrostriction.

A permanently-polarized material such as quartz (SiO2) or barium titanate (BaTiO3) will produce an electric field when the material changes dimensions as a result of an imposed mechanical force. This phenomenon is known as the piezoelectric effect.

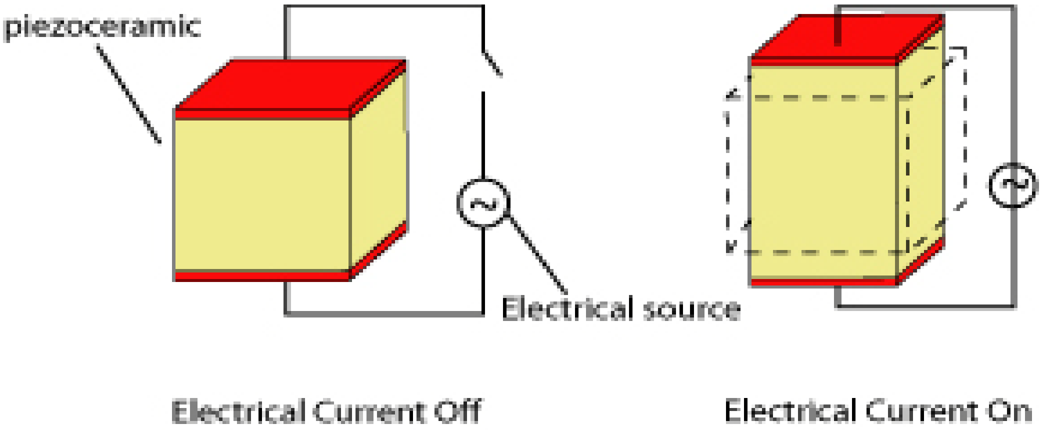

Fig. 2.9 Piezoelectric Crystal with Current Off and On

Main components of Transducer/Probe head as shown in **Fig 2.10** are,

1. Active element

2. Backing material

3. Matching layer

The backing is most commonly a highly attenuative and very dense material and is used to control the vibration of the transducer crystal by absorbing the energy that radiates from the back face of the piezoelectric element. When the acoustic impedance of the backing material matches that of the piezoelectric crystal, the result is a highly damped transducer with excellent resolution. By varying the backing material in order to vary the difference in impedance between the backing and the piezoelectric crystal, a transducer will suffer somewhat and resolution may be much higher in signal amplitude or sensitivity.

2.5.1 Components of Transducer

As shown in the **Fig. 2.11**, the components of the transducer and their functions are as follows:

The main purpose of the wear plate is simply to protect the piezoelectric transducer element from the environment. Wear plates are selected to generally protect against wear and corrosion. In an immersion-type transducer, the wear plate also serves as an acoustic transformer between the piezoelectric transducer element and water, wedge or delay line. [7]

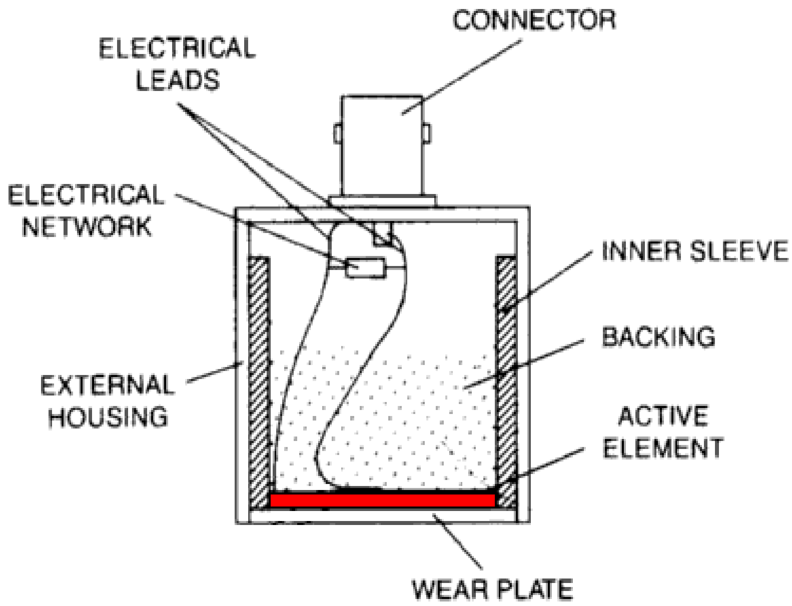

Fig. 2.10 Piezoelectric Transducer

The backing material supporting the crystal has a great influence on the damping characteristics of a transducer. Using a backing material with impedance similar to that of the active element will produce the most effective damping. Such transducer will have a narrow bandwidth resulting in higher sensitivity. As the mismatch in impedance between the active element and the backing material increases, material penetration increases but transducer sensitivity is reduced.

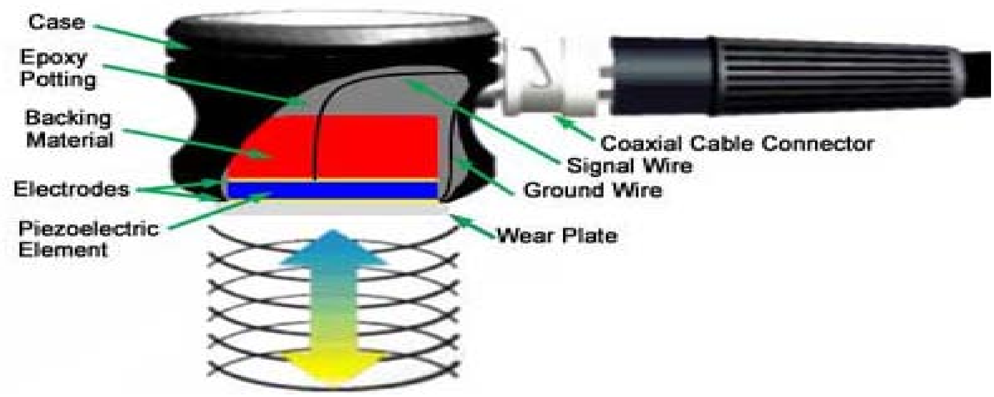

Fig. 2.11 Components of Transducer

2.5.2 Radiated Fields of Ultrasonic Transducers

The sound that emanates from a piezoelectric transducer does not originate from a point, but instead originates from most of the surface of the piezoelectric element. Round transducers are often referred to as piston source transducers because the sound field resembles a cylindrical mass in front of the transducer. The sound field from a typical piezoelectric transducer is shown below.

The intensity of the sound in **Fig. 2.12** is indicated by colour, with lighter colours indicating higher intensity. Since the ultrasound originates from a number of points along the transducer face, the ultrasound intensity along the beam is affected by constructive and destructive wave interference as discussed in a previous page on wave interference. These are sometimes also referred to as diffraction effects. This wave interference leads to extensive fluctuations in the sound intensity near the source and is known as the near field. Because of acoustic variations within a near field, it can be extremely difficult to accurately evaluate flaws in materials when they are positioned within this area.

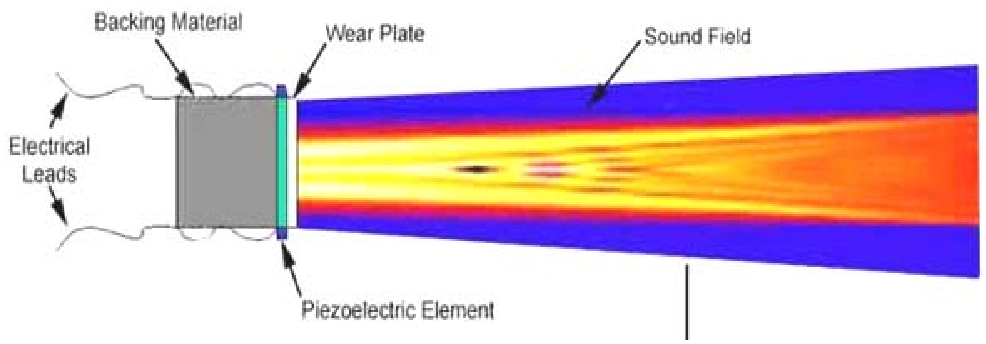

Fig. 2.12 Sound Field from a Typical Piezoelectric Transducer

2.6 Types of Transducer

Transducers are classified into groups according to the application [8].

- **Contact transducers** are used for direct contact inspections, and are generally hand manipulated, as shown in **Fig. 2.19**. They have elements protected in a rugged casing to withstand sliding contact with a variety of materials. These transducers have an ergonomic design so that they are easy to grip and move along a surface. They often have replaceable wear plates to lengthen their useful life. Coupling materials of water, grease, oils, or commercial materials are used to remove the air gap between the transducer and the component being inspected.

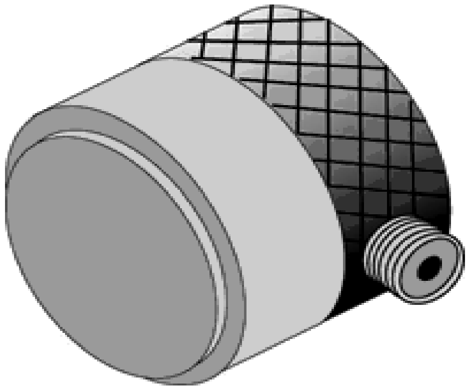

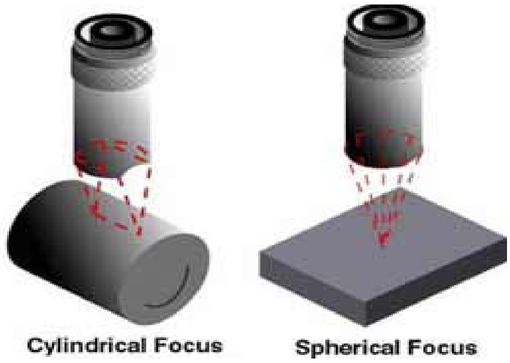

Fig. 2.13 Contact Transducer **Fig. 2.14 Immersion Transducer**

- **Immersion transducers** do not contact the component. These transducers are designed to operate in a liquid environment and all connections are watertight, as shown in **Fig. 2.14**. Immersion transducers usually have an impedance matching layer that helps to get more sound energy into the water and, in turn, into the component being inspected. Immersion transducers can be purchased with a planer cylindrically focused or spherically focused lens. A focused transducer can improve the sensitivity and axial resolution by concentrating the sound energy to a smaller area. Immersion transducers are typically used inside a water tank or as part of a squirter or bubbler system in scanning applications.

2.7 More on Contact Transducers

Contact transducers are available in a variety of specifications to improve their usefulness for a variety of applications. The flat contact transducer shown above is used in normal beam inspections of relatively flat surfaces, and where near surface resolution is not critical. If the surface is curved, a shoe that matches the curvature of the part may need to be added to the face of the transducer. If near surface resolution is important or if an angle beam inspection is needed, one of the special contact transducers described below might be used.

- **Dual element transducers** contain two independently operated elements in a single housing, as shown in **Fig. 2.15**. One of the elements transmits and the other receives the ultrasonic signal. Active elements can be chosen for their sending and receiving capabilities to provide a transducer with a cleaner signal, and transducers for special applications, such as the inspection of course grained material. Dual element transducers are especially well suited for making measurements in applications where reflectors are very near the transducer since this design eliminates the ring down effect that single-element transducers experience (when single-element transducers are operating in pulse echo mode, the element cannot start receiving reflected signals until the element has stopped ringing from its transmit function). Dual element transducers are very useful when making thickness measurements of thin materials and when inspecting for near surface defects. The two elements are angled towards each other to create a crossed-beam sound path in the test material.

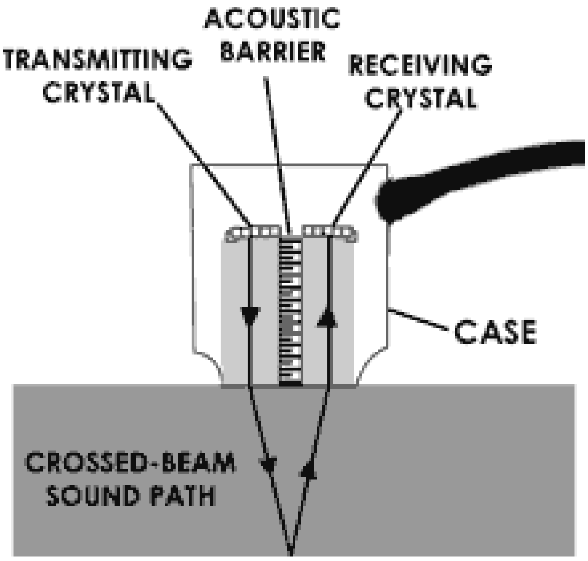

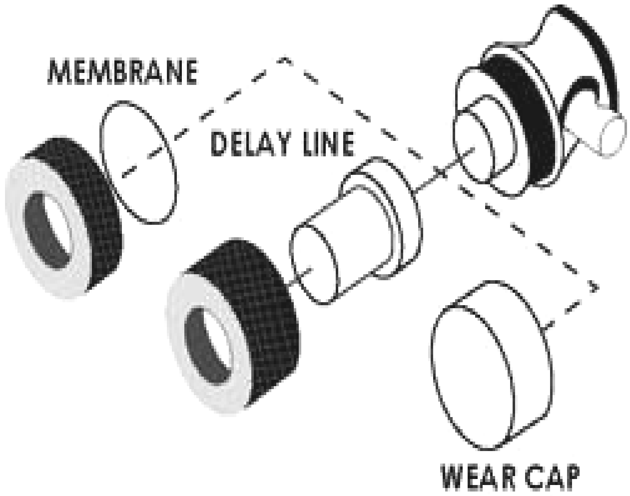

Fig. 2.15 Dual Element Transducers **Fig. 2.16 Delay Line Transducers**

Delay line transducers provide versatility with a variety of replaceable options. Removable delay line, surface conforming membrane, and protective wear cap options, as shown in **Fig. 2.16** can make a single transducer effective for a wide range of applications. As the name implies, the primary function of a delay line transducer is to introduce a time delay between the generation of the sound wave and the arrival of any reflected waves. This allows the transducer to complete its "sending" function before it starts its "listening" function so that near surface resolution is improved. They are designed for use in applications such as high precision thickness gauging of thin materials and de-lamination checks in composite materials. They are also useful in high-temperature measurement applications since the delay line provides some insulation to the piezoelectric element from the heat.

- **Angle beam transducers** and wedges are typically used to introduce a refracted shear wave into the test material. Transducers can be purchased in a variety of fixed angles or in adjustable versions where the user determines the angles of incidence and refraction. In the fixed angle versions, the angle of refraction that is marked on the transducer is only accurate for a particular material, which is usually steel. The angled sound path allows the sound beam to be reflected from the back wall to improve detect ability of flaws in and around welded areas. They are also used to generate surface waves for use in detecting defects on the surface of a component.

- **Normal incidence shear wave transducers** are unique because they allow the introduction of shear waves directly into a test piece without the use of an angle beam wedge. Careful design has enabled manufacturing of transducers with minimal longitudinal wave contamination. The ratio of the longitudinal to shear wave components is generally below -30dB.
- **Paint brush transducers** are used to scan wide areas. These long and narrow transducers are made up of an array of small crystals that are carefully matched to minimize variations in performance and maintain uniform sensitivity over the entire area of the transducer. Paint brush transducers make it possible to scan a larger area more rapidly for discontinuities. Smaller and more sensitive transducers are often then required to further define the details of a discontinuity.

2.8 Methods of Ultrasonic Testing

Ultrasonic energy striking at an interface of two different materials, either at normal or at inclined incidence, is partially reflected back or partially transmitted into the other medium. It is the transmitted part of energy which is utilized in inspection work. Depending on conditions of test and information required, a number of techniques are used for the ultrasonic inspection. Following are the three methods generally used:

1. Pulse Echo Method.
2. Through Transmission Method
3. Two transducer method
4. Resonance method

2.8.1 Pulse Echo Method

In the pulse-echo method, a piezoelectric transducer with its longitudinal axis located perpendicular to and mounted on or near the surface of the test material is used to transmit and receive ultrasonic energy, as shown in **Fig. 2.17**. The ultrasonic waves are reflected by the opposite face of the material or by discontinuities, layers, voids, or inclusions in the material, and received by the same transducer, where the reflected energy is converted into an electrical signal as shown in the Figure. The electrical signal is computer processed for display on a video monitor or TV screen. The display can show the relative thickness of the material, depth into the material where flaws are located, and (with proper scanning hardware and software), where the flaws are located in the X-Y plane

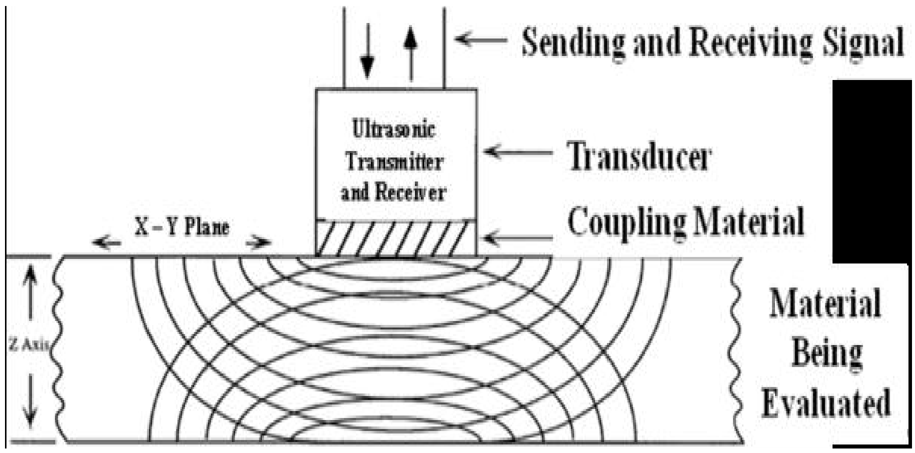

Fig. 2.17 Pulse Echo Method

2.8.2 Two Transducer Method

The pulse echo method can be used with either single or double crystal unit in single transducer unit the probe acts as both transmitter and receiver. In two transducer arrangement, one transmits and other receives the ultrasonic waves. These are placed on same side of specimen .pulse wave is send in to the specimen by the transducer T. And the echoes reflected from the back surface or any defect. Are received by the transducer R and displayed on the flaw detector screen. For specific applications like wall thickness measurement special type of transducers in which the transmitting and the receiving crystals are housed in a single unit are also used. These transducers are popularly known as “twin‟ or T-R probes.

2.8.3. Through Transmission Method

In the through-transmission method, an ultrasonic transmitter is used on one side of the material while a detector is placed on the opposite side as shown in the **Fig. 2.18**. One unit acts as transmitter and the other unit as receiver. The beam from the transmitter T travels through the material to its opposite surface where the receiving transducer R is placed. Scanning of the material using this method will result in the location of defects, flaws, and inclusions in the X-Y plane.

2.8.4 Resonance Method

The method uses resonance phenomenon to measure the material thickness or to determine the quality of bonding, in two materials. In a situation that the thickness of the material equals half the wavelength of the sound or it's multiple, resonance takes place. The frequency of the continuous longitudinal waves transmitted in the material is varied till standing waves are set up in the material.

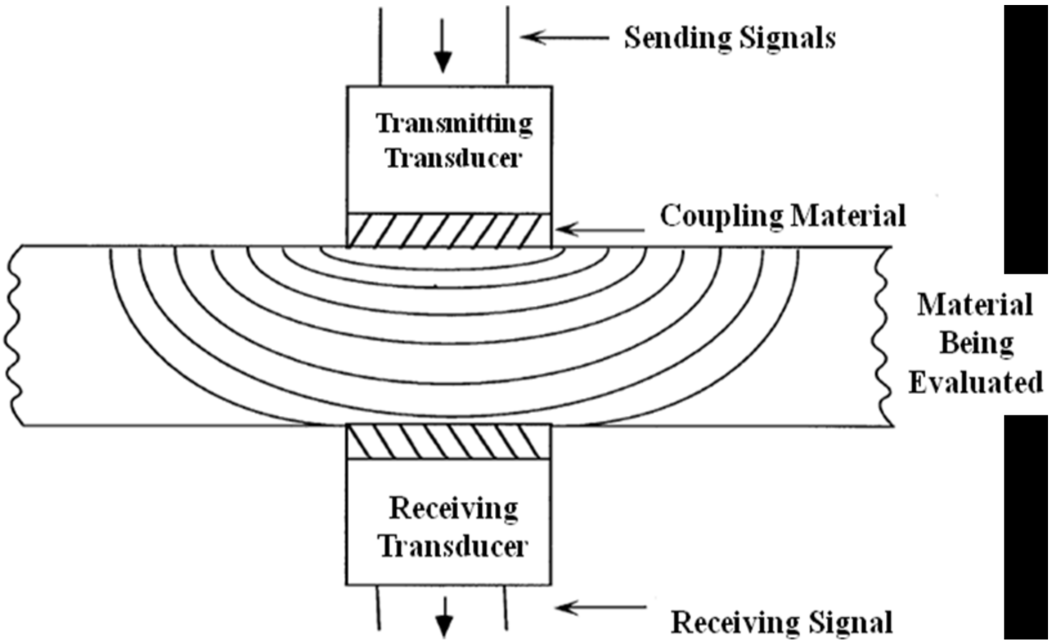

Fig. 2.18 Through Transmission Method

Presence of resonance is indicated by an increase in amplitude as the probe is moved and a change of resonant frequency is seen, which cannot be accounted for by a change in material thickness, if any, it is usually an indication of discontinuity.

From the above methods, Pulse Echo method is mostly used in Ultrasonic testing to find location of defect in specimen and Through Transmission is mostly used in testing using ultrasonic's to find the magnitude of the defect in Specimen.

2.9 Methods of Data Presentation

Ultrasonic data can be collected and displayed in a number of different formats. The three most common formats are known in the NDT world as **A-scan**, **B-scan** and **C-scan** presentations. Each presentation mode provides a different way of looking at and evaluating the region of material being inspected. Modern computerized ultrasonic scanning systems can display data in all three presentation forms simultaneously.

2.9.1 A-scan presentation

The **A-scan** presentation displays the amount of received ultrasonic energy as a function of time. The relative amount of received energy is plotted along the vertical axis and the elapsed time (which may be related to the sound energy travel time within the material) is displayed along the horizontal axis. Most instruments with an a-scan display allow the signal to be displayed in its natural radio frequency form (*rf*), as a fully rectified *rf* signal, or as either the positive or negative half of the *rf* signal. In the **A-scan** presentation, relative discontinuity size can be estimated by comparing the signal amplitude obtained from an unknown reflector to that from a known reflector. Reflector depth can be determined by the position of the signal on the horizontal sweep.

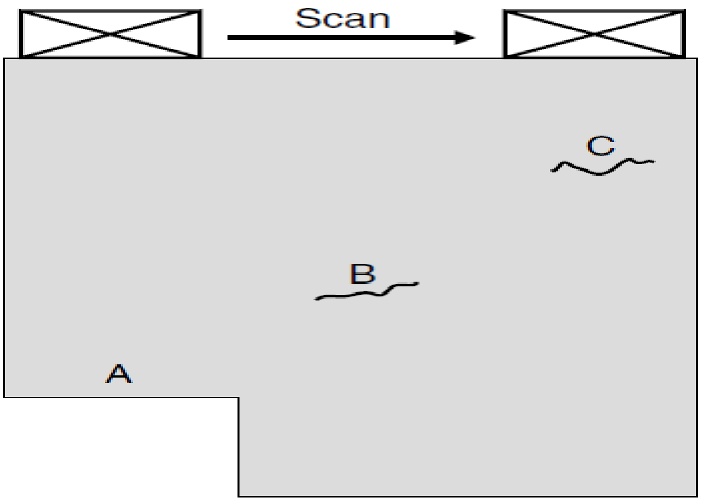

Fig. 2.19 Component for scanning

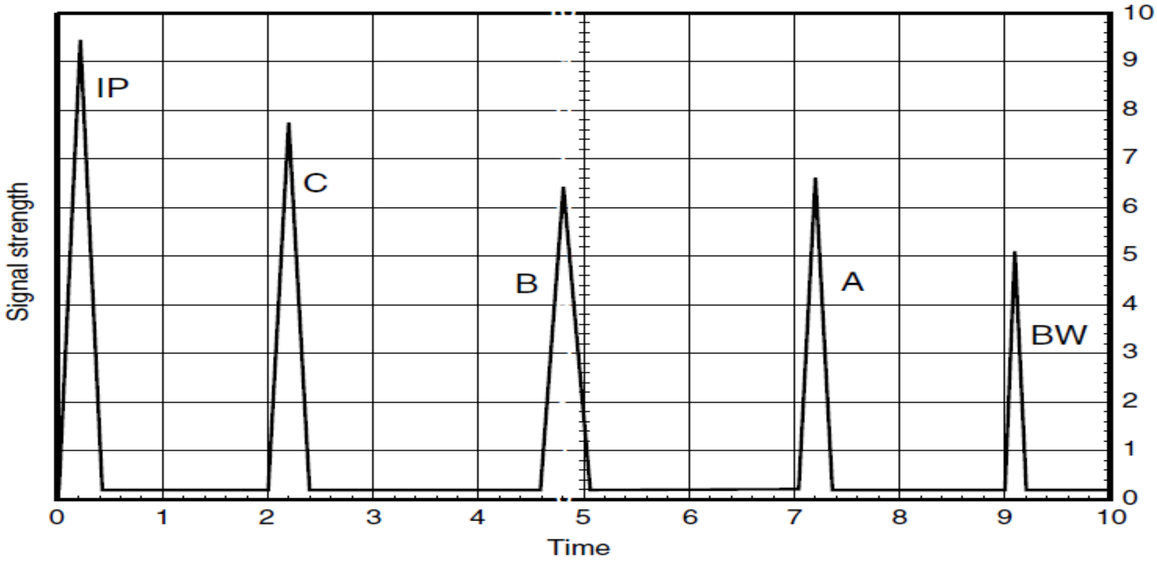

Fig. 2.20 A-scan presentation

For the component as shown in fig. 2.19, the A-scan presentation will be as shown in Fig. 2.20.In the **Fig. 2.20** of the **A-scan** presentation to the right, the initial pulse generated by the transducer is represented by the signal ***ip,*** which is near time zero. As the transducer is scanned along the surface of the part, four other signals are likely to appear at different times on the screen. When the transducer is in its far left position, only the ***ip*** signal and signal ***a***, the sound energy reflecting from surface ***a,*** will be seen on the trace. As the transducer is scanned to the right, a signal from the back wall ***bw*** will appear later in time, showing that the sound has travelled farther to reach this surface. When the transducer is over flaw ***b***, signal ***b*** will appear at a point on the time scale that is approximately halfway between the ***ip*** signal and the ***bw*** signal. Since the ***ip*** signal corresponds to the front surface of the material, this indicates that flaw ***b*** is about halfway between the front and back surfaces of the sample. When the transducer is moved over flaw ***c,*** signal ***c*** will appear earlier in time since the sound travel path is shorter and signal ***b*** will disappear since sound will no longer be reflecting from it.

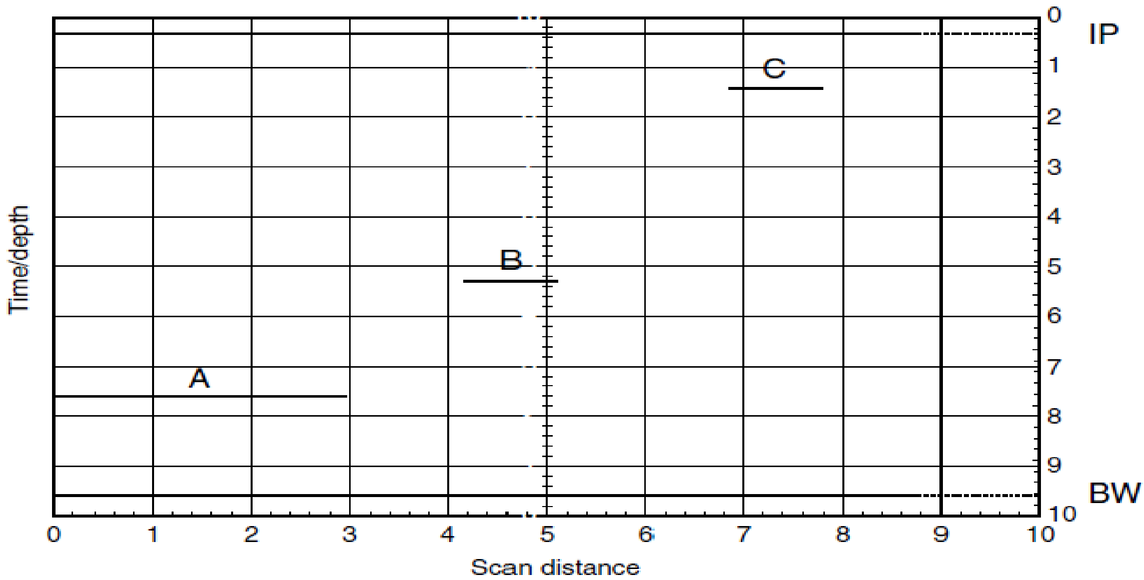

Fig. 2.21 B-scan presentation

2.9.2 B-scan presentation

The B-scan presentation is a profile (cross-sectional) view of the test specimen. In the B-scan, the time-of-flight (travel time) of the sound energy is displayed along the vertical axis and the linear position of the transducer is displayed along the horizontal axis. As shown in **Fig. 2.21** from the b-scan, the depth of the reflector and its approximate linear dimensions in the scan direction can be determined. The b-scan is typically produced by establishing a trigger gate on the a-scan. Whenever the signal intensity is great enough to trigger the gate, a point is produced on the b-scan. The gate is triggered by the sound reflecting from the back wall of the specimen and by smaller reflectors within the material. For the component as shown in Fig. 2.19, in the b-scan image, line “**a”** is produced as the transducer is scanned over the reduced thickness portion of the specimen. When the transducer moves to the right of this section, the back wall line “**bw”** is produced. When the transducer is on flaw **b** and **c** respectively, lines those are similar to the length of the flaws and at similar depths within the material are drawn on the b-scan. It should be noted that a limitation to this display technique is that reflectors may be masked by larger reflectors near the surface.

2.9.3 C-Scan presentation

The c-scan presentation provides a plan-type view of the location and size of test specimen features, as shown in **Fig. 2.22**. The plane of the image is parallel to the scan pattern of the transducer. **C-scan** presentations are produced with an automated data acquisition system, such as a computer controlled immersion scanning system. Typically, a data collection gate is established on the a-scan and the amplitude or the time-of-flight of the signal is recorded at regular intervals as the transducer is scanned over the test piece. The relative signal amplitude or the time-of-flight is displayed as a shade of grey or a colour for each of the positions where data was recorded. The c-scan presentation provides an image of the features that reflect and scatter the sound within and on the surfaces of the test piece.

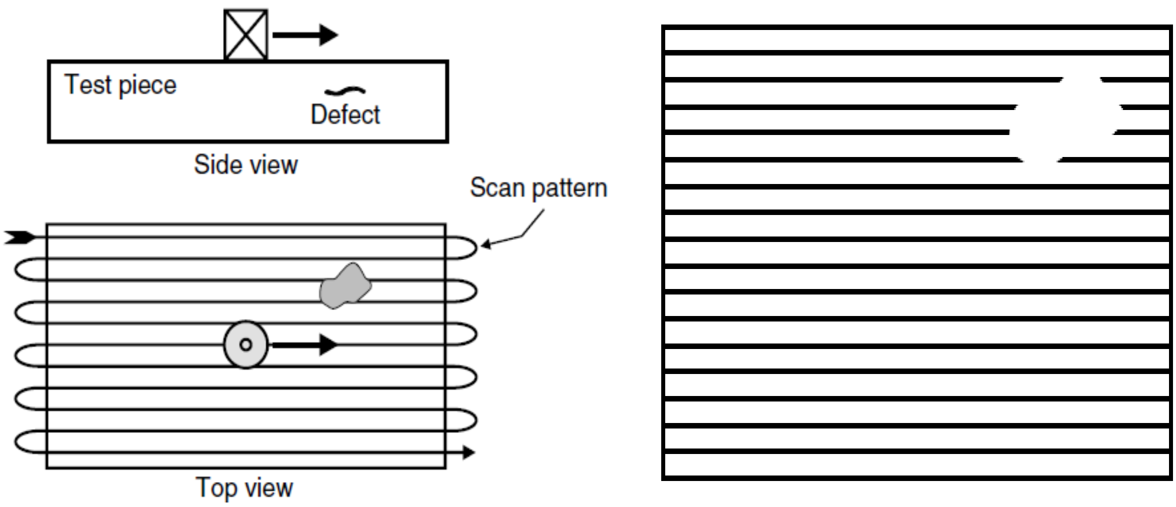

Fig. 2.22 C-Scan presentation

2.10 Probe Selection Parameters

The selection of probe suitable for a particular job is an important step before starting the work. The probe must comply with the conditions dictated by the material of the work piece, its shape and the test information requirements. This is naturally only possible provided that the basics of acoustics allow it.

2.10.1 Size of the Probe

The size or diameter of the active element has its own significance. Generally it is not considered important that a choice of diameter would also be helpful in several situations, a probe of any available diameter is accepted and used for the inspection.

A number of parameters are dependent on the diameter, e.g., near zone and beam profile etc. due to limitation of mode of vibration of the piezoelectric disc. It is always possible to choose any diameter for any desired frequency.

2.10.2 Contour Matching Soles

In the case of using contact method for the inspection of pipes, rods etc. having small diameter, the contact area between the job and probe can be very small. According to Bureau of Indian Standards, it is recommended that wherever the surface is curved and the curvature is of regular nature having a minimum radius of 225mm, it may be tested with flat face probe. If the surface is extremely smooth, standard flat face probe may be used on convex surface with a minimum radius of 50 mm and where it is concave with a minimum radius 300mm, flat face probe may be used. In all such cases the contact is not good resulting in heavy loss of energy. A small amount of sound energy is transmitted into the job. In such case it is helpful if the contact area is increased by providing the probe with a sole having a curvature matching with the curvature of the job. This Plano-concave sole can either be cylindrical or spherical depending on the job to be inspected. Such soles can be provided in the case of normal or angle beam probe.

2.10.3 Frequency

Frequency of probe plays an important role as it affects its testing capability in several ways. In practice, it is seen that in several situations the requirements are conflicting and a compromise is to be made between favourable and adverse effects to achieve the best possible choice of frequency. Sensitivity, resolution, penetration and beam spread are largely dependent of the probe and can be modified to an extent by chances in other parameters. Frequency selection requirements are:

(i) Penetration
(ii) Detect ability of small flaws.

Sound propagation in a medium depends on a number of factors such as absorption, scattering, diffraction effects and beam spreading. Their influence with relation to frequency selection for inspection becomes very important.

2.10.4 Grain Size and Flaw Size

Higher frequencies suffer higher attenuation of ultrasonic energy in the material. It s necessary to note the small reflector to be detected and the structure of the material while selecting the frequency. Coarse or large grain material can cause scatter and loss of reflected energy, particularly when the grain size and the wavelength are comparable. If the frequency is lowered to a point where the wavelength is considerably greater than the grain size, scattering losses are reduced but the sensitivity is also lowered.

CHAPTER 3

ULTRASONIC GUIDED WAVES

3.1 Introduction

On present day, many types of NDT techniques [10, 11] such as liquid penetrant technique, radiography , ultrasonics, eddy current, magnetic flux leakage, thermography etc. are available today, the elastic wave-based techniques have become the most popular for SHM applications. This is because crack initiation and propagation generate detectable sonic or ultrasonic waves. These waves can propagate at long distance through the structure under inspection and can be picked up by a sensor placed at another location. The received signal at the sensor can be analyzed in order to locate and estimate the degree of damage in the structure. Often the elastic waves that propagate from one point to another in the structure after being generated by the new crack formation or by a transducer are beyond our hearing range and are called ultrasonic waves.

3.2 Classification of Ultrasonic Waves

Ultrasonic waves can be classified in two types:

- Body waves or bulk waves
- Surface waves or guided waves.

Body waves propagate through a bulk material, hence attenuate, while the surface waves propagate along the surface of a body as shown in **Fig 3.1**.

Surface waves are often called guided waves because the geometry of the body guides them.

Advantages of using guided waves:

- Variable mode selection, by using various combinations of different striking angles and frequencies.
- Sensitivity to different type of flaws.
- Propagation to long distances.
- Guiding character, that enables them to follow curvature and hard to reach places.

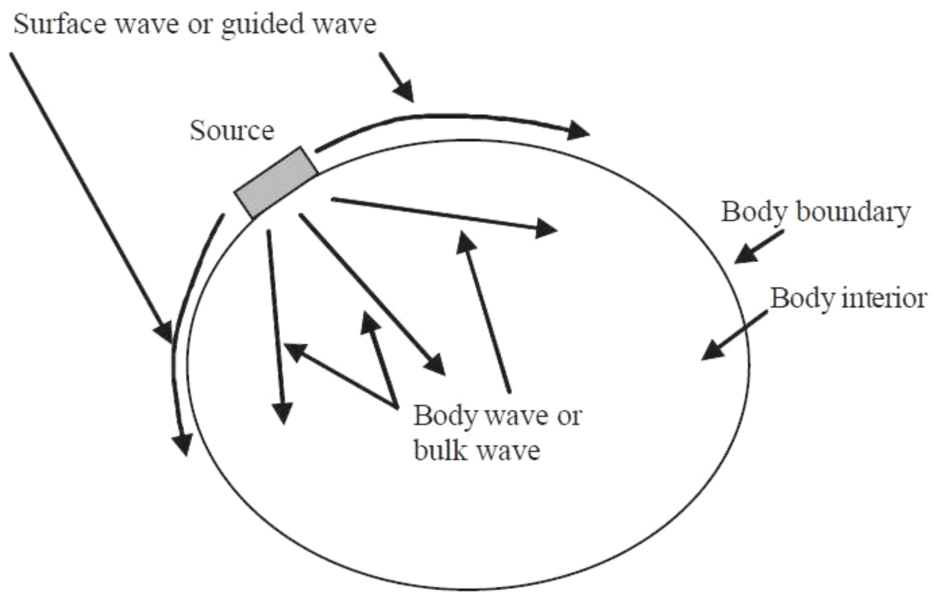

Fig. 3.1 Body waves and surface waves generated by an ultrasonic source

Guided waves can further be classified into following types, as shown in **Fig. 3.2**:

- Bar waves
- Cylindrical wave
- Rayleigh waves
- Lamb waves
- Rayleigh-Lamb waves

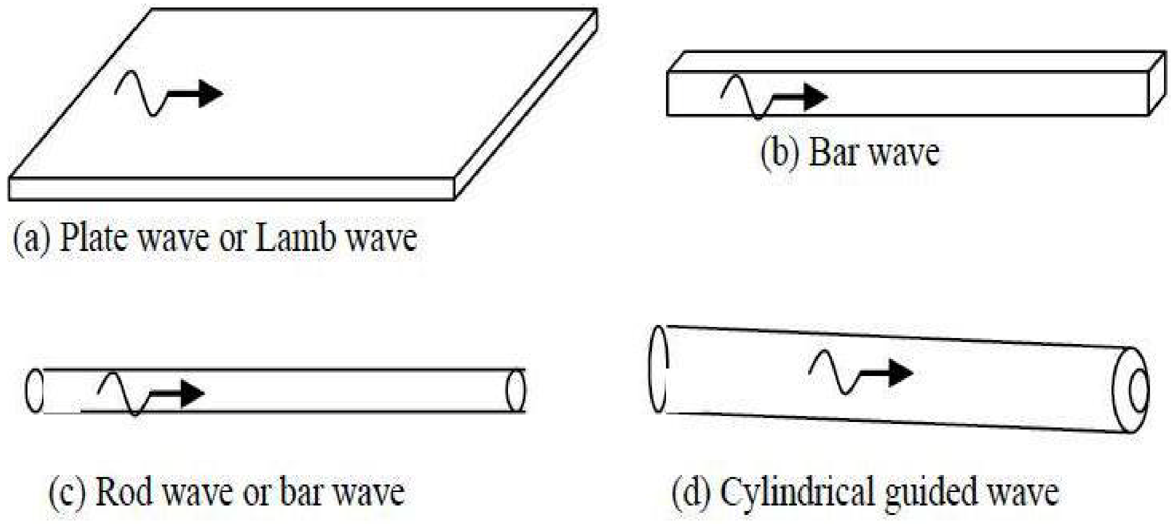

Fig 3.2 Different types of guided waves in various problem geometries

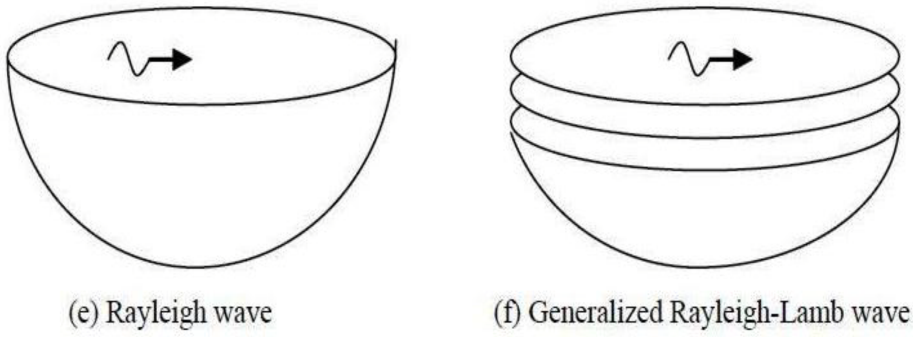

Fig 3.2 Different types of guided waves in various problem geometries

Cylindrical Guided Waves: Elastic waves propagating through a hollow cylinder or pipe are called cylindrical guided waves (**Fig. 3.2(d))**. Since for a cylinder the two stress-free surfaces- inner and outer surfaces – are parallel to each other as in a plate, sometimes the cylindrical guided waves are also called Lamb waves.

Bar waves: When guided waves propagate through a rod or bar they are known as bar waves (**Fig. 3.2(c))**.

Rayleigh wave: If the structure is a homogenous half-space then the guided wave propagating along the surface of the half-space is called Rayleigh wave (**Fig. 3.2(e))**.

Lamb waves: Waves propagating through a plate type structure with two parallel stress-free boundaries are known as Lamb waves, again named after its inventor. Lamb waves are also known as plate waves because they propagate through plates (**Fig. 3.2(a))**.

Rayleigh-Lamb waves: Waves propagating parallel to the free surface of a multilayered solid half-space are known as generalized Rayleigh-Lamb waves or simply Rayleigh waves (**Fig. 3.2(f))**.

3.3 Ultrasonic Guided Waves in Plated Structures

Guided waves are waves whose propagation characters depend on structural geometries, such as plates, rods, pipes, etc. These waves are generated by impinging the plate obliquely with a piezoelectric transducer.

The ultrasonic waves propagate in two ways:

- Longitudinal ultrasonic wave (L): displacement of particles is parallel with the energy transport direction,

- Shear ultrasonic wave (S): displacement occurs in the direction perpendicular to energy transport.

Shear wave, can further propagate in two modes **(Fig 3.3)**:

- Shear horizontal wave (SH): displacement describes in the direction parallel to plate surface.
- Shear vertical wave (SV): displacement occurs in the direction perpendicular to the plate surface.

In a thin plate (up to a few wavelengths thick), longitudinal wave are polarized in the direction perpendicular to the surface and SV wave formed and combined with L wave. These combined SV+L is known as lamb wave. In an isotropic plate, lamb waves are either symmetric (Si) or anti symmetric (Ai), where i is order of mode. The symmetric modes associate with a Compressional rarefaction expansion of the plate and anti symmetric modes associated with a flexural propagation. Lamb wave have a dispersive nature and its phase and group velocities not only depend on the material characterization but also depend on the thickness, frequency and lamb wave mode.

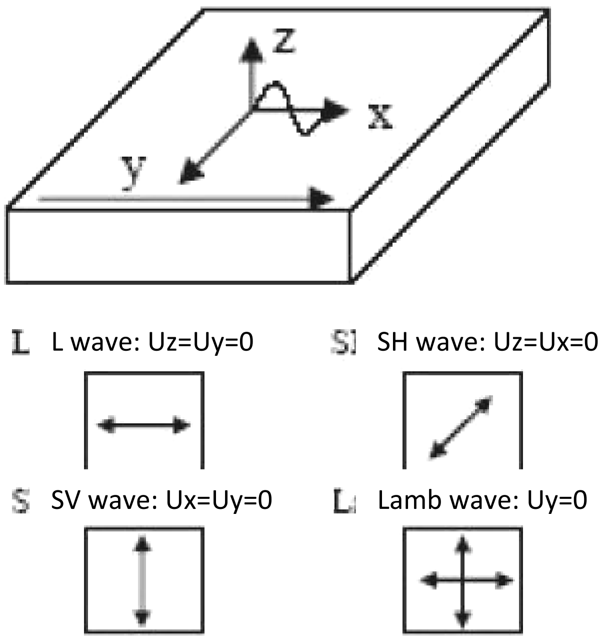

Fig. 3.3 Various Modes of Shear Waves

The resulting refection and refraction at the interfaces produces many new signal packets. If angle of incidence and frequency is adjusted properly, the reflected and refracted energy within the plate will constructively interfere and form a plate wave.

To use lamb waves for defect detection in plated structures, knowledge of the lamb modes is must for detecting the defects at specific depth. To study the modes, Detri et al. [12] studied the energy distribution inside a plate for different lamb modes and related the energy distribution curve to defect detection capabilities of different lamb modes. It is proved that both symmetric and anti symmetric modes have maximum energy flow rate at the central plane of the plate.

3.4 Dispersion Effect in Plates

This phenomenon of the wave speed dependence on the frequency is called dispersion phenomenon and these waves are called dispersive waves. The Lamb wave speed is not only dispersive but also multi-valued. At a given frequency multiple values of the wave speed are obtained for these waves. Different wave speeds correspond to different modes of the propagating Lamb wave. Such multiple modes do not exist for the longitudinal wave, shear wave [13].

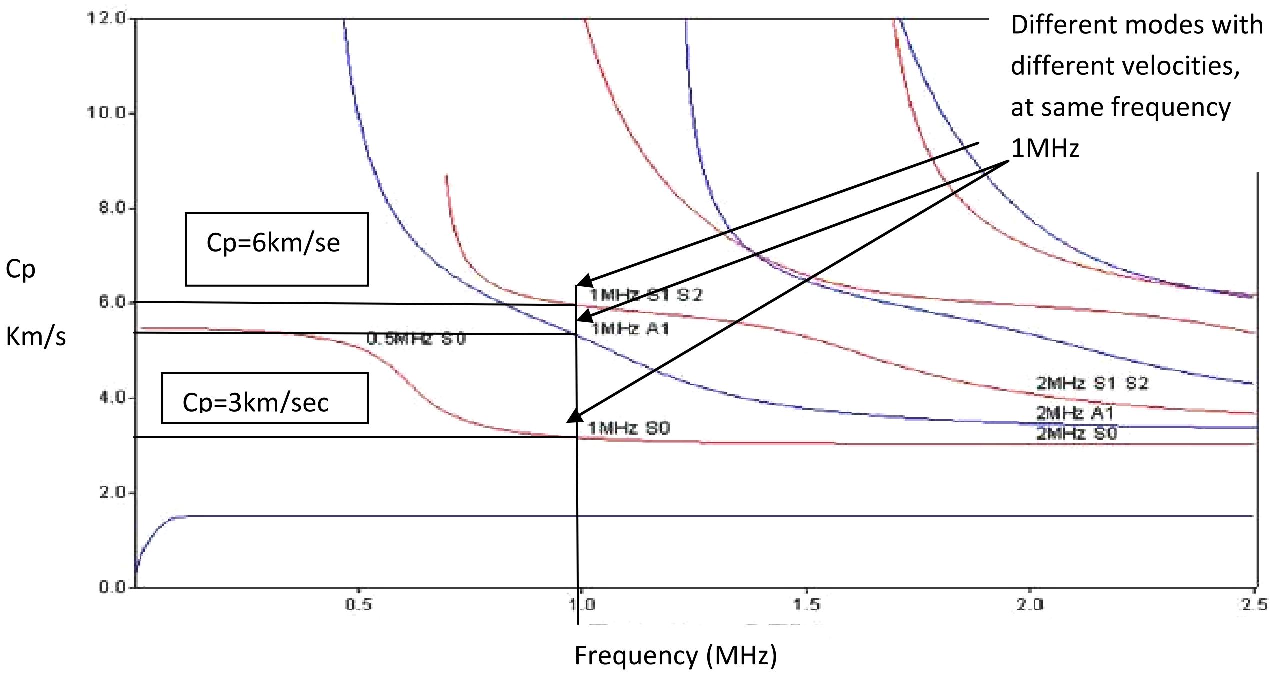

Fig. 3.4 Dispersion curves for Lamb wave propagation in a 4 mm steel plate, immersed in water

For example, in the **Fig 3.4**, at the particular frequency e.g. 1MHz, the dispersion curve shows the existence of four modes (S_0, A_1, S_1 and S_2, where S1 and S2 are overlapped) propagating through the plate, of which S_0, S_1 and S_2 are symmetric modes and A_1 is anti-symmetric mode.

At the given frequency, the velocity of mode S_0 is 3 km/s, mode S_1-S_2 is 6km/s and A_1 is 5.5 km/s

The particular mode at 1MHz frequency can be obtained by varying the striking angle, calculated by Snell's law i.e. for S1 mode, the phase velocity is 6km/s, so the striking angle (A_1) for S_1 mode at 1MHz is calculated as follows by Snell's law:

Let the angle required is $A_{1,}$

$$\frac{\sin A_1}{C_1} = \frac{\sin 90}{C_2}$$

C_1 is velocity of lamb wave in water (1.5 km/sec).

C_2 is phase velocity of lamb wave in Steel (6 km/sec)

$$A_1 = \sin^{-1}\frac{C_1}{C_2}$$

$$A_1 = \sin^{-1}\frac{1.5}{6}$$

$$A_1 = 14.7^{o}$$

So at an angle of 14.7^{o} (of both transmitter and receiver) at 1MHz, we get S_1 mode

The dispersion curves of Lamb wave modes could be obtained by solving wave equation with boundary conditions. For the traction free boundary conditions at the surface of plate, the frequency equations are [14]

$$\frac{\tan(\beta d/2)}{\tan \alpha d/2} = -\frac{4\alpha\beta k^2}{(k^2-\beta^2)^2} \qquad \ldots 3.1$$

$$\frac{\tan(\beta d/2)}{\tan \alpha d/2} = -\frac{(k^2-\beta^2)^2}{4\alpha\beta k^2} \qquad \ldots 3.2$$

Where

$$\alpha^2 = \frac{\omega^2}{c_l^2} - k^2$$

$$\beta^2 = \frac{\omega^2}{c_t^2} - k^2$$

c_l= longitudinal wave velocity in steel plate (5670 m/s),

c_t= shear wave velocity in steel plate (3136m/s),

ω is angular frequency

k is the wave number

d is plate thickness

Eq. 3.1 and Eq. 3.2 could calculate anti symmetric (A) and symmetric(S) modes respectively.

The modes can be represented in phase velocity Cp versus frequency (f) that is dispersion curves shown in **Fig 3.4.**

Phase velocity C_p = fλ and

The Group Velocity C_g = dω/dk,

Can be calculated as functions of d/λ

Phase velocity could be controlled by the angle of incident so that the phased velocity dispersion curves could be used to find the excitation conditions, such as frequency and angle of incident, of a desired mode [15].

Group velocity indicate the wave propagation velocity so that it is possible to predict the wave propagation velocity of an excited mode under certain excitation conditions obtained from phased velocity dispersion curves.

3.5 Mode Selection

Since there are infinite Lamb wave modes in a steel plate at a given frequency, it is necessary to select a proper mode for the experimental purpose. Mode selection could be performed by two-dimensional tuning, that is frequency and phase velocity tuning.

In this case, the phase velocity is continuously controlled by variable angle setting, so that the phased velocity tuning could be performed by incident angle tuning. **Fig 3.5** shows the frequency tuning results for the fixed incident angle of 30 degrees. The pulse-echo signals indicated by arrows were reflected from 380mm away free edge of the steel plate. Frequency was swept from 650 kHz to 1000 kHz. In case of 840 kHz shown in Fig 2.4 (c), the strongest signal was received and the wave form was compact [16].

Fig 3.6 shows the effect of incident angle for the fixed frequency of 840 kHz. For the incident angle of 25 degrees, a tiny amount of energy was received as shown in **Fig 3.6 (a).** The result was same for the angle between 0 and 25 degrees. For the angle between 30 and 37 degrees, the results were very close to **Fig3.6 (b)** that was the result for the incident angle of

35 degrees. There was no signal received for the angle between 40 and 70 degrees. For 85 degrees, there was a signal received as shown in **Fig 3.6(c).**

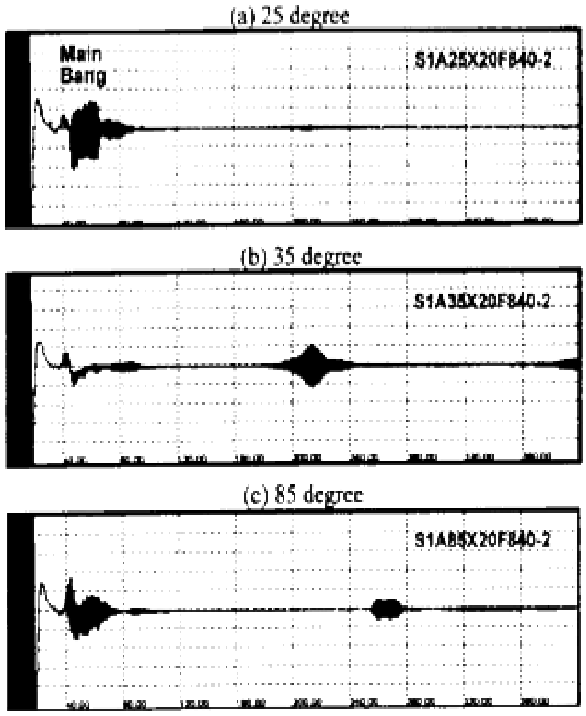

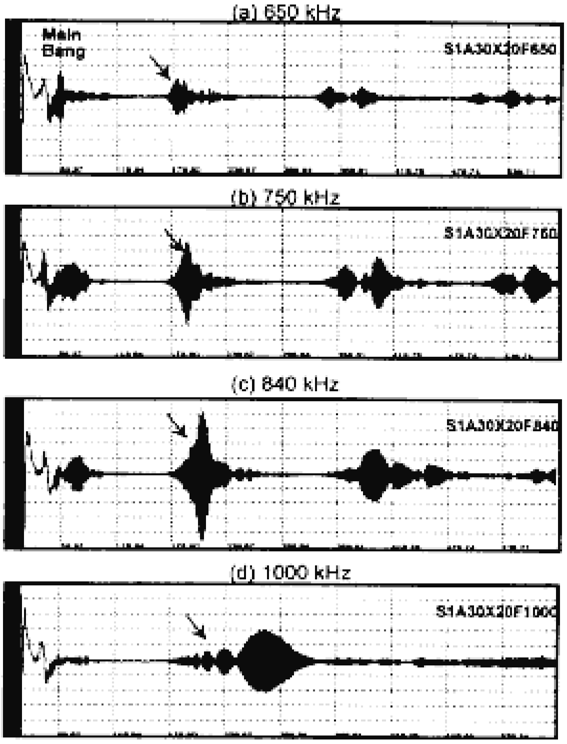

Fig. 3.5 Effects of tuning ultrasonic on Frequency On wave reflection

fig. 3.6 Effects of tuning incident angle the generation of Lamb waves

3.6 The Zero-Order Modes

The symmetrical and anti-symmetric zero-order modes are very important; as they are the only modes that exist over the entire frequency spectrum from zero to indefinitely high frequencies. In the low frequency range (i.e. when the wavelength is greater than the plate thickness) these modes are often called the “extensional mode” and the “flexural mode" respectively, terms that describe the nature of the motion and the elastic stiffness that govern the velocities of propagation. The elliptical particle motion is mainly in the plane of the plate for the symmetrical, extensional mode and perpendicular to the plane of the plate for the anti-symmetric, flexural mode. These characteristics change at higher frequencies.

These two modes are the most important because (a) they exist at all frequencies and (b) in most practical situations they carry more energy than the higher-order modes.

The zero-order symmetrical mode (S_0) travels at the "plate velocity" in the low-frequency regime where it is properly called the "extensional mode". In this regime the plate stretches in the direction of propagation and contracts correspondingly in the thickness direction. As the frequency increases and the wavelength become comparable with the plate thickness, curving of the plate starts to have a significant influence on its effective stiffness. The phase velocity drops smoothly while the group velocity drops somewhat precipitously towards a minimum.

The zero-order anti-symmetric mode (A_0) is highly dispersive in the low frequency regime where it is properly called the "flexural mode". For very low frequencies the phase and group velocities are both proportional to the square root of the frequency; the group velocity is twice the phase velocity. This simple relationship is a consequence of the stiffness/thickness relationship for thin plates in bending. At higher frequencies where the wavelength is no longer much greater than the plate thickness, these relationships break down. The phase velocity rises less and less quickly and converges towards the Rayleigh wave velocity in the high frequency limit.

The group velocity passes through a maximum, a little faster than the shear wave velocity, when the wavelength is approximately equal to the plate thickness. It then converges, from above; to the Rayleigh wave velocity in the high frequency limit.

In experiments that allow both symmetric and anti-symmetric modes to be excited and detected, the symmetric mode often appears as a higher-velocity, lower-amplitude precursor to the anti- symmetric mode. The anti-symmetric mode is the more easily excited of the two, and often carries most of the energy [17].

CHAPTER 4

LITERATURE REVIEW

One of the most commonly used NDT techniques is Ultrasonic Testing, utilizing guided waves. This chapter presents a review of literature on utilization of ultrasonic guided waves for damage defection in plated structures. This gives an idea of study carried out in this area up to this stage.

Junker et al (1992) [18] developed a device and method for guided testing of an object, and in particular, an internal structural component in an object, using non-destructive ultrasonic techniques is provided. A housing containing at least one ultrasonic transducer probe is adapted to be placed directly on the surface of the object to be tested. Eddy current probes are provided in the housing to guide the ultrasonic probe such that the ultrasonic energy will be directed at the appropriate internal structural design component of the object to be inspected. A microcomputer is then used to record the data obtained using ultrasonic signals and the position on the object using the information designed from the eddy current probes.

Cawley et al (1992) [19] discusses the selection of the appropriate mode and frequency range for different inspection requirements and reviews the possible methods of excitation, response measurement and signal processing. It is usually desirable to transmit a single, non-dispersive mode, and excitation methods to achieve this are discussed. A variety of signal processing techniques from simple time domain to relatively complex two-dimensional Fourier analysis are available. Time domain processing can often be applied satisfactorily in low frequency-thickness regions where only two modes can propagate, but tends to be unreliable above the cut-off frequency of the a_1 mode. As an example of the design of a Lamb wave testing regime, a set of tests on a butt-welded steel plate with simulated weld defects of different depths is described. It was observed that by operating below the a_1 cut-off frequency with judicious selection of testing technique, the presence of defects can be detected reliably from changes in the shape of the received waveform.

Cawley et al (1996) [20] discusses the selection of an appropriate mode and its excitation and reception. Lamb waves are very attractive for the quick inspection of large structures because they can propagate long distances along plates and shells. The chief drawback of

Lamb wave inspection is that at least two modes exist at all frequencies and the modes are generally dispersive, which means that the received signals can be very complicated. As a result, the potential advantages of Lamb wave inspection have seldom been realized in practice. The key to the successful application of Lamb waves is the excitation of a single mode in a non-dispersive region. Examples of the use of Lamb waves for the detection of delamination in composite materials and corrosion in pipes are then given.

Kundu et al (1997) [21] describes an investigation on the Lamb wave propagation through a two-layered glass plate with different interface conditions between the layers is carried out to study the effectiveness of Lamb waves in detecting defects at the interface as well as estimating the interface strength. To this end the stress field inside the two layered plate is theoretically calculated for different interface conditions and for a number of propagating Lamb modes. It is observed that, for every Lamb mode, the stress field inside the plate varies significantly with depth. Symmetric modes generate maximum normal stress and zero shear stress at the central plane; the situation is reversed for the anti-symmetric modes. It is found that the Lamb modes which produce large shear stress at the interface position are most sensitive to the shear stiffness of the interface. Void and delamination type defects that releases the interface stress affect those Lamb modes most significantly which produce high stress at the interface position.

Rose et al, (1997) [22] described that guided waves improved efficiency, sensitivity and choice of mode to be used. Depending on the frequency, plate thickness and mode selected, the particle motion distribution through the thickness of the plate can be varied to increase the sensitivity to different defects. As a result of edge reflection studies, it is known fact that a guided wave scattering problem can show different mode conversions depending on incident mode, frequency, and reflector geometry. This means a defect shape change can provide a variety of scattering patterns even under identical incident modes and frequency. Similarly, each guided wave mode on the dispersion curve can interact differently even with the same defect shape.

Chimentia et al (1997) [23] examined the behaviour of guided elastic waves in the presence of rough surfaces. These investigations lead to a broader understanding of the phenomenon of rough-surface interactions with elastic guided waves. Extensive measurements in immersion, contact mode, and with a knife-edge coupler demonstrate the wide range of physical behaviour of elastic guided waves and their dependence on the condition of the guiding surfaces. Author configured experimental conditions to maximize the rough-surface damping contrast, by measuring below and above the Compressional critical angle.

Kundu et al (1998) [24] discusses about closed cracks under compressive normal stresses that are difficult to detect by the conventional ultrasonic techniques. When the crack surfaces stay in very close contact with each other then the bond between the two surfaces of the crack is called a ‘kissing bond’. Catastrophic failures can result if the system is subjected to crack opening normal stresses or shear stresses. When the crack surfaces are smooth then kissing bonds cannot transmit shear stress very well but can carry compressive normal stress, these bonds are called ‘slip bonds’. Conventional P-wave scans (C-scan or A-scan) are based on the assumptions that P-waves are reflected by the defective interface. However, an interface subjected to a large compressive stress cannot reflect P-waves effectively; hence these bonds remain invisible to the conventional P-wave based C-scan or A-scan techniques. In this paper it is shown that the kissing bonds can be effectively detected by some leaky Lamb mode. Theoretical and experimental results are presented to show that using the Lamb waves is an effective way of detecting kissing bonds.

Kundu et al. (1998) [25] has studied the lamb wave propagation in large plates and its use in internal defect detection. The lamb wave modes which are most efficient for detecting different types of defects are identified. Stress fields inside the plate for different modes of lamb waves are computed. From these stress plots, the most efficient mode for detecting the particular types of defect can be identified.

Rose et al. (2000) [26] carried out an experimental investigation to establish a technical concept for detection of defects in thin steel plates. The goal was to find the most efficient testing parameters, in context to relationship between excitation frequency of tone burst and various incident angles.

Kundu et al. (2001) [27] has investigated the difficulties in detection of internal defects in mirror symmetric composite plates using lamb wave modes. In a symmetrically layered composite plate stress, displacement magnitudes and energy distribution profiles for all lamb modes are symmetric about central plane of the plate. As a result, ability of lamb mode to detect a defect in corresponding layer of mirror symmetry. Hence form lamb wave image generated, it is difficult to distinguish between the defects in two layers of mirror symmetry. The authors discuss to solve the problem by fine tuning of frequency used and striking angle of incident beam.

Rose (2002) [28] studied that the major difference between bulk wave propagation and guided wave propagation is that a boundary is required for guided wave propagation. As a result of a boundary along a thin plate or interface, variety of different waves is reflected and mode converting inside a structure and superimposes with areas of constructive and destructive interference that finally leads to the guided wave packets that can travel in the structure. As a result of refraction at the interface, a variety of different waves can propagate in the structure.

Worden et al. (2002) [29] states that a practical complication of Lamb wave inspection mainly lies in the propagation characteristics of the elastic waves. The propagation is typically characterized by the product of the wave frequency and the sample thickness, or frequency-thickness product (FT). For a low value of this parameter (typically less than 1 MHz-mm in aluminium media), only the fundamental symmetric, S_0, and anti-symmetric, A_0, modes can propagate. As the FT product increases, so does the number of allowed modes. However, these higher modes have widely different phase velocities and often experience considerable phase-velocity dispersion as a function of the FT value. Note that damage diagnosis is much simplified if a known single mode of the Lamb waves is generated over a non dispersive region of the FT product.

Lindenb et al (2003) [30] describes about the online monitoring of fatigue cracks using ultrasonic waves. Most of the currently available non-destructive testing methods are off-line, i.e. The operational loading and the inspection are considered as two distinct stages. In this article, an experimental methodology based on ultrasonic surface waves is developed to continuously inspect a structure during its operation. The proposed method uses spectral information of transmitted surface waves at several working points of the operational load. Simple statistical indicators of the transmitted wave energy during loading are introduced in order to be able to monitor the structural health on-line. As a validation experiment, a propagating fatigue crack in a sinusoidal loaded beam is considered.

Rose et al (2003) [31] discusses that a microprocessor, when utilized in connection with an ultrasonic flaw detector, can reliably regulate an ultrasonic inspection process. By means of several concentrated laboratory trials and accompanying analysis with the microprocessor-flaw detector combination, it was demonstrated that dependable, speedy, and cost-effective flaw detection is within the realm of reality. Specifically, this particular study focuses on the microprocessor controlled evaluation of steel plates. While it is true that the overall procedure employed here involves itself with flaw classification in one area (welds in steel plates), it will become apparent that applications are not restricted to steel plates.

Cawley et al (2004) [32] studied the efficient monitoring of the structural integrity of large areas of such structures from a single monitoring location can be achieved using a guided ultrasonic waves array. Guided waves have stress distributed through the thickness of the structure and can propagate over large distances [25]. In this paper the array design and operation are described briefly. The guided wave array consists of a ring of 32 piezoelectric transducer elements, equally spaced on a diameter of 70 mm. Each transducer element consists of a PZT disc and backing mass. Measurements were performed on a 5 mm thick steel plate with a variety of machined defects to simulate corrosion damage.

Movafeghi et al (2005)[33] stated that the biggest difficulty of lamb wave inspection is the dispersive nature of lamb wave and its multimode propagation and so need to signal processing as well as experienced operators. The author evaluates the defects in thin Aluminium plates. For this; two lamb wave testing techniques (pulse-echo and emission), with different lamb modes as transmitter and receiver, have been used and the sensitivity of these methods has been compared with each other. The symmetric modes associate with a Compressional rarefaction expansion of the plate and anti-symmetric modes associated with a flexural propagation.

Edalati et al. (2005) [34] studied the dispersion and displacement curves of ultrasonic lamb wave, propagated in Aluminium thin plates. Two ultrasonic lamb wave techniques, pulse-echo (a1 mode as emitter) and emission (s1 mode as emitter), were used for interpretation of notch defects with depths of 10%, 30% and 60% of plate thickness. Thickness of plate was 2 mm and the nominal centre frequency of transducers was 2 MHz It was observed that these techniques are sensitive to evaluate defects, especially in short probe to defect distances. Amplitude analysis gives qualitative and quantitative information about defects depth.

Fromme et al. (2006)[35] explained Guided ultrasonic waves can propagate over large distances in thin structures like the hull plates of a ship and allow for efficient non-destructive testing of such structures with limited access. The sensitivity of guided ultrasonic wave inspection and monitoring for damage detection close to structural features, e.g., stiffeners, in plate like structures, has been investigated in a two dimensional Finite Element Model (FEM). The combined interaction of the guided ultrasonic waves with defects and structural features in large structures has been modelled numerically to predict and improve the sensitivity and reliability of damage detection.

Rose et al (2006) [36] discusses**,** theoretical and experimental issues of acquiring dispersion curves for bars of arbitrary cross-section are discussed. Since a guided wave can propagate over long distances in a structure, guided waves have great potential for being applied to the rapid non-destructive evaluation of large structures such as rails in the railroad industry. Such fundamental data as phase velocity, group velocity, and wave structure for each guided wave mode is presented for structures with complicated cross-sectional geometries as rail. Phase velocity and group velocity dispersion curves are obtained for bars with an arbitrary cross-section using a semi-analytical finite element method. Since a large number of propagating modes with close phase velocities exist, dispersion curves consisting of only dominant modes are obtained by calculating the displacement at a received point for each mode.

Balasubramaniam et al (2007) [37] discuss about the non-dispersive propagation of ultrasonic guided wave higher order modes travelling along the circumferential direction in a hollow cylinder and its interaction with defects in pipe support regions. These circumferential guided waves were generated in mild steel pipe specimens containing artificially created axial notches (simulating axial cracks) and pinholes (simulating pinhole-like defects) of different sizes in order to simulate conditions such as cracking and corrosion under pipe supports. The characteristics of these guided waves were also studied as a function of parameters related to how they were generated. These higher frequency modes were explored for their ability to detect and size defects. The defect position along the circumference was ascertained from the time of flight while the defect size was estimated using the amplitude data.

Zoofan et al (2007) [38] discuss about the sizing and locating of internal defects in fatigue samples. For the monitoring of crack initiation and evolution ultrasonic Lamb waves are excited and acquired in the sample continuously during fatigue tests at different levels of fatigue load using a high-speed data acquisition system. The cracks were localized and sized using the vertical C-scanning technique (VC-scan). The scanned ultrasonic images were compared with micro radiographic images and were found to be in good agreement. Data fusion from three NDE techniques enables one to determine the initiation times, shapes, orientations and sizes of fatigue cracks.

Kundu et al (2007) [**39**] in this paper, the DPSM method is extended to model the ultrasonic field generated in a homogeneous isotropic solid plate immersed in a fluid. The objective of this study is to model the generation of guided waves in a solid plate when ultrasonic beams from transducers of finite dimension strike the plate at different critical angles. DPSM results for a solid half-space problem are compared with the finite element predictions to show the superiority of the DPSM technique. The predicted results are also compared with the experimental visualization of the mode patterns of Lamb waves propagating in a glass plate obtained from stroboscopic photo- elastic method. The DPSM technique is applied to study the mode patterns in aluminium plates immersed in water.

CHAPTER 5

DAMAGE DETECTION IN PLATES- AN EXPERIMENTAL STUDY

Damage detection has been an important area of concern in the design, operation, maintenance and repair of many military, industrial and civil structures and equipment involving plate structures, submerged in water. Current chapter discusses the experimental set up and methodology for using ultrasonics to monitor damage in the plates utilizing Lamb Waves which subsequently would be made incident on the submerged specimens, with some inherent irregularities, at varying critical angles. The reflected /scattered signals would be received at particular angles. The variations in the signals received lead one to identify, locate and evaluate damage and determine the residual life of the subject plate specimens.

5.1 Selection of Lamb Wave Modes

The key problem associated with the quantitative measurement of the characteristics of propagating Lamb modes is that more than one mode exists at any given frequency, as discussed in Chapter 3, section 3.4. Excitation with transducers of finite dimensions inevitably means that all the modes possible at any particular frequency of excitation are produced and are present. So it is not possible to separate the modes simply by transforming from the time domain to the frequency domain. Also, since the excitation will not be single frequency, dispersion will also be present leading to complicated time domain signal. Therefore, the time history of the response of the plate has been usually multi-mode and dispersive.

In such cases the shape of the lamb wave packet has been strongly dependent on propagation distance. When the wave hits the interface different modes are generated with different velocities and energy. Each mode can be separately excited in the plate using SNELL’S law. Since velocity of each mode for each frequency will be different, by using SNELL’S law required mode can be excited. Dispersion curves have been generated to find the velocity of any particular mode by using DISPERSE software as shown in Fig. 3.4., and thereafter, by using SNELL’S law, as shown in section 3.4, required angles to excite a particular mode can be excited.

After calculating the angle of incidence for the particular mode, the transducers are arranged as shown in Fig. 5.1.

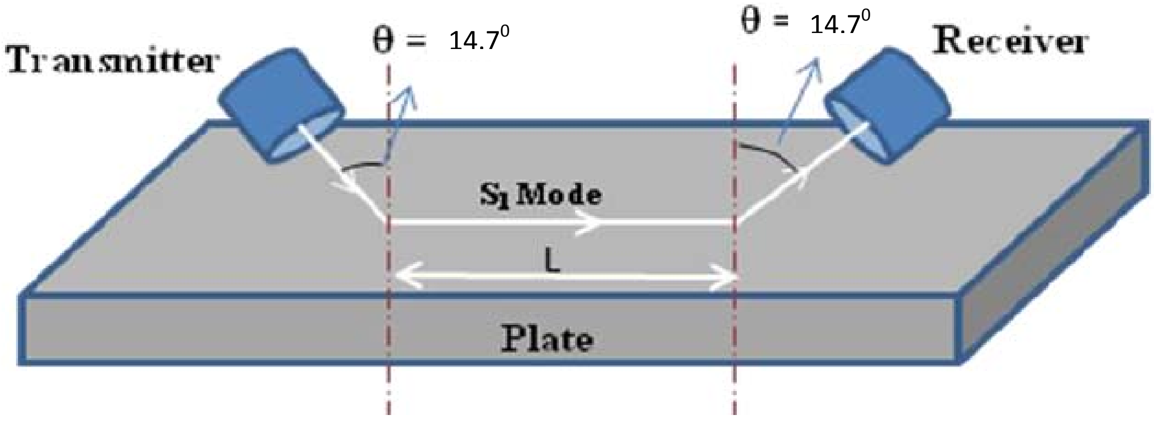

Fig. 5.1 Transducers arranged at an angle to the plate

5.2 Experimental Setup

The experimental setup consists of pulser/receiver which generates the pulse for every given time interval. The pulse generated has been sent to the transducer which transfers the pulse to an ultrasonic wave. Transmitter transducer has been in contact with the plate through the couplant and the other end the receiver transducer has been also arranged in the same way. Since the testing has been carried out in water, so water acts as a natural couplant .This transducer has been connected back to the pulser/receiver, sends the signals to the digitizer card which has been connected to computer hardware.

Driven by the pulser/receiver, the compressional transducer generates ultrasonic pulse that propagates through the plate in the form of longitudinal waves. When there is an interface such as a crack, void or flaw in the wave path, part of the energy is reflected back from the interface and received by the same transmitting transducer. The reflected energy has been converted into an electrical signal which has been processed in a computer and digitized for display.

Pulse echo and through transmission methods are used for characterizing the damage. The presence of the defect and extent of damage can be ascertained by through transmission. However pulse- echo method has been used to locate the defect and also to ascertain the extent of damage. Longitudinal wave has been generated by placing the transducers at an angle to the plate as shown in Fig 5.1. In this study, a single transducer has been used to generate and receive wave signatures in the pulse-echo method. Two transducers are used for sending and receiving the waveforms in through transmission method. Transducers having longer wave form duration and a relatively narrow frequency bandwidth with centre frequency of 1 MHz and 0.5MHz has been used for the 4mm and 6mm thick plate specimens.

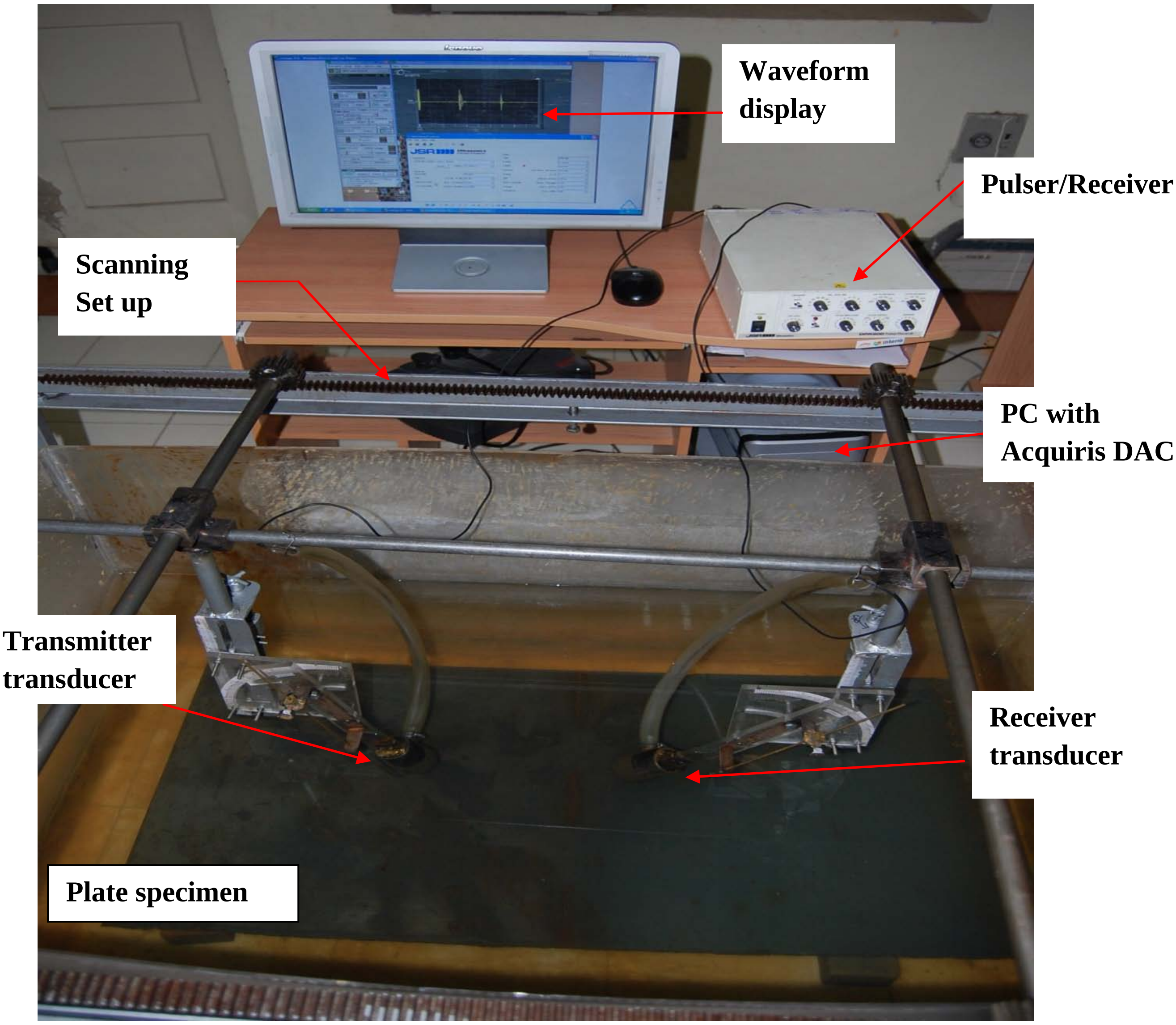

Fig. 5.2 Experimental Set up

A computer with an ACQUIRIS digitizer card has been used to capture the received signal and its subsequent processing. The transducers were mounted in holders and attached to the scanning set up, as shown in **Fig.5.2**.

Features of the equipment used are as follows:

(a) Transducer:

It is a single element longitudinal wave transducer. It can be used in straight beam flaw detection and thickness gauging, detection and sizing of delamination, material characterization and sound velocity measurements, inspection of plates, billets, bars, forgings castings, extrusions, and a wide variety of other metallic and non-metallic components. S 24 HB 1 (KARL DEUTSCH) Standard transducer of 1 MHz frequency and 24 mm diameter and S 24 HB 0.5 (KARL DEUTSCH) Standard contact transducer of 0.5 MHz frequency and 24 mm diameter has been used, as shown in fig. 5.3.

Fig. 5.3 Standard KARL DEUTSCH transducer

(b) JSR Ultrasonics DPR 300 Pulser/ Receiver System:

DPR300 pulser produces a high voltage electrical excitation pulse (up to 475 Volt) and applies this pulse to the instrument’s T/R connector. An ultrasonic transducer connected to the T/R connector via a length of 50Ω coaxial cable has been then employed to convert the electrical energy of the excitation pulse into an ultrasonic pulse that has been propagated into a test material or medium.

With the DPR300 configured for pulse-echo mode operation, acoustic echoes reflected from interfaces or defects within the test material are converted by the transducer into electrical signals that are presented to the T/R connector of the DPR300. The low-noise DPR300 receiver amplifies these electrical signals, and the signals then pass through adjustable high pass and low pass filters. The DPR300 receiver gain has been adjustable between -13 dB and 66 dB, and there are six high pass and six low pass filter settings for band-limiting the receiver frequency response. The amplified and filtered signals are available on the instrument’s Receiver Output connector.

The DPR300 may also be used in transmission mode operation wherein a separate receiving transducer has been used to detect acoustic pulses that have propagated through a test material or medium. Fig. 5.4 gives the details of the inside layout of the JSR pulse generator. The details of the specifications of the JSR pulse generator are given in Table 5.1.

The sub-units of the JSR pulse-receiver are as given below:

PRF Oscillator & Pulser Trigger control:

The internal PRF oscillator generates repetitive trigger pulses for the pulser subsystem under the control of the PRF control. Pulser Trigger control selects between the internal PRF oscillator and an external source applied to the Trig/Sync connector as trigger sources for the DPR 300 Pulser.

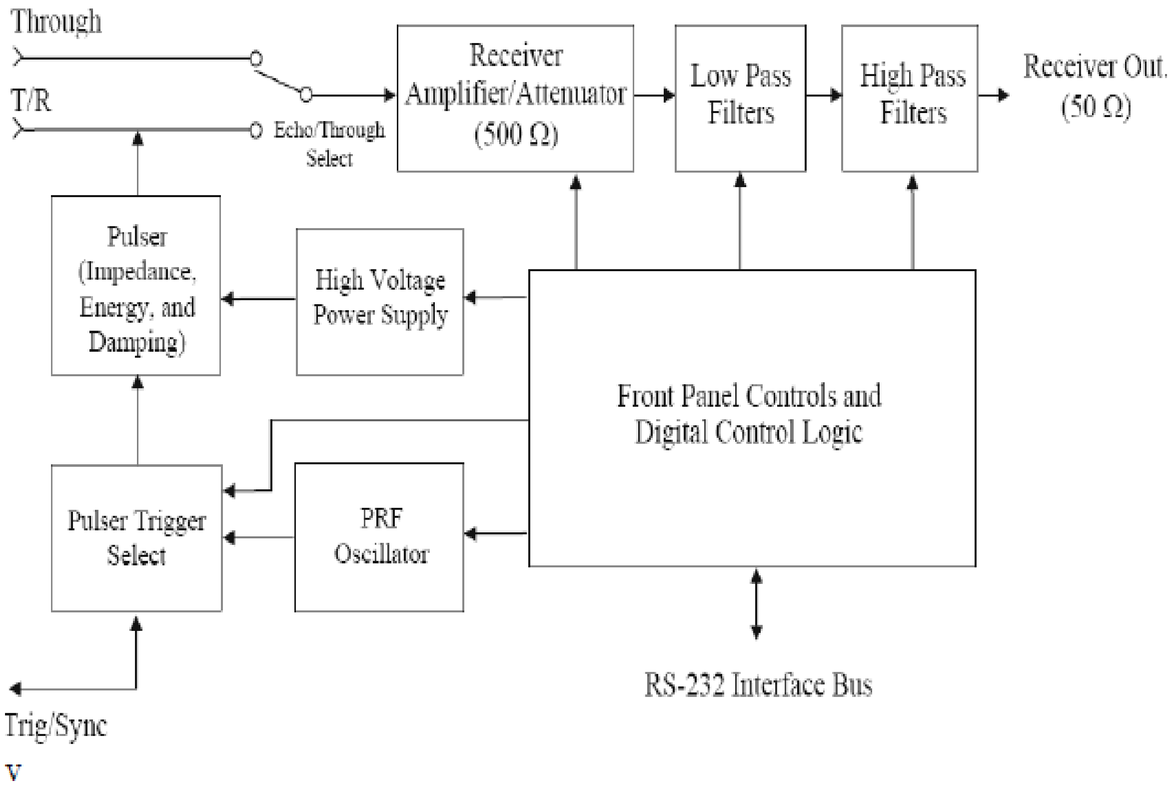

Fig.5.4. Layout of JSR Pulse Generator

Pulser (Impedance/Energy/Damping):

The pulser generates an excitation pulse upon receiving a trigger event from a selected source. There are four energy and two impedance values, and the single Energy and impedance control adjusts the pulse energy and the pulser impedance.

Receiver amplifier:

It controls the amplification or attenuation of signals processed by the DPR300 receiver. The receiver gain can be varied from -13dB to 66 dB.

Low Pass and High Pass filters:

Low filters are available for reducing the bandwidth of the DPR300 receiver. High Pass filters are available for eliminating undesirable low frequency energy from the DPR300 receiver signal. High pass filtering can be used as a means of providing faster receiver recovery from strong signals such as the excitation pulse or strong interface echoes. Table 5.1 gives the specifications of JSR pulse-receiver.

Table 5.1: Specifications of JSR pulse-receiver

Pulser	
Pulse Type	Negative Spike Pulse
High Voltage Supply	100V to 475V
Initial Transition (Fall Time)	<5 ns (10-90%) typical for 475V pulsers
Pulse Amplitude	-475V peak. Amplitude depends on Energy, Impedance, Damping control settings, and pulser type
Pulse Energy	1.55 µJoules minimum, 304 µJoules maximum for 475V pulsers. Dependent upon energy and voltage setting
Pulse Duration	Typically 10-70 ns FWHM for 50Ω load. Function of the Energy, Impedance, and Damping controls
Damping	16 Damping values: 331, 198, 142, 110, 92, 77, 67, 59, 52, 47, 43, 39, 37, 34, 32, and 30 Ω
Mode	Pulse-echo or through transmission
Through Mode Isolation	Typically 80 dB at 10 MHz
Pulser Repetition rate	Internal: 100 Hz -5 kHz for 475V pulsers. External: 0-5 kHz for 475V pulsers.
Sync Output	Maximum +5 V, tr <30 ns, tw=50 ns.min. TTL and CMOS compatible. Minimum value of load impedance is 50 Ω
Pulser Trigger Source	Selectable by computer between internal oscillator and external source
External Trigger Input	3 - 5 V positive going pulse. Triggering will occur synchronously with leading edge of trigger signal. TTL and CMOS compatible
Receiver	
Gain	-13 to 66 dB in 1 dB steps controlled by the host computer

Phase	0° (non inverting)
Input Impedance	500 Ω (through transmission)
Bandwidth	.001-35 MHz (-3 dB) or .001-50 MHz
High Pass Filter	DC,1,2.5,5,7.5 and 12.5 MHz
Low Pass Filter	3,7.5,10,15,22.5 (35 MHz BW) or 5,10,15,22.5,35 (50 MHz BW)
Receiver Noise	Typically 49 µV pk-pk input referred (measured at 60dB,35 MHz bandwidth)
Output Impedance	50 Ω
Output Voltage	± 0.5 V into 50 Ω

(c) Dual-Channel High-Resolution Waveform Digitizer:

Model DC438 Dual-channel, 12-bit, 100 MHz, 200 MS/s, 4-M point acquisition memory card had been used to capture the waveform. Waveforms are transferred directly into the digitizer large acquisition memories so that complex signals can be stored over very long time periods. Large memories are essential for maintaining fast sampling rates and therefore timing resolution. Table 5.2 gives the specifications of the Digitizer Card.

Table 5.2: Specifications of Digitizer Card

Model DC438	
Bandwidth (-3 dB)	DC to 100 MHz
Full Scale Range (FSR)	250 mV, 500 mV, 1 V, 2 V, 5 V and 10 V
Impedance	50 Ω ± 1% @ DC
Connector	BNC, gold-plated
Channels	Two
Coupling	DC
Maximum Input Voltage	±10 V DC (2 W) or 10 V RMS at 50 Ω
Bandwidth Limit Filter	35 MHz 2-pole Bessel filter (DC438)
Minimum Amplitude	1 V pk-pk
Impedance	50

(d) 4 axis- scanning set up:

In this testing, an acrylic tank of size 106cmx70cmx60cm and set up to move and set the transducers at a given angle has been used for testing as shown in the Fig. 5.5.

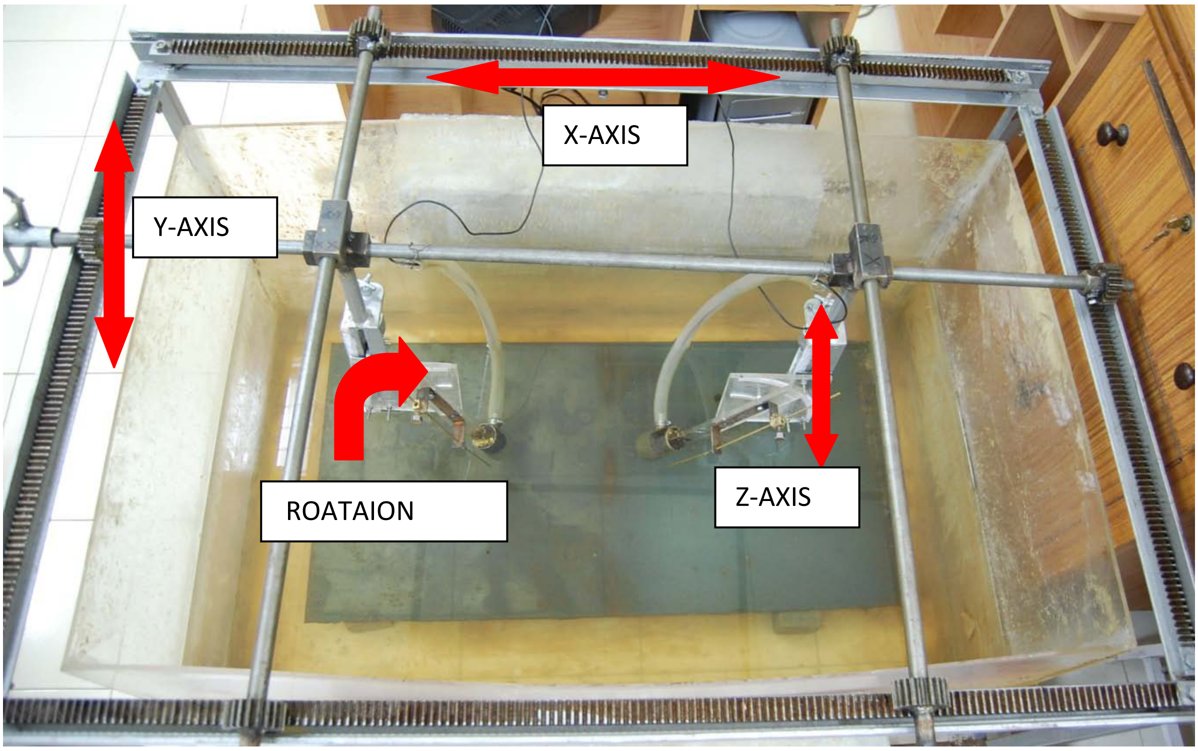

Fig. 5.5 4-Axis scanning set up

This set up has four degree of freedom, three translations for positioning of transducer over plate and one rotational to arrange the transducers at a specific angle so as to get a desirable mode. The transducers are mounted in a holder and naturally coupled with water. The excitation signal consisted of a negative spike pulse with pulse duration ranging from 10-70 ns. The least count for the translational motion is 1mm and least count for rotational motion is 0.1 degree. The maximum movement in X-direction is 120 cm, Y-direction is 70 cm, Z-direction is 10 cm, and rotation allowed is 0-90 degree.

5.3 Testing of Plates in Water

The plate and the transducers are immersed in water where water becomes couplant for the transducer to send ultrasonic waves in the plate. In this the transducers are kept at an angle to the surface of the plate as shown in the Fig. 5.5. For generating different modes, the incident angles are changed. The study has been carried out on two different M.S. plates of thicknesses 4mm and 6mm.

The testing has been done for notch type defects, of different depth, size and location.

5.3.1 Selection of the Frequency

Transducers with central frequencies of 0.5MHz and 1 MHz have been used for the experiments. The transducers were driven by a Pulser/receiver system with maximum gain of 67 dB and maximum input voltage of 475V. An external PC and Digitizer card has been used to capture the received signal and for further processing. Different frequencies and modes have different dispersion characteristics with a trend toward higher frequencies having slower energy transport velocities.

5.3.2 Mode Selection in Mild Steel Plate

Plate with water on both sides has been modelled in disperse software as shown in Fig 5.6. The angle of incidence has been calculated by using SNELL'S Law. The velocity of a particular mode that has to be excited is found from the DISPERSE curves, as shown in fig 5.7. Table 5.3 shows all the corresponding angles of incidence, for the modes, required for excitation in 4mm plate.

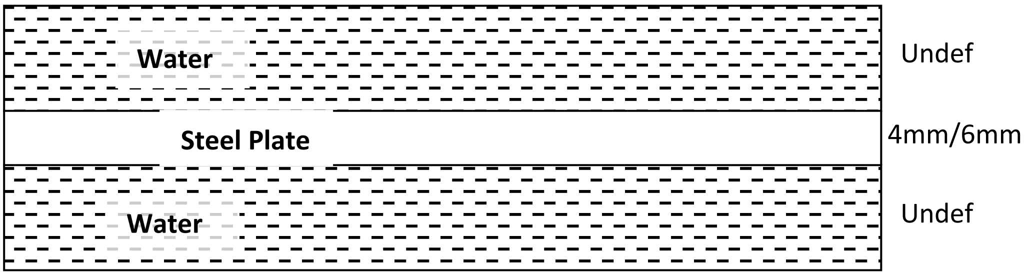

Fig. 5.6 Modelling of Mild Steel Plate in DISPERSE software

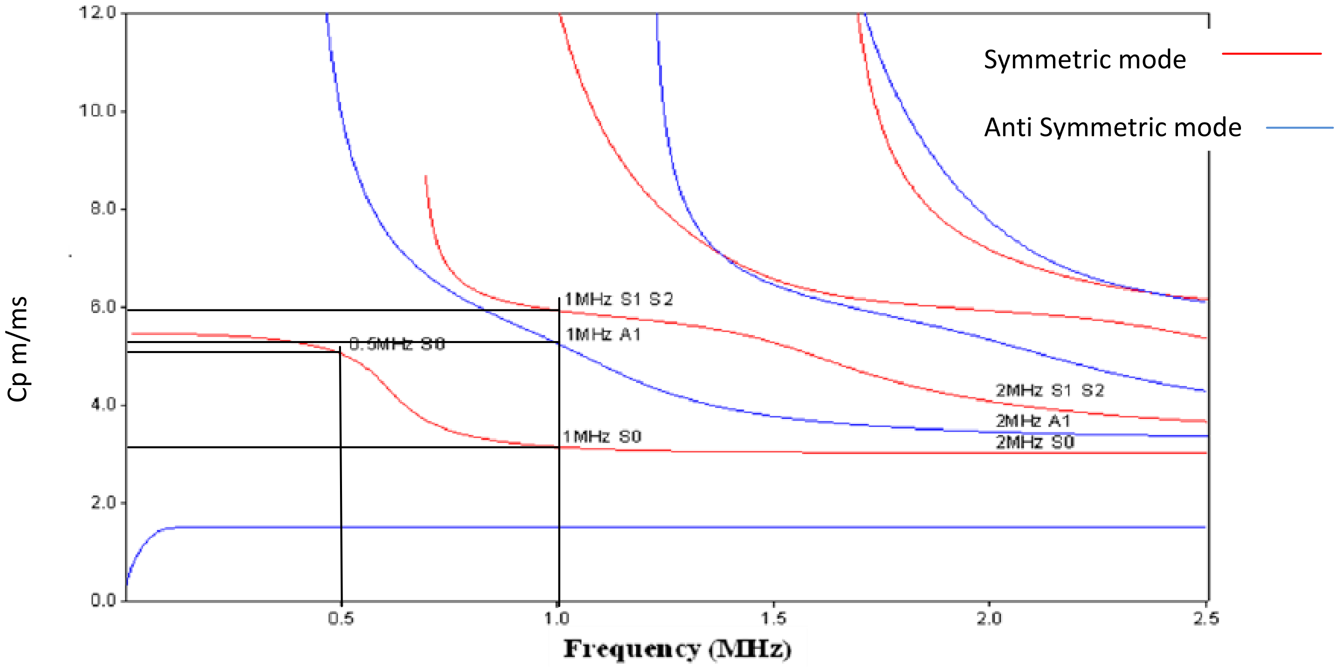

Fig. 5.7 DISPERSE curves showing various modes at various frequencies in 4mm plate

Table 5.3 Angles to excite modes in 4 mm plate

Frequency / Mode	0.5 MHz	1 MHz
S0	17.4 ^{o}	28.6 ^{o}
S2	-	14.7 ^{o}
S4	-	7.3 ^{o}
A1	8.8 ^{o}	16.7 ^{o}

Similarly, in 6 mm mild steel plate with water on both sides has been modelled in DISPERSE software. The angle of incidence has been calculated using the velocity of the mode which has to be excited has been found using the fig 5.8. Table 5.4 shows the corresponding angles of incidence, for the modes, required for excitation in 6mm mild steel plate.

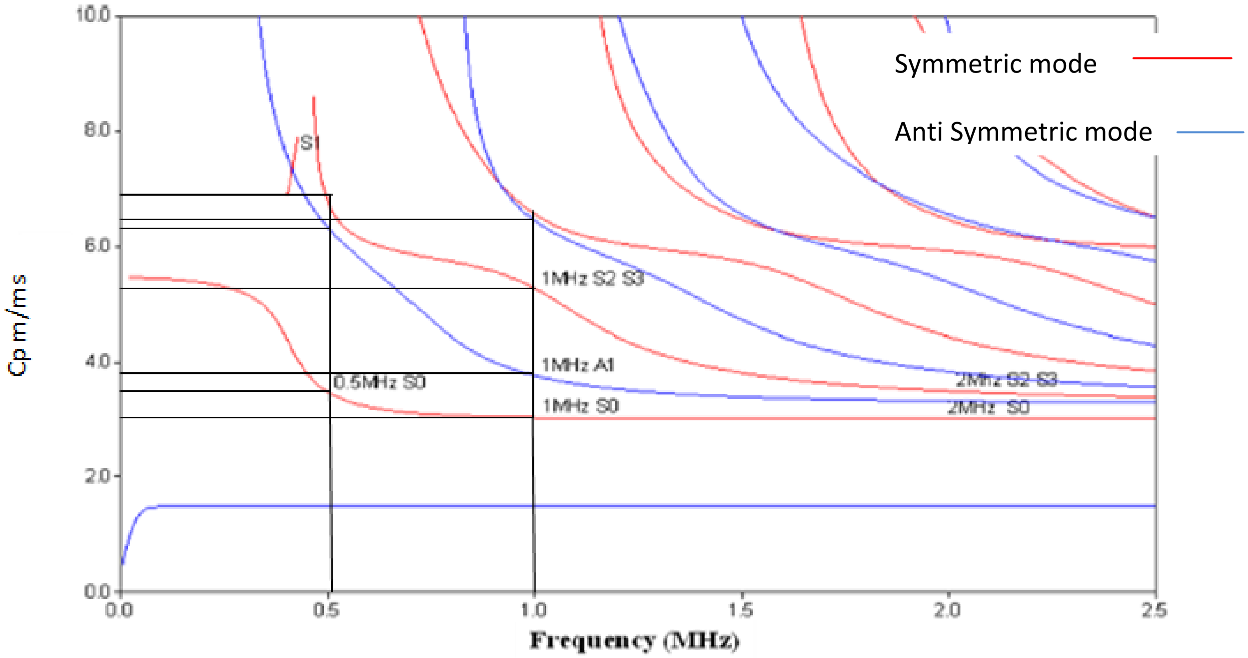

Fig. 5.8 DISPERSE curves showing various modes at various frequencies in 6mm plate

In fig. 5.7 and fig. 5.8 it has been observed that for 2MHz frequency, different modes generated, have very near phase velocities. So while calculating the critical angle for each mode, the angles are very close, hence difficult to obtain. Also at higher frequency like 2MHz, scattering of the waves increases, due to which wave cannot travel long distances efficiently. So 2 MHz frequency has not been considered for the testing.

The modes with phase velocity more than 6 m/ms are not considered for testing because these modes are not stable, and do not give very clear signal during the testing. Also these modes have high attenuation, as compared to the modes with lower phase velocity.

Table 5.4 Angles to excite modes in 6 mm plate

Frequency / Mode	0.5 MHz	1 MHz
S0	25.8^o	29.6^o
S2	12.9^o	16.6^o
S4	-	13.2^o
A1	13.8^o	23.5^o
A2	-	13.4^o

Thus any available mode can be obtained by just arranging the transmitting transducer and receiving transducer at a specific incident angle in case of through transmission scanning. However in case of pulse-echo scanning, any available mode can be obtained by arranging only the transmitting transducer at the specific angle.

The selection of a particular mode depends in its sensitivity to the defect, which has been explained in detail in next chapter.

5.4 Scanning of Plate Specimen

Scanning of plates has been done by arranging the transducers at the angle as given by the selected modes of each frequency. The plate to be tested has been then divided into grid points as shown in Fig. 5.9. The total length and width of the plate has been divided into equal intervals. Each interval in X- direction and in Y-direction may be equal or unequal depending on plate dimensions. In this experimental study, a plate of size 20″x20″ had been taken and grid of size 1″x1″ had been formed.

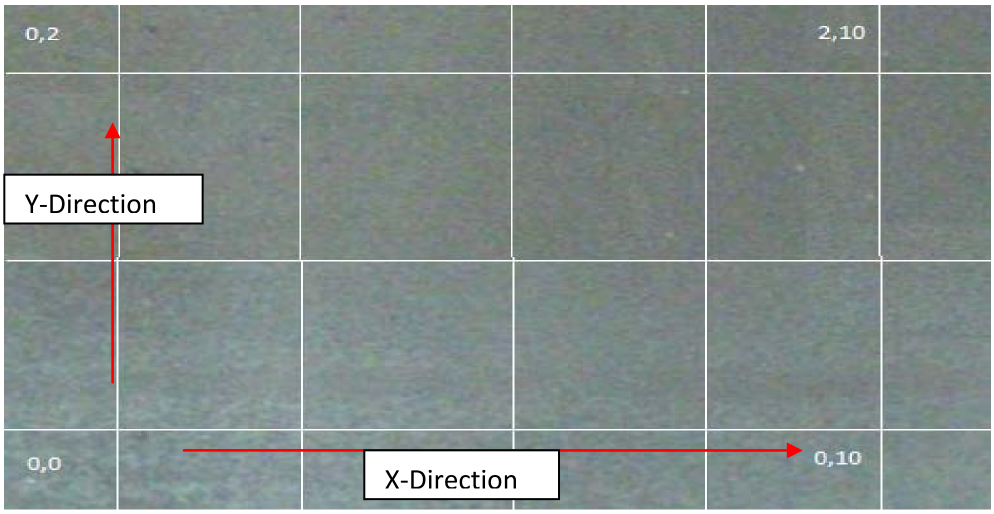

Fig. 5.9 Plate with grid points for testing.

Before starting the scanning process, the transmitter transducer has been placed at (0, 0) and receiver transducer has been placed at (0, 2) of the grid, then through transmission has been taken at every grid point by moving in x-direction. If there is a fall in through transmission amplitude, it suggests some discontinuity between the grid points, which needs to be located. The setup is then switched to Pulse echo mode and scanning has been carried out in y-direction, as the defect is approached, there is a rise in the amplitude of the signal.

5.5 Correction Factor

As a thumb rule for NDT using ultrasonic waves, a healthy specimen needs to be inspected first, before inspecting a defected specimen. This serves as a reference for the defect ridden specimens, with which the inspection results of healthy specimen are compared and the decision about the presence and extent of the defects is arrived at.

So the healthy plate of 4mm thickness has been scanned by through transmission at 0.5MHz frequency, S0 mode, before introducing the defects on the same plates. Since the specimen was completely healthy, uniform readings were expected, but iconoclastic results were obtained, as shown in fig. **5**.10.

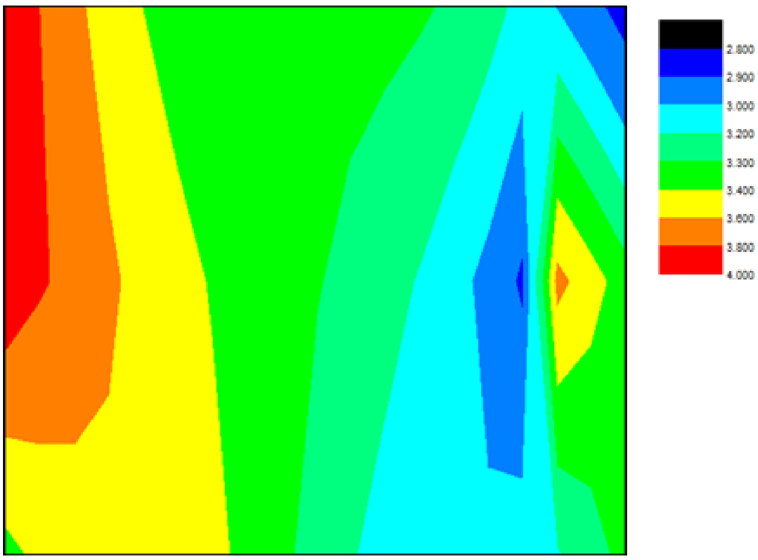

Fig. 5.10 Scanning result of 4mm healthy plate at 0.5MHz, S0 mode

The possible reasons for the variation in the scanning results of a healthy plate could be attributed to:

- Inherent irregularities in the specimen.
- Play in the moving parts of the scanning set up due to wear and tear.

So 6mm thick plate was tested for same frequency and same mode in healthy state. The scanning results are shown in fig. 5.11

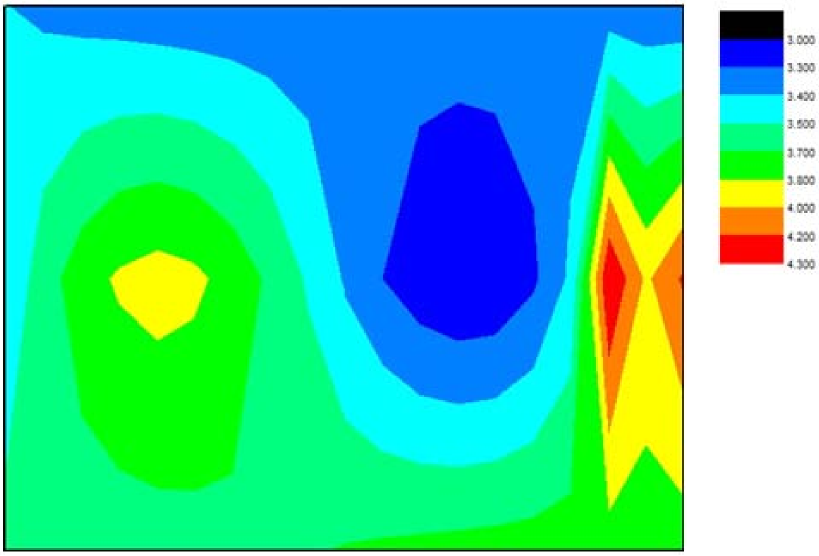

Fig. 5.11 Scanning result of 6mm healthy plate at 0.5MHz, S0 mode

Since these results were not uniform and also did not had any particular trend, both the plates of 4mm and 6mm thickness were tested at 1MHz frequency, S0 mode. The results obtained are shown in fig. 5.12(a) and fig. 5.12 (b). These kinds of trends of readings were observed for other modes on 0.5MHz and 1MHz frequency.

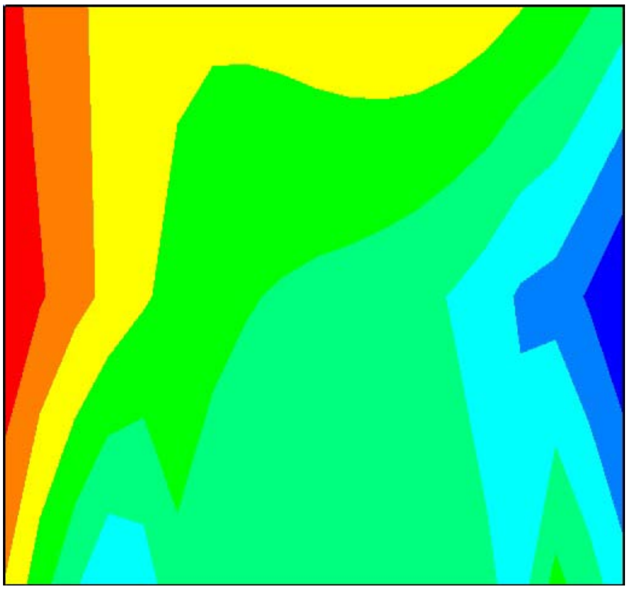

Fig. 5.12(a) Scanning results of 4mm thick healthy plates for 1MHz, S0 mode.

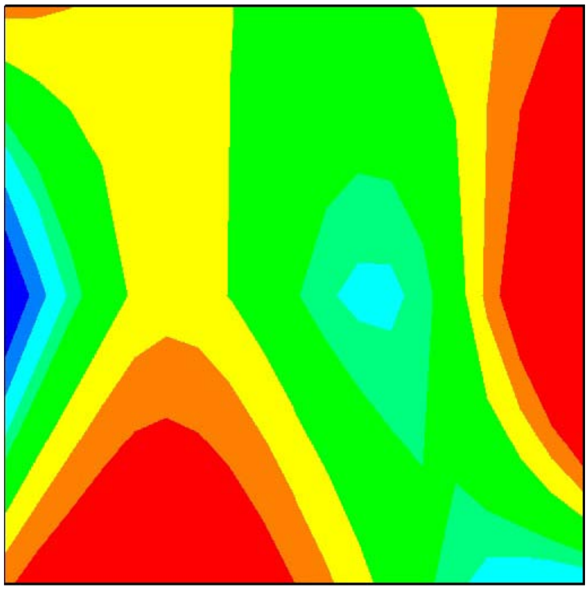

Fig. 5.12(b) Scanning results of 6mm thick healthy plates for 1MHz, S0 mode.

As observed from the fig. 5.10, 5.11, 5.12(a) and 5.12(b), the trends for different plates and different modes had no similarity. So the play in the scanning set up was ruled out, and the defects were attributed due to inherent irregularities. Here it is also observed that different modes respond in a different manner to these inherent irregularities.

5.5.1 Formulation of Correction Factor

To deal with the inherent irregularities in the plate specimens, the trend line had been formed for the modes selected in section 5.3.2 for both 0.5MHz and 1MHz frequency. Then from the trend line, a correction factor was formulated, which had been applied to normalize any set of given readings in that mode.

To formulate the correction factor for a given mode, five readings were taken on a plate of size 20″x20″, at locations 3″ apart, as shown in Fig. 5.13 and were plotted on a graph. A particular trend had been observed as shown in fig. 5.14 and trend lines of different orders (2, 3 and 4) were fitted to this plot as shown in fig. 5.14

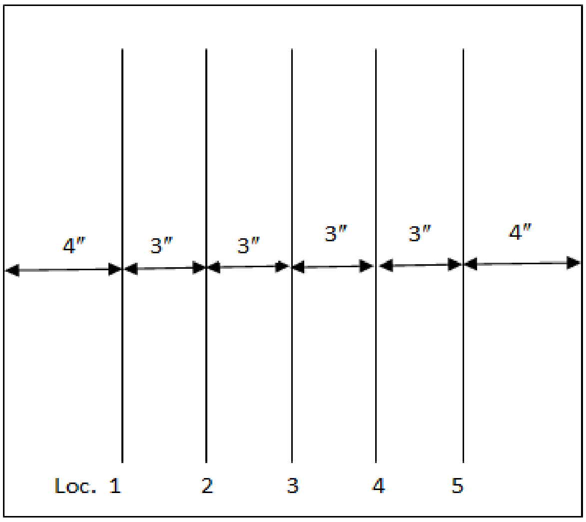

Fig. 5.13 Schematic diagram of a plate showing 5 locations selected for the readings.

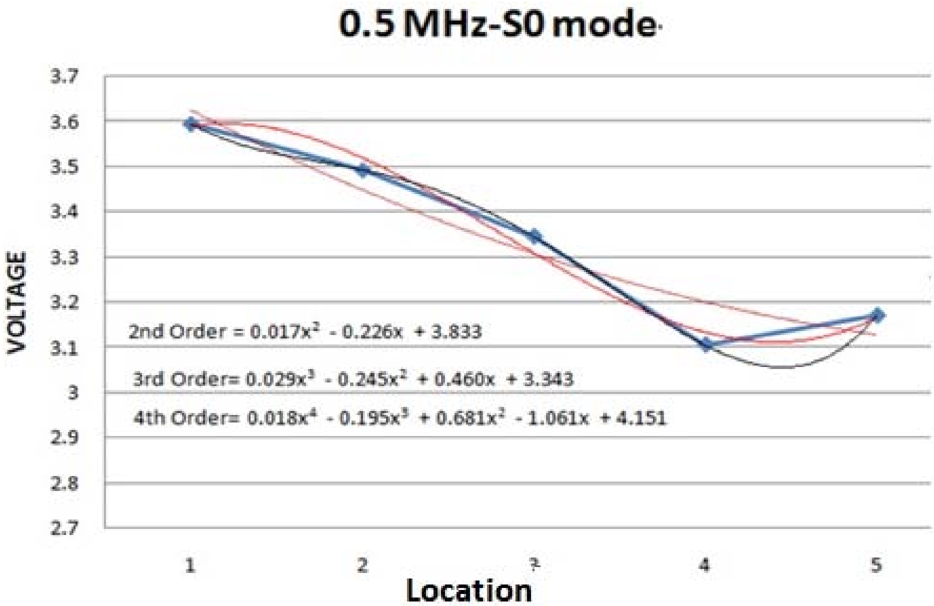

Fig 5.14 Trend-lines of 2^{nd}, 3^{rd} and 4^{th} Order with their equations.

From fig. 5.14, 3rd order curve appears to be the best fitting. Then the plate has been divided into 19 locations, 1″ apart, similar to the manner as shown in fig. 5.13. The readings for the locations were then parameterised using the equation of the trend line i.e.

$$G=f(x) = 0.029x^3 - 0.245x^2 + 0.46x + 3.343 \quad 5.1$$

Taking parameter value as a variable, the reading for the healthy location had been calculated from the equation 5.1. From the calculated healthy results, the maximum value had been divided by each result. This gives a value ranging between zero to 1, where 1 is for the maximum value, and less than 1 for subsequent values. This value is the correction factor. Table 5.5 show the calculations for calculating the correction factor. Then readings are again taken on the same plate, and same location, after introducing the defects. The correction factor is then divided by these readings to obtain the true value of the reading at the given location.

Table 5.5 Calculations for calculating the correction factor.

Location	Parameter	Healthy (calculated from 3RD order equation)	Correction Factor	Healthy readings-corrected	Healthy (calculated from 4th order equation)	Correction Factor	Healthy readings-corrected
1	0.25	3.638219	0.95898	3.79384375	4.393262	1	4.393262
2	0.5	3.64125	0.959779	3.79384375	4.052813	0.922506	4.393262
3	0.75	3.645906	0.961006	3.79384375	3.83423	0.872753	4.393262
4	1	3.652	0.962612	3.79384375	3.71	0.844475	4.393262
5	1.33	3.661927	0.965229	3.79384375	3.64918	0.830631	4.393262
6	1.66	3.673601	0.968306	3.79384375	3.661344	0.8334	4.393262
7	2	3.687	0.971838	3.79384375	3.708	0.84402	4.393262
8	2.33	3.700894	0.9755	3.79384375	3.754546	0.854615	4.393262
9	2.66	3.715227	0.979278	3.79384375	3.779936	0.860394	4.393262
10	3	3.73	0.983172	3.79384375	3.77	0.858132	4.393262
11	3.33	3.7439	0.986836	3.79384375	3.720884	0.846952	4.393262
12	3.66	3.756934	0.990271	3.79384375	3.63749	0.82797	4.393262
13	4	3.769	0.993452	3.79384375	3.53	0.803503	4.393262
14	4.33	3.778947	0.996073	3.79384375	3.427712	0.78022	4.393262
15	4.66	3.78672	0.998122	3.79384375	3.359048	0.764591	4.393262
16	5	3.792	0.999514	3.79384375	3.366	0.766173	4.393262
17	5.25	3.793844	1	3.79384375	3.452012	0.785751	4.393262
18	5.5	3.79375	0.999975	3.79384375	3.634063	0.82719	4.393262
19	5.75	3.791531	0.99939	3.79384375	3.939855	0.896795	4.393262
	MAXIMUM-	3.793844		MAXIMUM-	4.393262		

From the above table, correction factors with 3rd and 4th order trend line are obtained and applied to the healthy readings. So it has been observed that 3rd order curve has been the best fitting curve, as the healthy reading obtained from the 3rd order trend line is below 4 Volt. As 4th order trend line gives the healthy readings above 4 Volt, which is not possible, because the pulser/receiver hardware used in the given experimental study can generate the maximum signal of 4 Volt. So the 4th order trend line has been rejected.

This process has been carried out for all modes at both 0.5MHz and 1MHz frequency, as different trend had been observed for each mode.

Similarly this trend has been also observed in the pulse echo scanning, and the inherent irregularities were observed. So in the same manner, the correction factor has been applied in pulse echo readings for plates of different thickness and different modes.

CHAPTER 6

RESULTS AND DISCUSSIONS

This chapter discusses about the experimental results of the notch defects of varying depth, size and location on plates of different thickness, submerged in water. Experiments as per the methodology discussed in last chapter have been carried out. Also the correction factor discussed in section 5.5 has been subsequently used to modify the readings.

6.1 Testing of 4mm Plate

Mild steel plate of thickness 4mm had been taken and divided into three regions, namely C1, C2 and C3. This plate has been seeded with notch type defects of varying depth, size and location at different locations. The depth of notch has been varied from 1mm, 2mm and 3mm to simulate 25%, 50% and 75% reduction in the area of the cross section. The location and size of the defects is as shown in Fig. 6.1. This plate has been tested with 0.5MHz and 1MHz frequency with different angles to excite different modes. For modes of each frequency, only few were taken for testing because the rest of modes at these frequencies which gave very weak output signal were ignored and also have less energy to detect the defect on the plate.

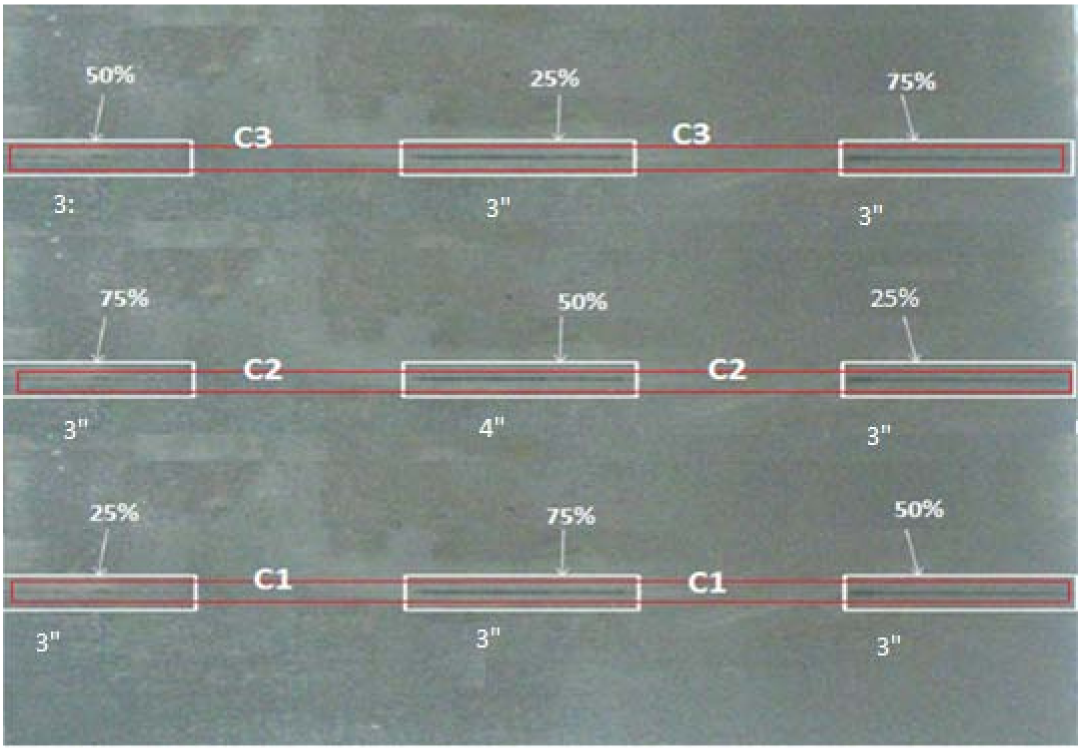

Fig. 6.1 4mm steel plate, showing the depth and location of defects

As discussed in chapter 5, section 5.3, out of different modes available at 0.5MHz and 1MHz frequency, the transducers were set on following angles:

- 17.4^0 to excite S0 mode in 0.5MHz
- 28.6^0 to excite S0 mode in 1MHz
- 14.7^0 to excite S2 mode in 1MHz
- 16.7^0 to excite A1 mode in 1MHz

The fig. 6.2 shows the signal for S0 mode at 0.5MHz frequency, for various depths of notch defect.

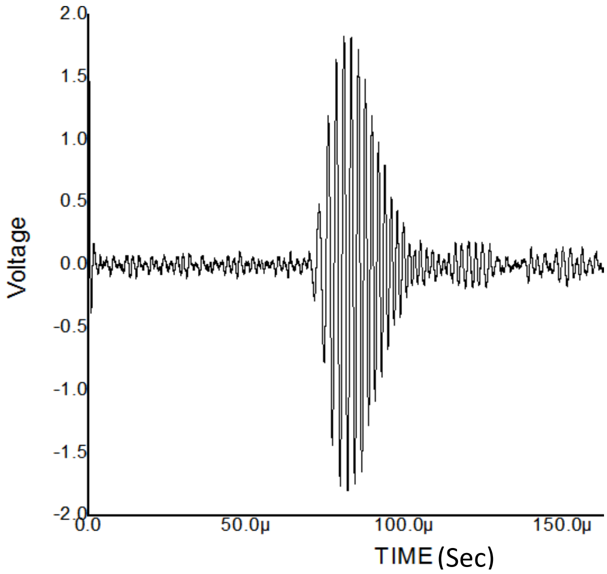

Fig. 6.2(a). Signal for healthy plate

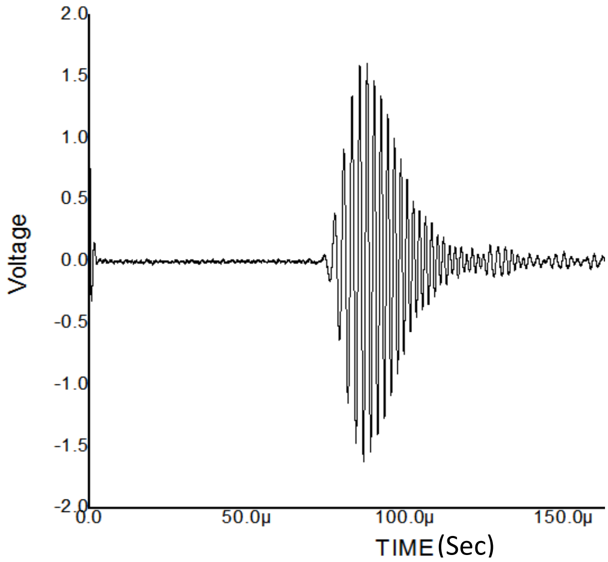

Fig. 6.2(b) Signal for plate with 1mm defect

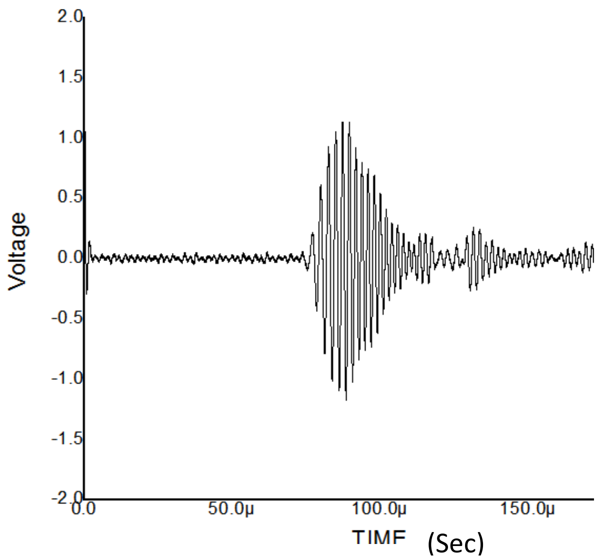

Fig. 6.2(c). Signal for plate with 2mm defect

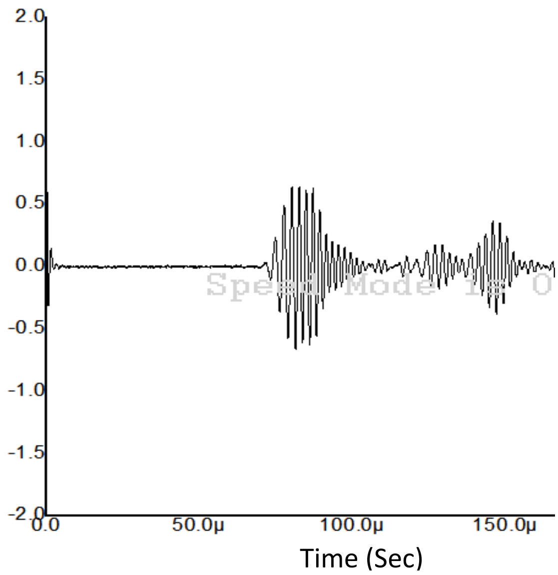

Fig. 6.2(d). Signal for plate with 3mm defect

The amplitude of various modes when interacting with defects of various depths is shown in fig. 6.3.

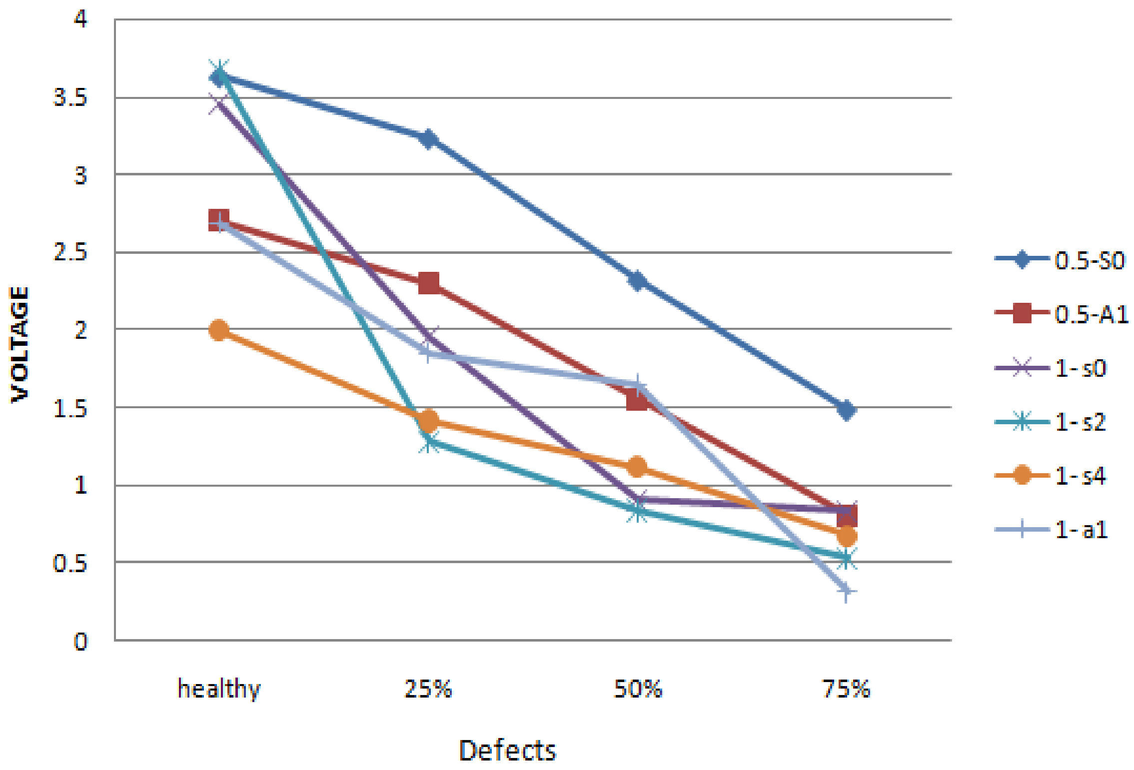

Fig. 6.3 Trends of various modes for Notch defects in 4mm plate

It is evident from the above graph that for 1MHz S1 and S2 modes and for 0.5MHz, S0 mode is most sensitive to the notch defect. In 1MHz S1 and S2 modes and in 0.5MHz, S0 mode is highly energized mode and is least attenuative. The peak to peak voltage amplitude with this mode is higher when compared with other modes.

Attenuation curves given by DISPERSE, as shown in fig. 6.4 also show that these modes suffer least attenuation in comparison to other modes in 4mm plate. Here it has been also observed that mode A1, though sensitive enough for the testing, is very attenuative. So it loses its energy when distance between the probes is increased. So this mode is also avoided.

The through transmission readings for healthy plate were taken at 5 different locations, in regions C1, C2 and C3 along the X-axis as shown in Fig.5.8 for all the modes selected above. A trend had been observed in the healthy readings as shown in fig. 6.5.

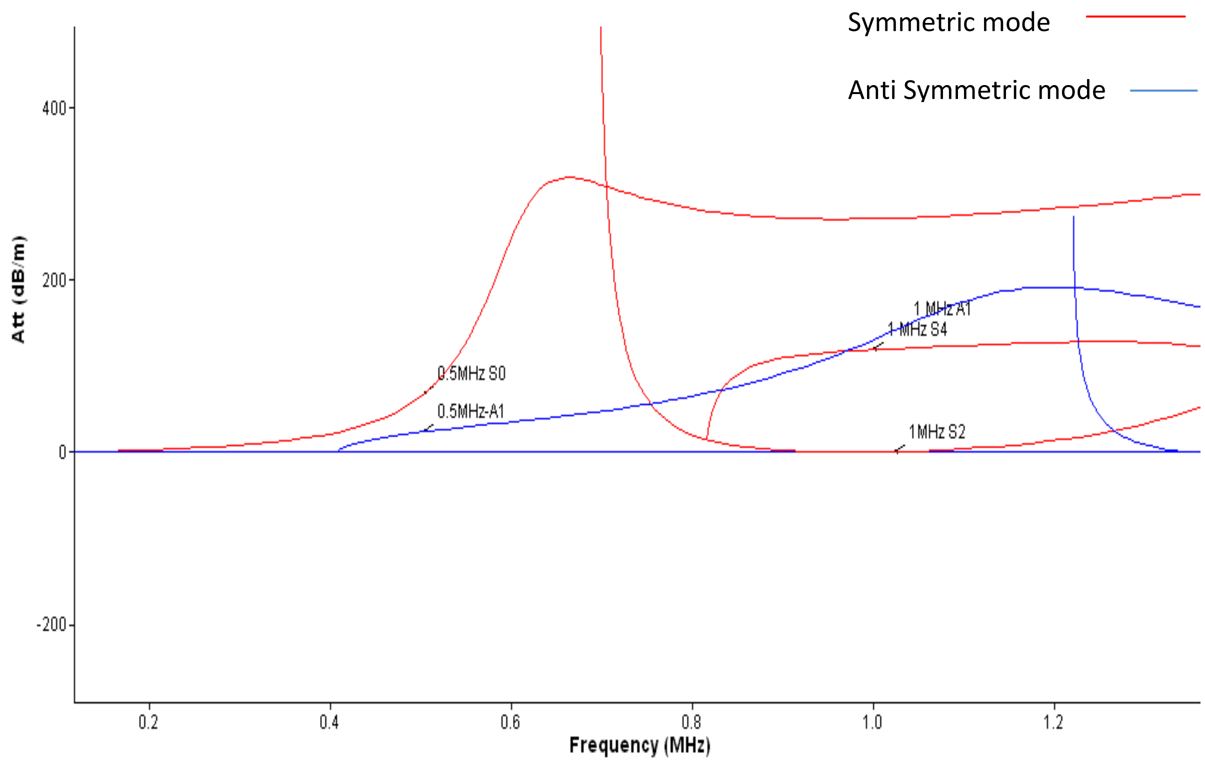

Fig. 6.4 Attenuation curves for 4mm plate

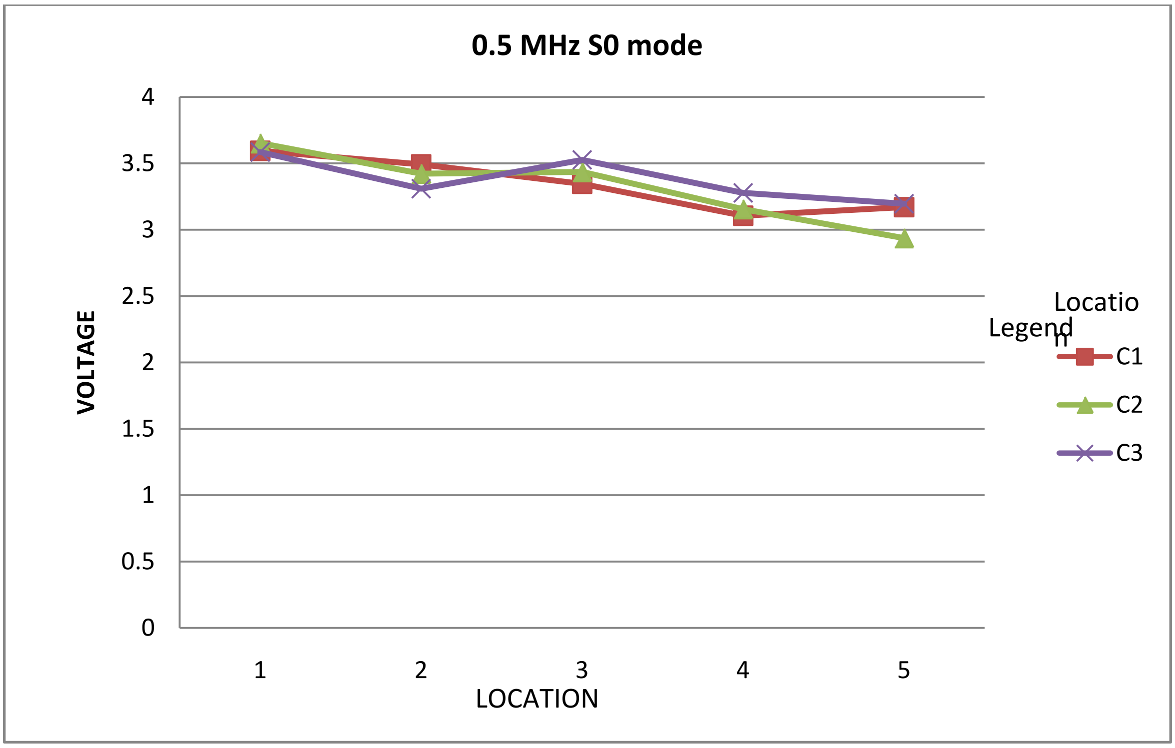

Fig. 6.5 Trend of readings for healthy plate at different locations

So a correction factor had been formulated from the trend-line of the healthy readings as discussed in Chapter 5, section 5.5.1.

After taking readings on healthy plate, the defects are seeded in the plate, as shown in fig. 6.1. After seeding the defects, the through transmission scanning has been done for the same modes used in scanning the healthy plate. Fig. 6.6 shows the readings for various defects and locations with the application of correction factor and without the application of the correction factor.

Table 6.1 shows the application of the correction factor for the given set of readings. It is observed that the readings at various locations are significantly increased or decreased, depending on the inherent irregularity in that location and much accurate readings are obtained which give much clear information about the extent of the damage.

Table 6.1 Application of the correction factor for the given set of readings.

Location	Parameter	Healthy (Calculated Form Trend Line Equation)	Correction Factor	Experimental Readings At Location C1	Experimental Readings With Correction Factor Applied
1	0.25	3.443140625	0.959186686	3.538574	3.68914003
2	0.5	3.515375	0.979309666	3.187256	3.254594649
3	0.75	3.562421875	0.992415938	3.105469	3.129201055
4	1	3.587	0.999262887	3.249317	3.251713879
5	1.33	3.589645973	1	3.671777	3.671777
6	1.66	3.564132584	0.992892506	3.6958447	3.722300933
7	2	3.515	0.979205199	3.808594	3.889474855
8	2.33	3.451550273	0.961529437	3.643799	3.789586526
9	2.66	3.378889784	0.941287751	2.192382	2.32913049
10	3	3.301	0.919589292	1.586914	1.725676901
11	3.33	3.228874573	0.899496663	2.177735	2.421059566
12	3.66	3.166486984	0.88211679	3.1674316	3.590716824
13	4	3.119	0.868887914	3.3681641	3.876408047
14	4.33	3.095618873	0.862374423	3.2774414	3.800485398
15	4.66	3.100924184	0.863852371	3.270752	3.786239537
16	5	3.143	0.87557381	3.0769531	3.514213269
17	5.25	3.201578125	0.891892445	2.8106054	3.151282887
18	5.5	3.286625	0.915584719	2.650147	2.894485835
19	5.75	3.400859375	0.947408018	3.272705	3.454377564
	Maximum	3.589645973			

In the following figures, “H-Corrected” means readings of healthy plate, with correction factor applied. “Defects” means the experimental readings of the plate, seeded with notch defects. “Corrected” means the experimental readings, with the application of correction factor.

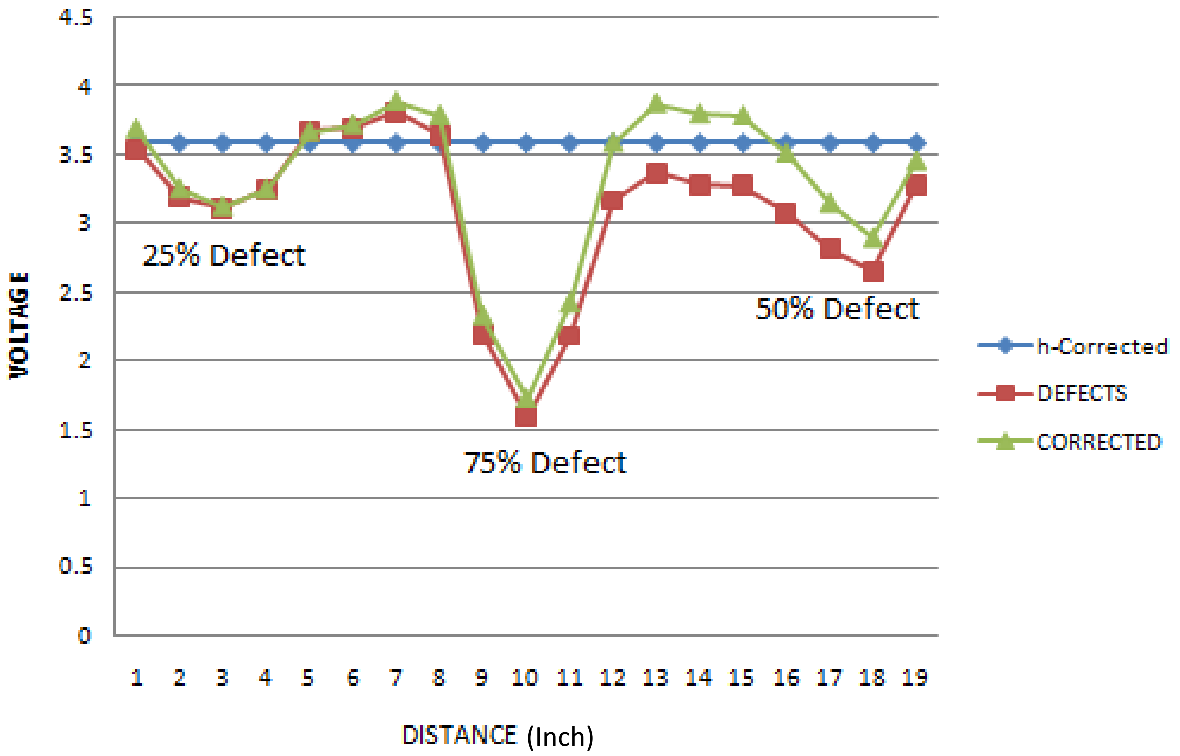

Fig. 6.6(a) 0.5MHz S0 mode C1 location

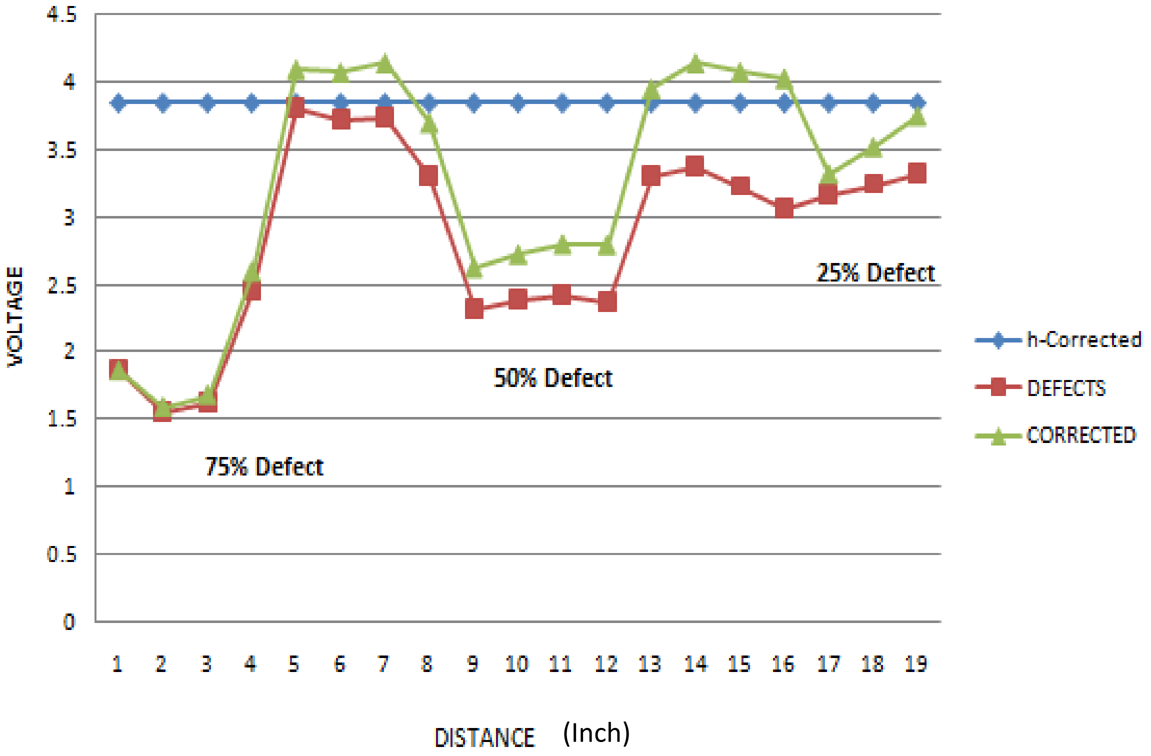

Fig. 6.6 (b) 0.5MHz S0 mode C2 location

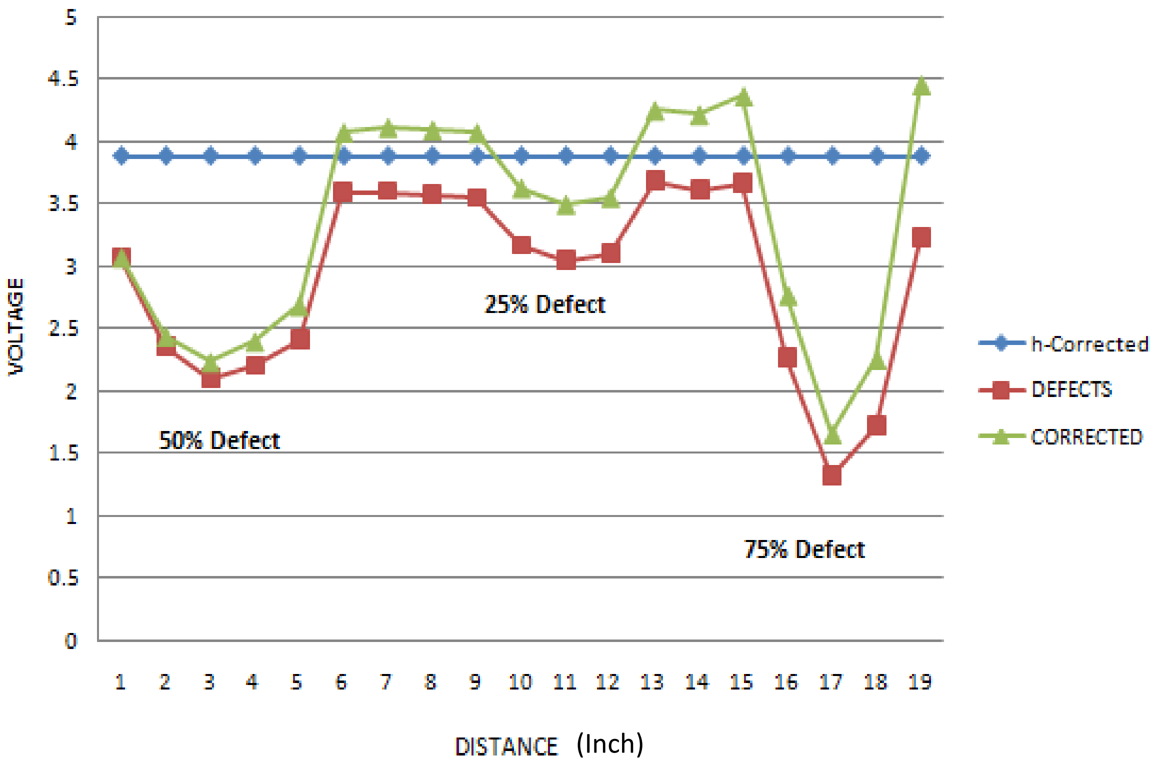

Fig. 6.6(c) 0.5MHz S0 mode C3 location

Fig. 6.6(d) shows the actual readings taken on the plate with seeded defects, taken at 1MHz frequency, S0 mode, locations C1, C2 and C3.

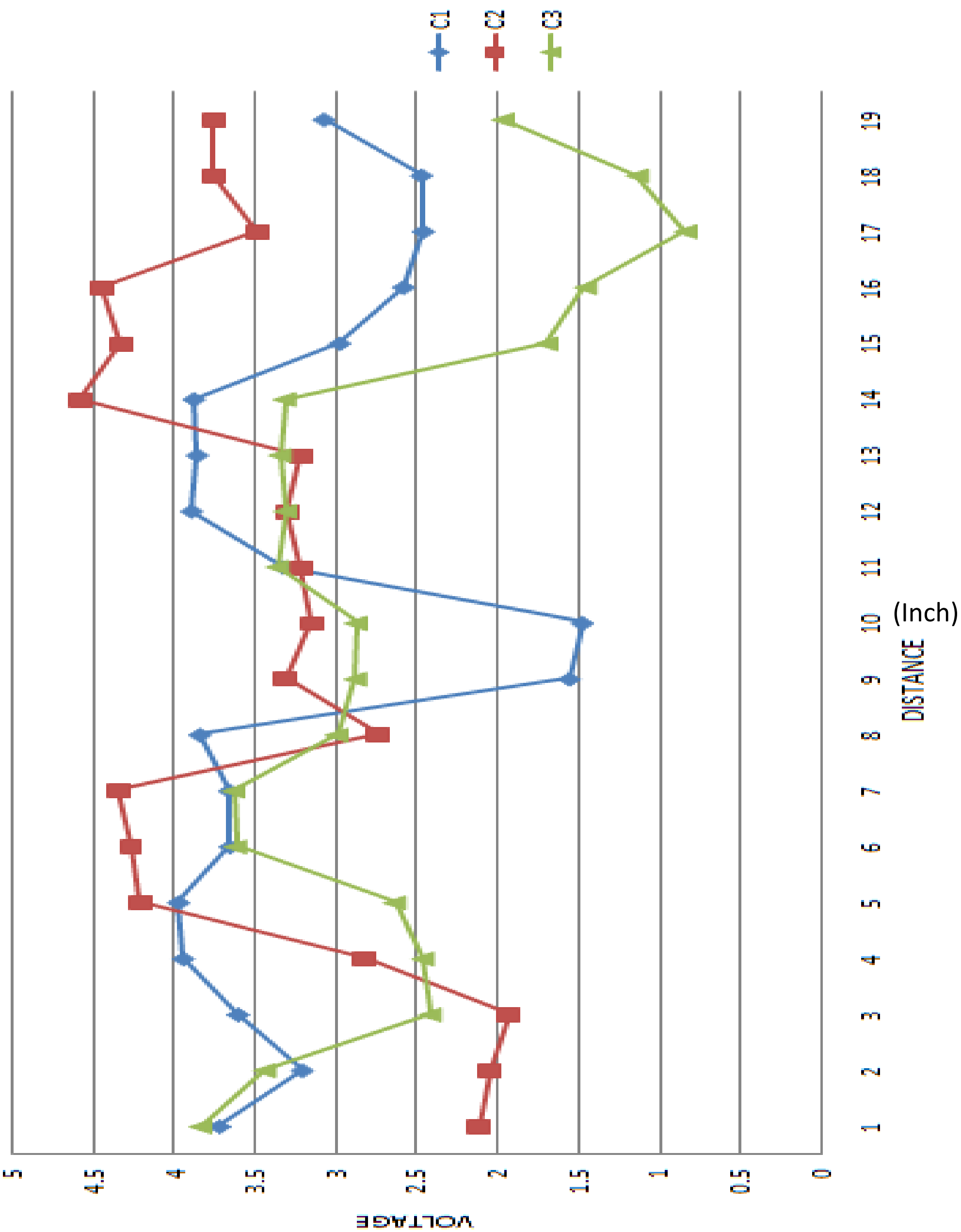

Fig. 6.6(d). 1MHz S0 mode C1, C2 and C3 location with corrected readings

6.1.1 Localizing the defects

Through transmission scanning gives an idea about the severity of damage. The plate had been seeded with 25%, 50%and 75% defects and had been scanned by through transmission. As the transducer reaches nears the notch, the voltage amplitude drastically falls as shown in Fig. 6.5. Fall in amplitude of the voltage indicates the presence of notch. When there is fall in amplitude in through transmission, the scanning is switched to pulse echo mode and scanning has been done in Y-direction. As the transducer approaches the defect, the amplitude of the voltage surges. Similar to through transmission, in pulse-echo scanning, trend is also observed for plates of different thickness and for different modes of different frequencies.

The effect of the inherent irregularities is also reflected in the results of the scanning, as shown by the values in table 6.2. So the correction factor is calculated and applied to pulse-echo reading also in a similar manner as done for through transmission scanning.

Table 6.2 results of Pulse-echo scanning of 4mm thick plate, at 1MHz S0.

1 MHz, S2 (4mm) CORRECTION FACTOR NOT APPLIED

	1	2	3	4	5	6	7	8	9	10	11	12	13	14	15	16	17	18	19
	0.979	0.9778	1.0034	0.9875	0.9766	0.9668	1.0242	0.9717	0.9753	1.0303	0.9729	0.9351	0.9143	0.9229	0.9192	0.7959	0.7983	0.802	0.7971
C3	1.2622	2.4561	2.9714	2.7749	0.9888	0.9595	0.9814	0.9888	2.6187	2.5865	1.0571	1.0095	1.0205	0.874	2.4561	3.8257	3.8147	2.4402	0.8801
	0.9363	0.907	0.9045	0.9058	0.9351	0.9265	0.9509	0.9729	0.9497	0.929	0.907	0.9033	0.9106	0.8789	0.8643	0.8728	0.8801	0.8801	0.78
	0.6803	0.7259	0.7528	0.7699	0.7861	0.7967	0.7943	0.7731	0.8195	0.8219	0.8325	0.8195	0.7731	0.7975	0.813	0.7609	0.7829	0.8407	0.8415
C2	3.8904	3.7866	3.5242	1.5242	0.8766	0.8668	0.9242	3.0728	3.1469	2.9115	3.1057	3.1655	0.6428	0.7891	0.7231	0.9282	2.1991	2.4652	2.1866
	0.7228	0.7423	0.7124	0.7112	0.6965	0.6935	0.6867	0.6617	0.7075	0.7014	0.6782	0.7759	0.6507	0.6874	0.655	0.7258	0.7179	0.7252	0.6758
	0.9583	0.9729	0.9399	0.9412	0.9302	0.9302	0.929	0.9314	0.9131	0.9131	0.9106	0.9143	0.9167	0.9155	0.8923	0.8801	0.8716	0.885	0.8679
C1	2.3376	2.3083	1.8023	0.9131	0.9375	0.9363	0.9338	0.9338	2.3135	2.998	3.8293	0.9141	1.0254	1.012	0.8813	0.9729	2.821	2.7435	1.6589
	0.7971	0.752	0.7373	0.7478	0.7227	0.7446	0.7458	0.7422	0.7312	0.7214	0.7288	0.7373	0.7385	0.7349	0.7459	0.7495	0.752	0.7727	0.78

1 MHz, S2 (4mm) CORRECTION FACTOR APPLIED

	1	2	3	4	5	6	7	8	9	10	11	12	13	14	15	16	17	18	19
	0.6507	0.6507	0.6507	0.6507	0.6507	0.6507	0.6507	0.6507	0.6507	0.6507	0.6507	0.6507	0.6507	0.6507	0.6507	0.6507	0.6507	0.6507	0.6507
C3	1.604	2.9094	3.0465	2.9896	1.0257	0.972	0.9833	0.9888	2.6334	2.6292	1.0899	1.0576	1.085	0.9404	2.6606	4.1401	4.099	3.6473	0.9142
	0.6507	0.6507	0.6507	0.6507	0.6507	0.6507	0.6507	0.6507	0.6507	0.6507	0.6507	0.6507	0.6507	0.6507	0.6507	0.6507	0.6507	0.6507	0.6507
	0.6507	0.6507	0.6507	0.6507	0.6507	0.6507	0.6507	0.6507	0.6507	0.6507	0.6507	0.6507	0.6507	0.6507	0.6507	0.6507	0.6507	0.6507	0.6507
C2	3.8904	3.8207	3.5882	1.5661	0.9117	0.9131	0.9858	3.3193	3.4446	3.2286	3.4895	3.606	0.7422	0.9237	0.8587	1.1179	2.6772	3.034	2.7211
	0.6507	0.6507	0.6507	0.6507	0.6507	0.6507	0.6507	0.6507	0.6507	0.6507	0.6507	0.6507	0.6507	0.6507	0.6507	0.6507	0.6507	0.6507	0.6507
	0.6507	0.6507	0.6507	0.6507	0.6507	0.6507	0.6507	0.6507	0.6507	0.6507	0.6507	0.6507	0.6507	0.6507	0.6507	0.6507	0.6507	0.6507	0.6507
C1	2.4896	2.4137	1.857	0.9301	0.945	0.938	0.9338	0.9354	3.3355	3.4463	3.9216	0.9473	1.0764	1.0771	0.952	1.0659	3.0125	3.0674	1.8717
	0.6507	0.6507	0.6507	0.6507	0.6507	0.6507	0.6507	0.6507	0.6507	0.6507	0.6507	0.6507	0.6507	0.6507	0.6507	0.6507	0.6507	0.6507	0.6507

*The values in red indicate the presence of the defect.

As shown in the above table, in which correction factor has not been applied, row C3 represents the location C3 as shown in fig. 6.1. in column 2, the reading for 2mm defect is less than the reading for the 1mm defect as shown in row C3, column 9. This discrepancy is attributed to the inherent irregularities. So in the next table, with correction factor applied, this discrepancy has been removed and the value of the reading for 2mm defect in row C3 and column 2 is higher than the values of the readings at 1mm defect. Fig. 6.7 shown the plots of pulse-echo scanning results for various modes done on 4mm thick plate.

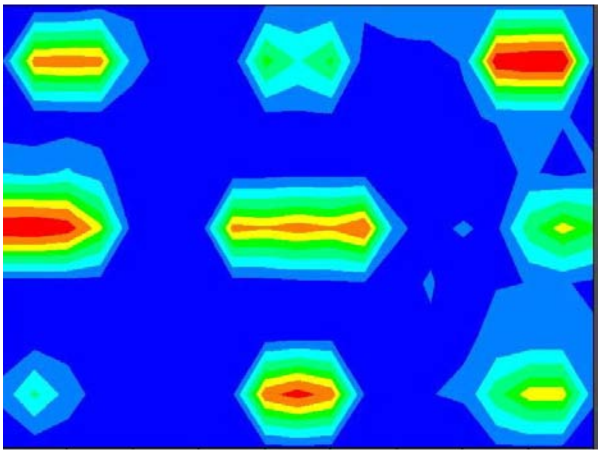

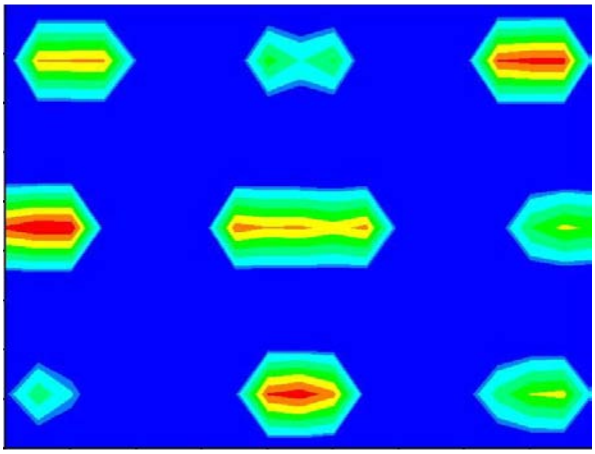

Fig. 6.7(a) 0.5 MHz S0 mode-before correction

Fig. 6.7(b) 0.5 MHz S0 mode-after correction

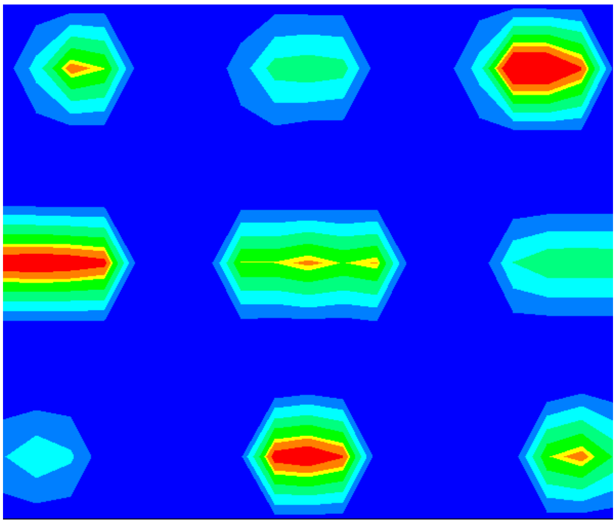

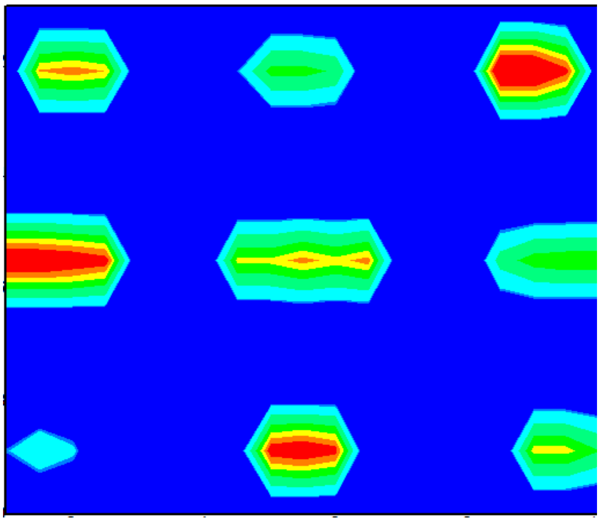

Fig. 6.7(c)1MHz S0 mode-before correction

Fig. 6.7(d) 1MHz S0 mode-after correction

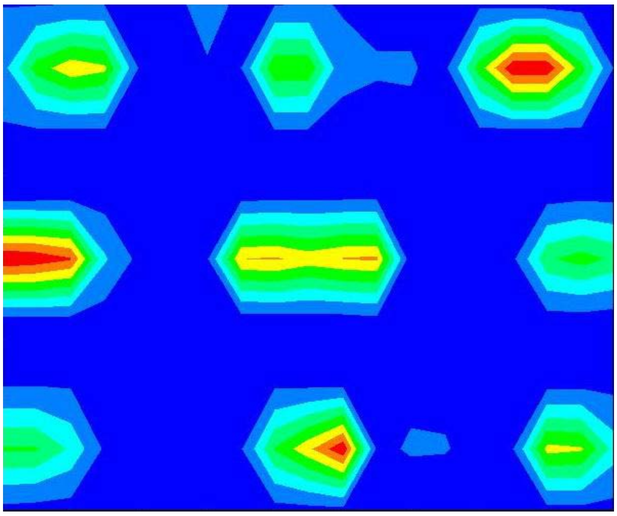

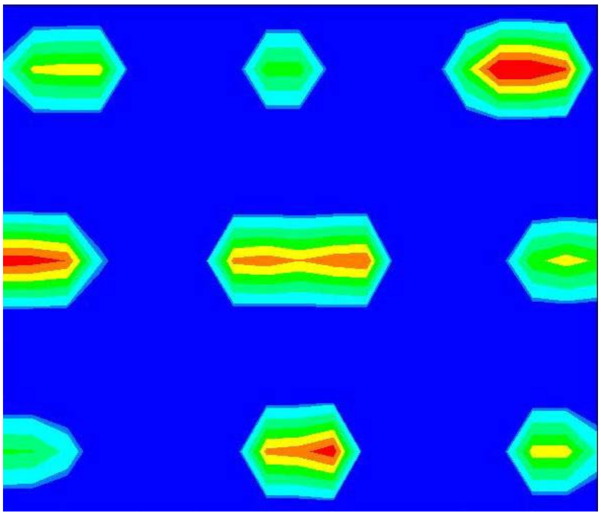

1 MHz S2 mode-before correction

1 MHz S2 mode-after correction

Hence it has been observed that after the correction factor had been applied, accurate readings about the depth and location of the defects were obtained, as compared to the readings prior to the application of the correction factor.

6.2 Testing of 6mm Plate

Mild steel plate of thickness 6mm has been taken and divided into three regions, namely C1, C2 and C3, similarly as done in 4mm thick plate. This plate has been seeded with notch type defects of varying depths and size at different locations. The depth of notch has been varied from 1mm, 2mm and 3mm to simulate 16.6%, 33.3% and 50% defect as shown in Fig.6.8. This has been tested with 0.5MHz and 1MHz with different angles to excite different modes. Out of these modes, only suitable modes were taken for testing. For different modes of each frequency, only few were taken for testing because the rest of modes of different frequencies which gave very weak output signal were and also have less energy to detect the defect on the plate.

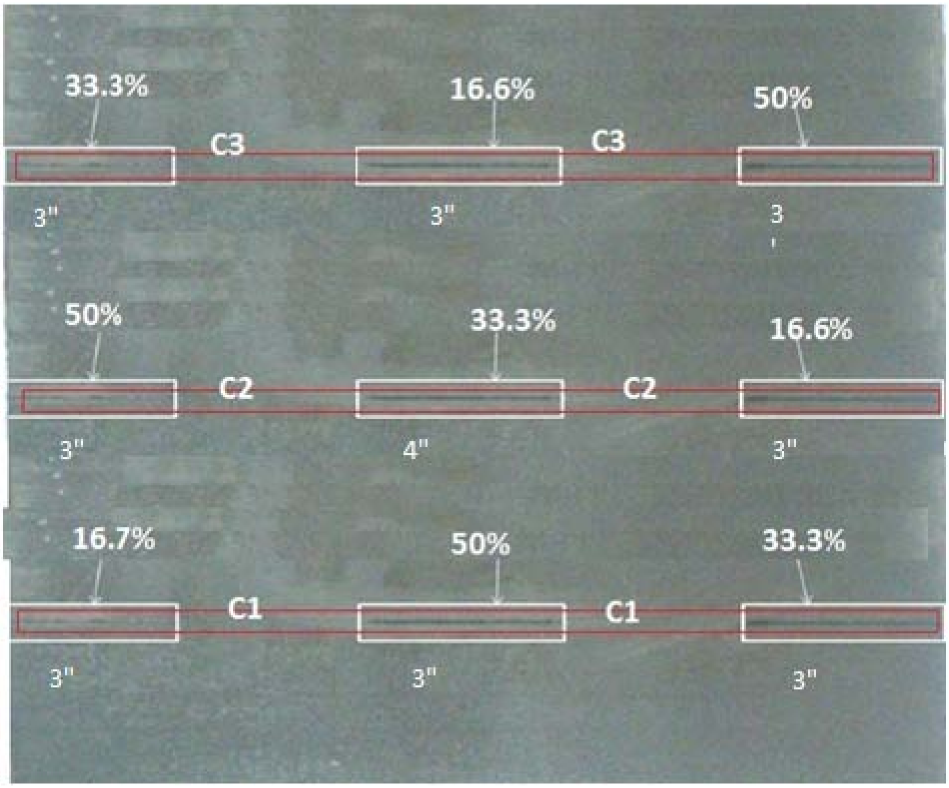

Fig. 6.8 6mm steel plate, showing the depth and location of defects

Following angles were used to excite various modes in 0.5MHz and 1MHz frequency:

- 25.8^0 to excite S0 mode in 0.5MHz
- 12.9^0 to excite S2 mode in 0.5MHz
- 13.8^0 to excite A1 mode in 0.5MHz

- 29.6^0 to excite S0 mode in 1MHz
- 16.6^0 to excite S2 mode in 1MHz
- 13.2^0 to excite S4 mode in 1MHz
- 23.5^0 to excite A1 mode in 1MHz
- 13.4^0 to excite A2 mode in 1MHz

The fig. 6.9 shows the fall in amplitude of various modes when interacting with defects of various depths.

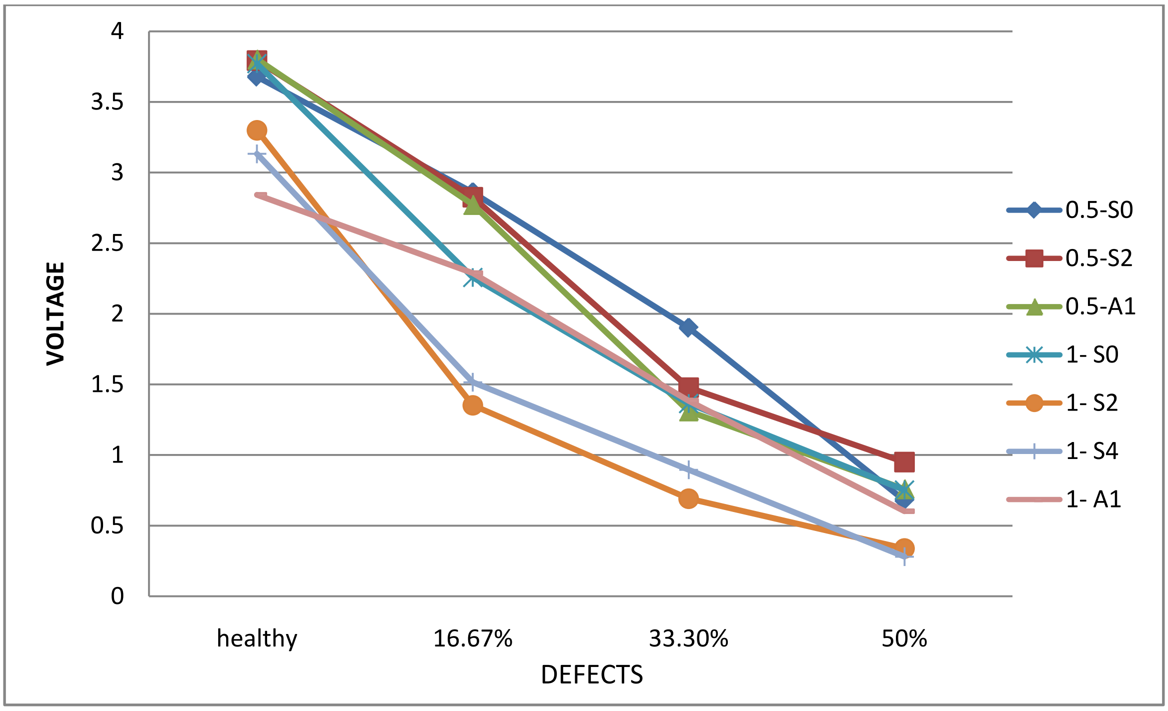

Fig. 6.9 Trends of various modes for Notch defects in 6mm plate

It is evident from the above graph that for 0.5 MHz S1 and S2 modes and for 1 MHz, S0 and S4 modes are most sensitive to the notch defect. In 1MHz S1 and S2 modes and in 0.5MHz, S0 mode is highly energized mode and is least attenuative. The peak to peak voltage amplitude with this mode is higher when compared with other modes. Attenuation curves given by DISPERSE, as shown in fig. 6.10 also show that these modes suffer least attenuation in comparison to other modes in 6mm plate. Here it has been also observed that in 0.5MHz, mode A1 and in 1MHz, mode A1 is sensitive to the defect, but is very attenuative. So it loses its energy when distance between the probes is increased. So this mode is also avoided.

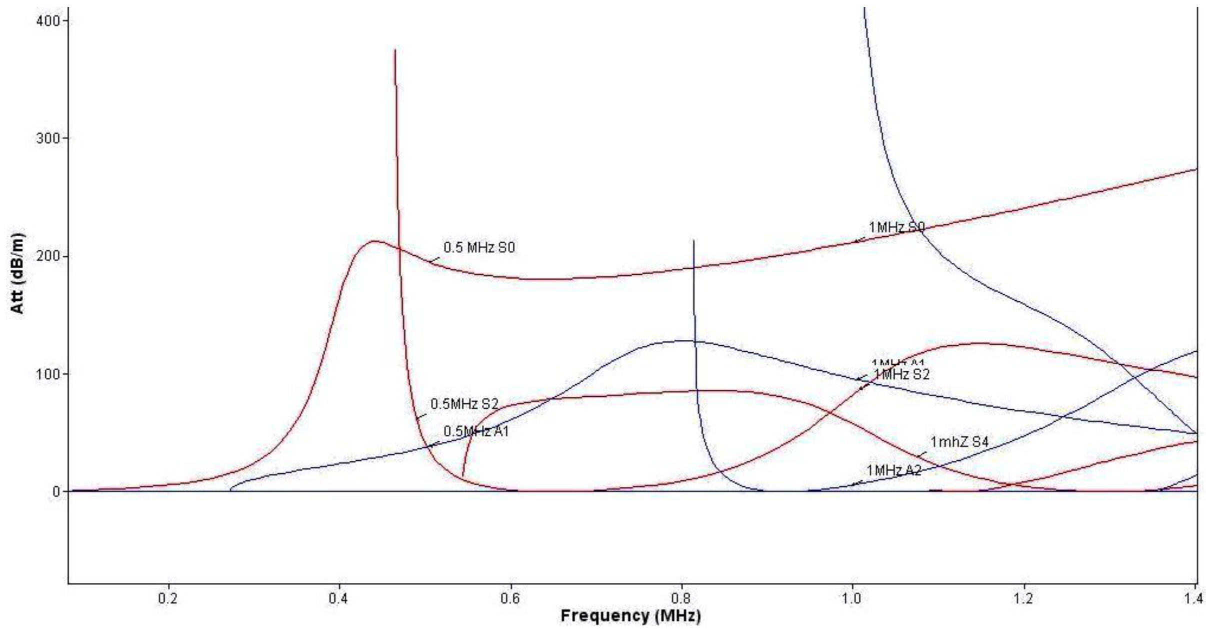

Fig. 6.10 Attenuation curves for 6mm plate

The through transmission readings for healthy plate were taken at 5 different locations, in regions C1, C2 and C3 along the X-axis as shown in Fig.5.8 for all the modes selected above. A trend had been observed in the healthy readings as shown in fig. 6.11

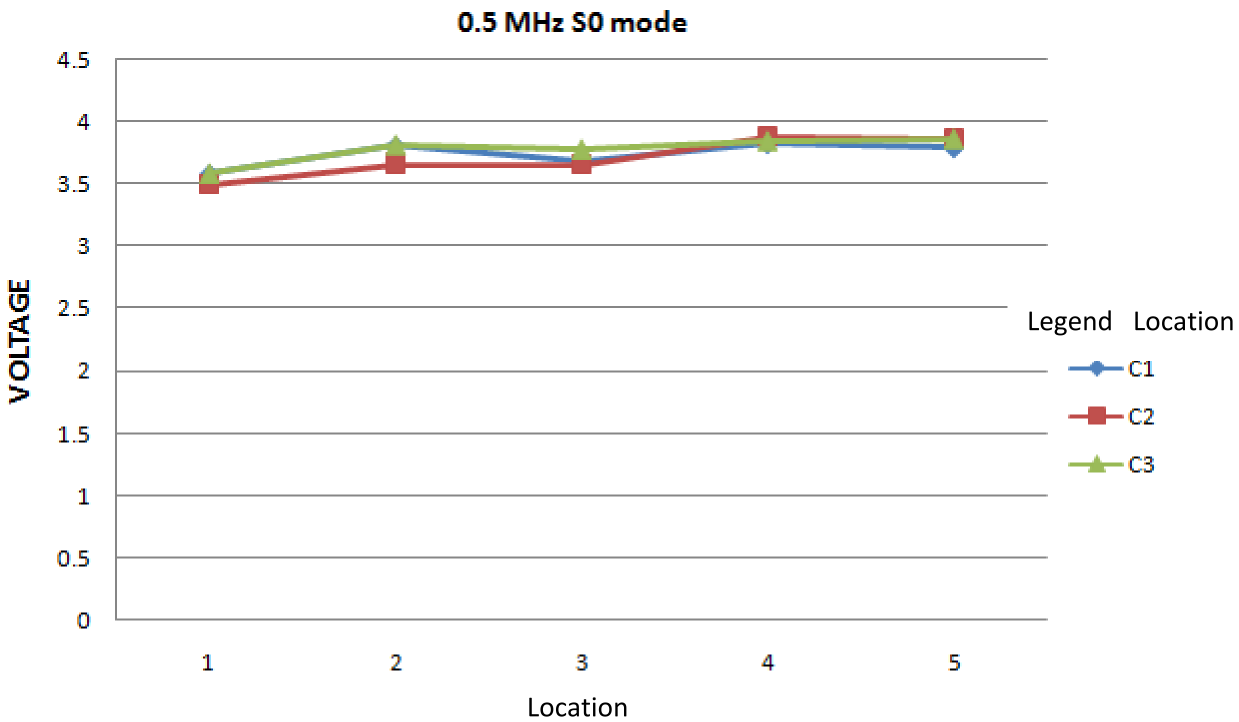

. **Fig. 6.11 Trend of readings for healthy plate at different locations**

So a correction factor had been formulated from the trend-line of the healthy readings as discussed in Chapter 5, section 5.5.1.

After taking readings on healthy plate, the defects had been seeded in the plate, as shown in fig. 6.8. After seeding the defects, the through transmission scanning has been done for the same modes used in scanning the healthy plate. The correction factor has been calculated in the similar manner as done for 4mm thick plate. Fig. 6.12 shows the readings for various defects and locations with the application of correction factor and without the application of the correction factor.

In the following figures, “H-Corrected” means readings of healthy plate, with correction factor applied. “Defects” means readings of defected part, without the application of correction factor. “Corrected” means the defected part readings, with correction factor applied. C1, C2, C3 give line of scan, as shown in fig. 6.11.

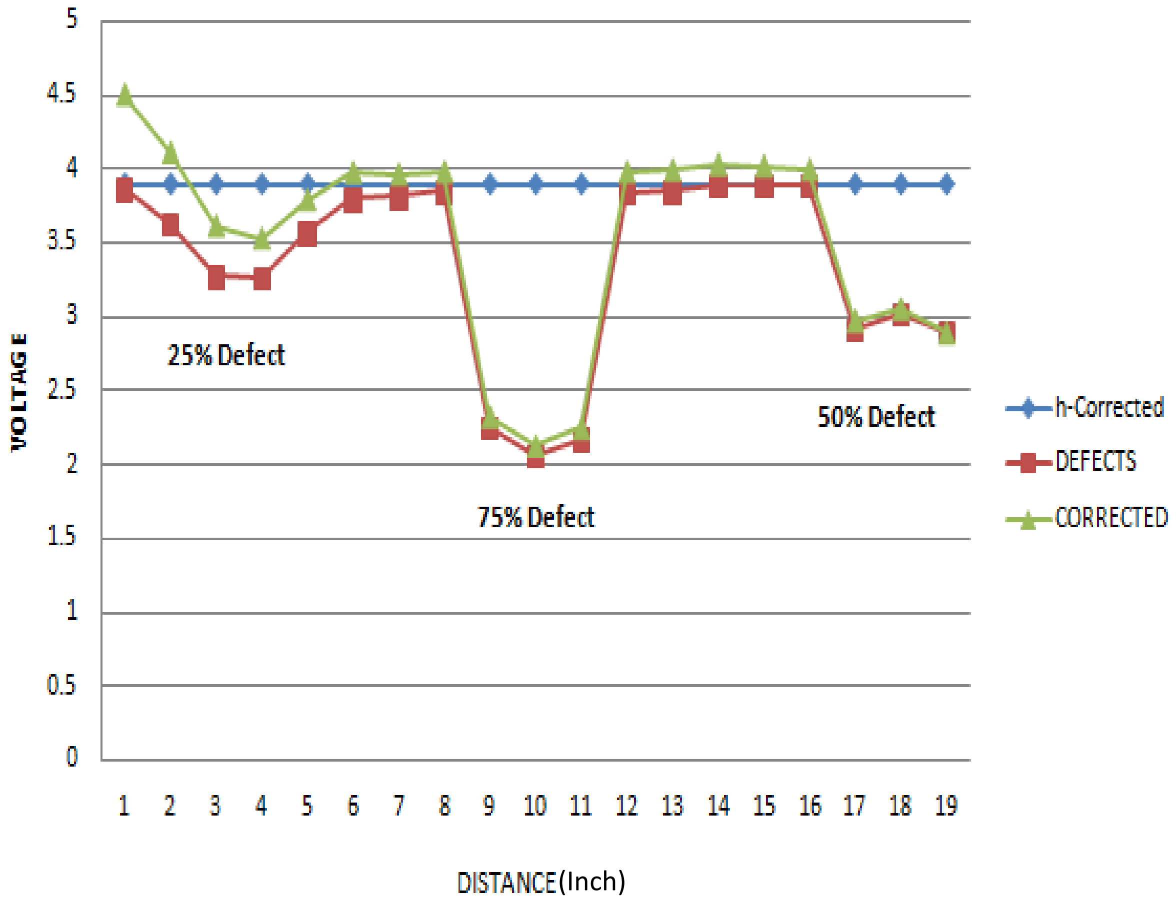

Fig. 6.12 (a) 0.5MHz S0 mode C1 location

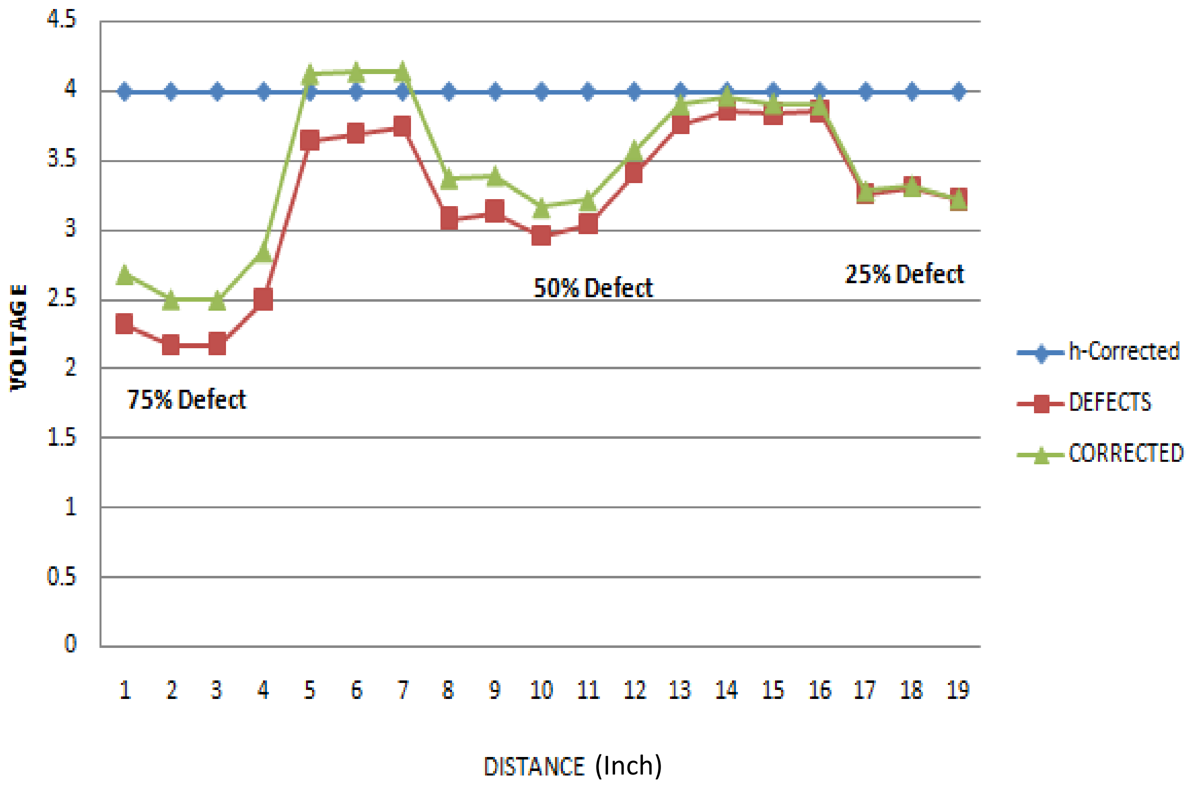

Fig. 6.12 (b) 0.5MHz S0 mode C2 location

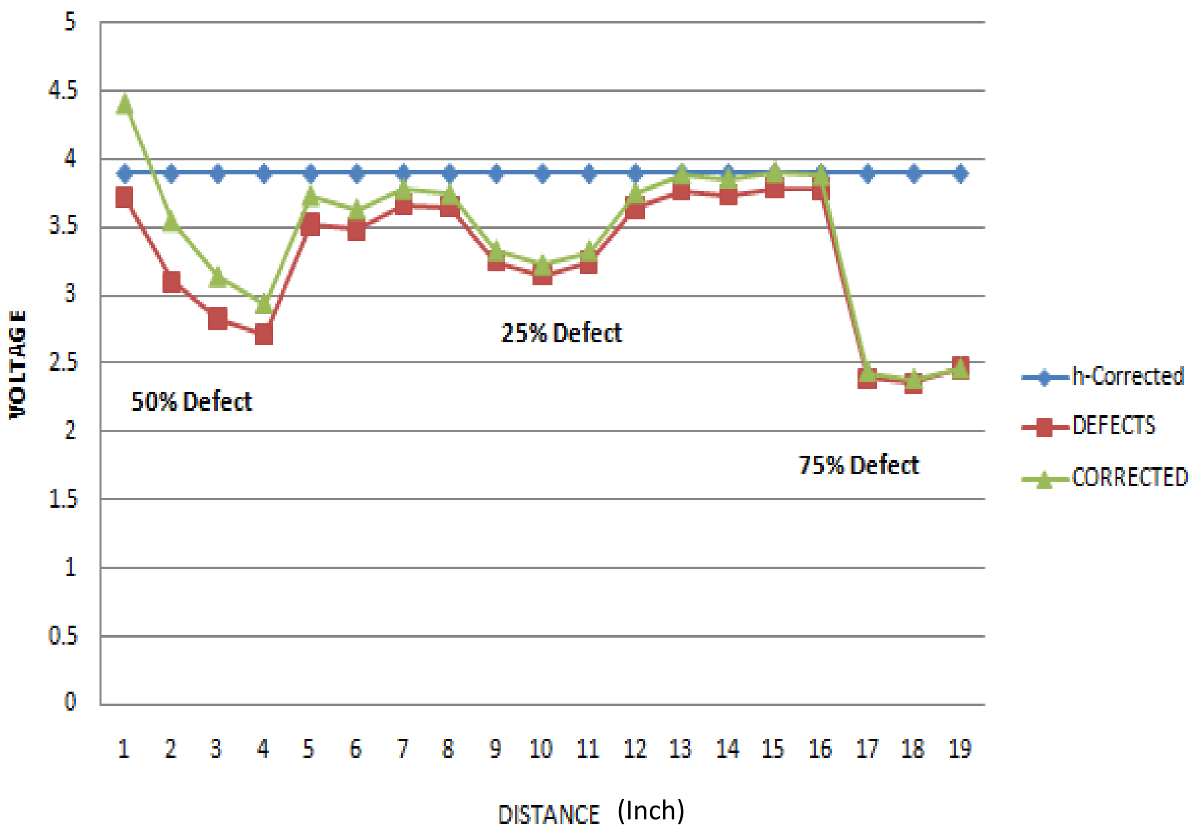

Fig. 6.12 (c) 0.5MHz S0 mode C3 location

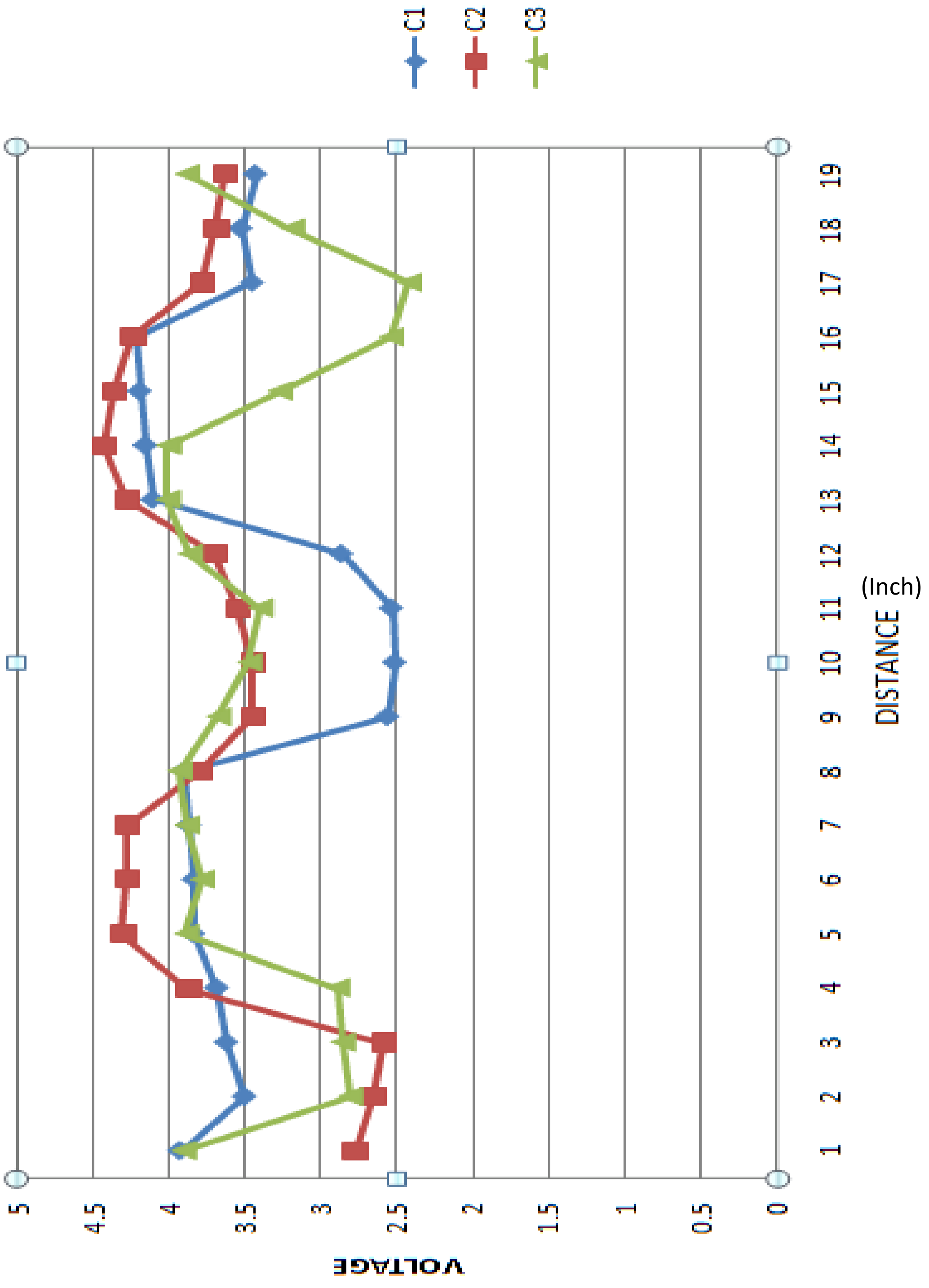

Fig. 6.12 (d) 0.5MHz S 2 mode C1, C2 and C3 locations

Fig. 6.6(d) shows the actual readings taken on the plate with seeded defects, taken at 1MHz frequency, S0 mode, locations C1, C2 and C3.

6.2.1 Localizing the defects

Through transmission scanning gives an idea about the severity of damage. The plate had been seeded with 16.6%, 33.3%and 50% defects and had been scanned by through transmission. As the transducer reaches nears the notch, the voltage amplitude drastically falls as shown in Fig. 6.11. Fall in amplitude of the voltage indicates the presence of notch. When there is fall in amplitude in through transmission, the scanning is switched to pulse echo mode and scanning has been done in Y-direction. The trends were observed in the scanning of the plate with pulse-echo method, so the correction factor was applied as discussed in section 6.1.1 and table 6.2. As the transducer approaches the defect, the amplitude of the voltage surges, as shown in Fig. 6.13

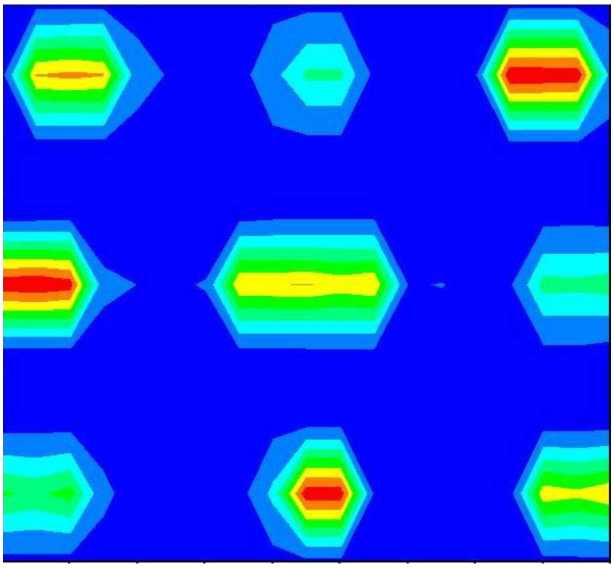

Fig. 6.13(a) 0.5 MHz S0 mode-before correction

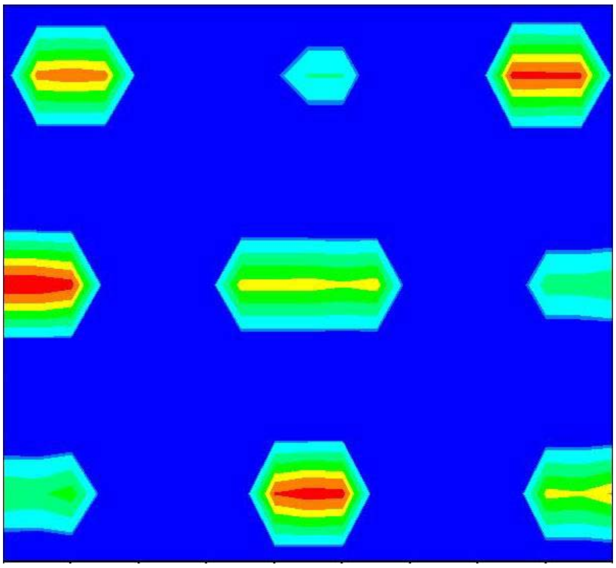

Fig. 6.13(b) 0.5 MHz S0 mode-after correction

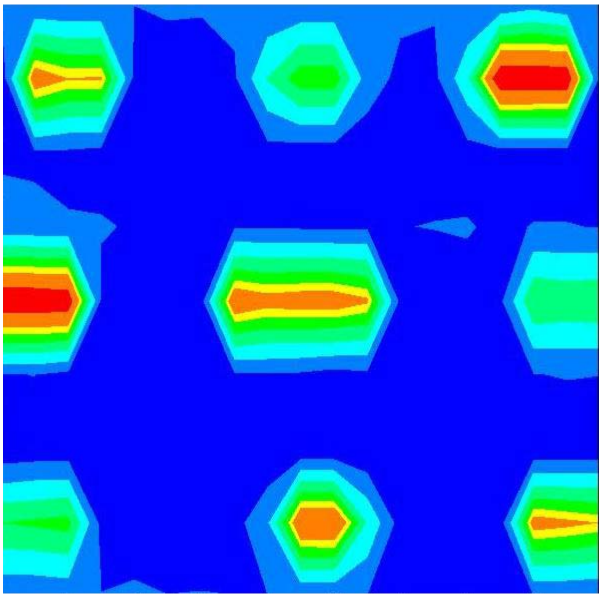

Fig. 6.13(c) 0.5 MHz S2 mode-before correction

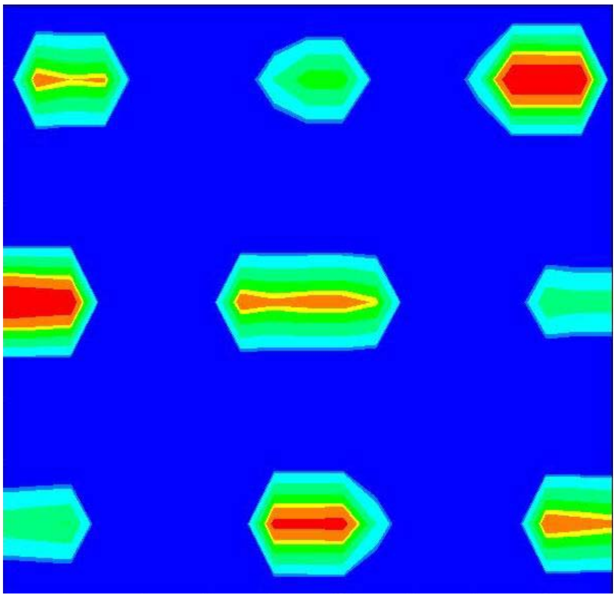

Fig. 6.13(d) 0.5 MHz S2 mode-after correction

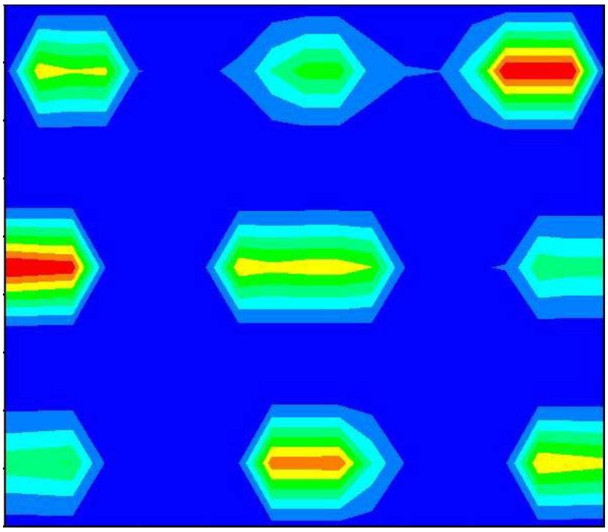

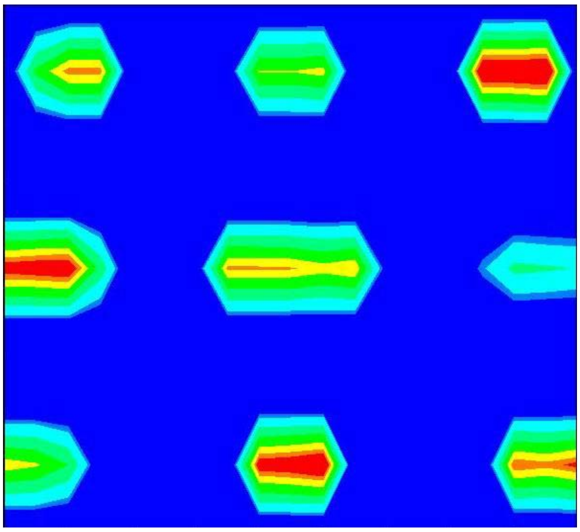

Fig. 6.13(e) 1 MHz S0 mode-before correction

Fig. 6.13(f) 1 MHz S0 mode-after correction

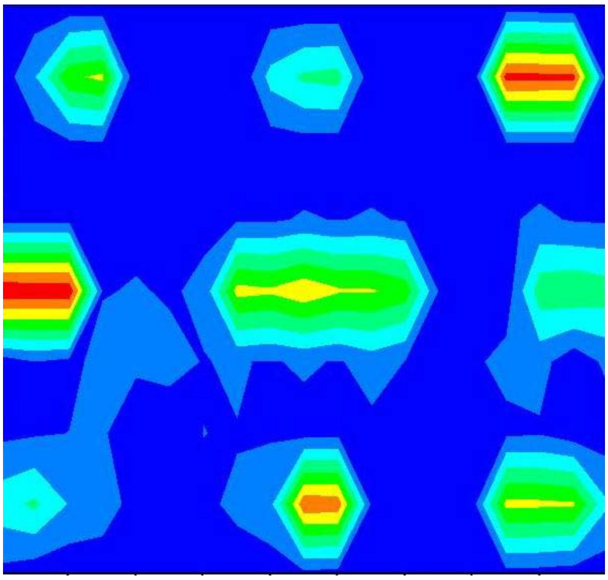

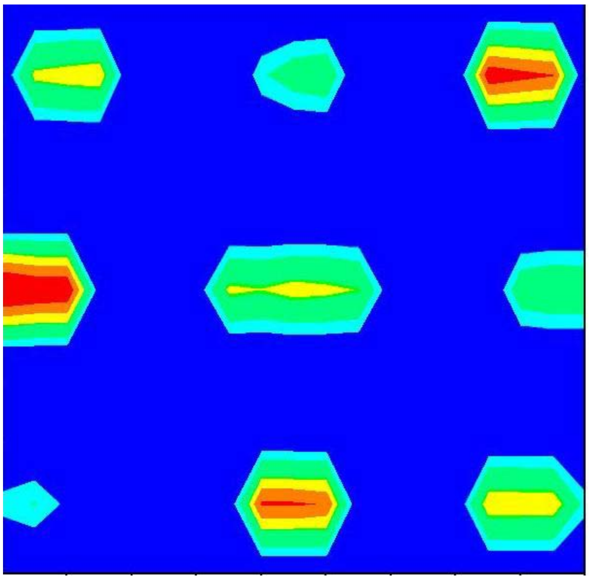

Fig. 6.13 (g) 1 MHz S4 mode-before correction

Fig. 6.13 (h) 1 MHz S4 mode-after correction

Hence it had been observed that after the correction factor had been applied, accurate readings about the depth and location of the defects were obtained, as compared to the readings prior to the application of the correction factor.

CHAPTER 7

CONCLUSIONS

The experimental study carried out on steel plates of different thickness with inherent irregularities seeded with notch defects show that ultrasonics is capable of detecting the notch damages effectively by using suitable modes. Different modes at different frequencies are sensitive to these defects.

Following conclusions can be drawn from this study.

- Higher frequency like 2MHz has been avoided because of scattering effect, which makes the modes at higher frequency inefficient to travel long distances. Also in 2 MHz, phase velocities of the modes are found to be very close to each other, which results in very close values for corresponding critical angles and are thus difficult to be used.
- Anti symmetric modes are not preferred over symmetric modes due to high attenuation and loss of energy.
- Before scanning a defected specimen, same specimen must be scanned in healthy condition to check for inherent irregularities.
- Variations if any in the scanning set up must also be observed, by scanning different healthy specimens, and observing any variation in the readings.
- Inherent irregularities if any, present in the specimen are reflected in the scanning of defects and lead to misinformation about the severity and location of the defect.
- Readings in healthy as well as defected specimen should be updated by evaluating and applying a position dependent correction factor, to compensate for inherent irregularities in the given specimen.

SCOPE OF FUTURE WORK

The field of NDT and damage detection constitutes important and challenging area of study, where wave propagation provides an efficient means of characterizing defects in structures. As the topic of ultrasonic guided wave propagation is very wide spread and has utilities in many areas of human endeavour, there is much scope for future work. The experimental methodology discussed in this work can be further extended for:

- Detection of welding defects.
- Detection of defects in corrugated plates.
- Water on one side of the plate to model real life problem of ship hulls.
- Detection of multiple cracks in steel plates.
- Scanning with different Pulser/Receiver like tone burst can be done.

REFERENCES

1. http://www.ndted.org/EducationResources/CommunityCollege/NDTIntro/cc_introBackground.htm
2. http://www.ndted.org/EducationResources/CommunityCollege/NDTIntro/cc_intro001.htm
3. Shull, P.J., Nondestructive Evaluation – Theory, Applications, and Applications, 2002
4. http://www.ndt-ed.org/GeneralResources/Method_Selection/MethodSelection.htm
5. "Transducers for ultrasonic flaw detection", by V.N.Bindal (1999).
6. http://www.ndted.org/EducationResources/CommunityCollege/Ultrasonics/Physics/modepropagation.htm
7. http://www.ndted.org/EducationResources/CommunityCollege/Ultrasonics/EquipmentTrans/characteristicspt.htm
8. http://www.ndted.org/EducationResources/CommunityCollege/Ultrasonics/Equipment Trans/transducertypes.htm
9. http://www.olympus-ims.com/en/ndt-tutorials/transducers/inside/
10. Kundu T., "Non destructive testing techniques for material characterization", Modeling in Geo mechanics, Chapter 12, Eds. M. Zaman, G. Gioda and J. Booker, Pub. John Wiley & Sons, 2000, p. 267-298.
11. Kundu T., Nondestructive Evaluation, Kirk-Othmer Encyclopedia of Chemical Technology, Pub. John Wiley and Sons, 2004
12. Ditri J J, J L Rose, Chen G.(1992) , " Mode Selection Criteria for Defect Detection Optimization Using Lamb Waves". Review of progress in quantitative non-destructive evaluation. Vol 11.
13. Kundu T., Maslov K., "Material Interface Inspection by Lamb Waves", International Journal of Solids and Structures, vol. 34, 1997, p. 3885-3901.
14. Hee Don Jeong, Hyeon Jae Shin, Joseph L. Rose," Detection of Defects in a Thin Steel Plate Using Ultrasonic Guided wave"
15. Graff, K. F., "Wave motion in elastic solids," Dover Publications, Inc., 1973.
16. Liu Zhenqing." Lamb Wave Analysis of Acousto-Ultrasonic Signals in Plate", Institute of Acoustics, Tongji University Shanghai 200092, P.R.China
17. http://www.ndt.net/article/wcndt00/papers/idn020/idn020.htm

18. Junker W.R., Michael M.J.”Apparatus and method for guided inspection of an object” United States Patent”, Patent Number: 5,161,413, Nov 10 1992.
19. Peter C., Allyne D.N., “Optimization of lamb wave inspection techniques.” NDT & E International Volume 25, Issue 1, 1992, Pages 11-22
20. Peter C., Allyne D.N., “the use of Lamb waves for long range inspection” Ultrasonics Volume 34, Issues 2-5, June 1996, Pages 287-290
21. Kundu, T., and K. I. Maslov, “Material Interface Inspection by Lamb Waves”, International Journal of Solids and Structures, Vol.34, pp.3885-3901, 1997.
22. Younho Cho, Hongcrholt Derrick D., and Rose Joseph L., “Lamb Wave Scattering Analysis for Reflector Characterization”, IEEE Transactions on Ultrasonics,
23. O.I. Lobkis, D. E. Chimentia (1997), “Elastic guided waves in plates with surface roughness” Acoustical Society of America, 102 (1), July 1997.
24. Kundu T., Maji A., Ghosh T. and Maslov K., “Detection of kissing bonds by lamb waves“Ultrasonics Volume 35, Issue 8, January 1998, Pages 573-580.
25. T. Gosh, T. Kundu, P. Karpur (1998) “Efficient Use of Lamb Modes for Detecting Defects in Large Plates”, Ultrasonics 36(2001) 791-801
26. Jeong H.D.,Hyeon .J.S., Rose J.L.,(2000),”Detection of Defects In a Thin Steel Plate Using Ultrasonic Guided Weave ”, Roma 2000 15th WCNDT.
27. Potel, J.F. De Belleval, T, Kundu (2001), “ Importance Of Near Lamb Mode Imaging Of Multi Layered Composite Plates” , Ultrasonics 39(2001) 283-290
28. Rose Joseph L. (2002) “A Baseline and Vision of Ultrasonic Guided Wave Inspection Potential” Journal of Pressure Vessel Technology, Vol. 124 / 273, ASME.
29. Worden, K., Allen, D., Sohn, H., and Farrar, C.R. (2002) “Damage Detection in Mechanical Structures using Extreme Values Statistics,” Los Alamos National Laboratory report LA-13903-MS.
30. Steve Vanlanduita, Patrick Guillaumea, Geert Van Der Lindenb (2003), “On-line monitoring of fatigue cracks using ultrasonic surface waves”, NDT&E International 36 (2003) 601–607.
31. J.L. Rose, J.B. Nestleroth and E.G. Poplawski, “Flaw classification in welded plates using microprocessor controlled flaw detector.”NDT International Volume 36, Issue 4, 2003, Pages 159-164
32. Fromme Paul, Wilcox Paul D., Lowe Mike J.S., Cawley Peter (2004), “On the Sensitivity of Corrosion and Fatigue Damage Detection using Guided Ultrasonic

Waves”. 2004 IEEE International Ultrasonics, Ferroelectrics, and Frequency Control Joint 50th Anniversary Conference.

33. Alleyne, D.N., Pavlakovic, B., Lowe, M.J.S., and Cawley, P., Insight43 (2), 93-96(2001) Benny, G., Steel, K., McNab, A., and Hayward, G., in Rev. Prog. QNDE, Vol. 23B, AIP Conference Proceedings 700, New York, 1484-1491 (2004).
34. Edalati K., Kermani A., M. Seiedi, M. Movafeghi (2005), “Defect Detection in Thin Plates by Ultrasonic Lamb Wave Techniques”. The 8th International Conference of the Slovenian Society for Non-Destructive Testing “Application of Contemporary Non-Destructive Testing in Engineering” September 1-3, 2005, Portorož, Slovenia, pp. 35-43
35. Fromme Paul, Wilcox Paul D., Lowe Mike J.S., Cawley Peter (2004), “On the Sensitivity of Corrosion and Fatigue Damage Detection using Guided Ultrasonic Waves”. 2004 IEEE International Ultrasonics, Ferroelectrics, and Frequency Control Joint 50th Anniversary Conference.
36. Takahiro Hayashi, Won-Joon Song and Joseph L. Rose, “Guided wave dispersion curves for a bar with an arbitrary cross-section ”Ultrasonics Volume 44, Issue 1, January 2006, Pages 17-24.
37. Satyarnarayan L., Chandrasekaran J., Maxfield Bruce, Balasubramaniam Krishnan 2007, “Circumferential higher order guided wave modes for the detection and sizing of cracks and pinholes in pipe support regions”, NDT&E International 41 (2008) 32–43.
38. Rokhlin S.I., m J.-Y. Kim, B. Xie, Zoofan B. (2007), “Nondestructive sizing and localization of internal micro cracks in fatigue samples”, NDT&E International 40 (2007) 462–470
39. Sourav Banerjee, Tribikram Kundu, “Ultrasonic field modeling in plates immersed in fluid”International Journal of Solids and Structures 44 (2007) 6013–6029”